공학박사학위논문

Fabrication of Endothelial Progenitor Cell-capturing Stents for Vascular Re-endothelialization

혈관내피화를 위해 혈관내피 전구세포를 포획하는 스텐트의 개발

2013년 2월

서울대학교 대학원

바이오엔지니어링 협동과정

강 찬 구

Fabrication of Endothelial Progenitor Cell-capturing Stents for Vascular Re-endothelialization

by

Chan-Koo Kang

Advisor: Professor Yoon-Sik Lee, Ph. D.

Submitted in Partial Fulfillment
of the Requirements for the Degree of
DOCTOR OF PHILOSOPHY

February, 2013

Interdisciplinary Program for Bioengineering
College of Engineering
Graduate School
Seoul National University

Abstract

Fabrication of Endothelial Progenitor Cell-capturing Stents for Vascular Re-endothelialization

Chan-Koo Kang
Interdisciplinary Program for Bioengineering
The Graduate School
Seoul National University

Endothelial progenitor cells (EPCs) have been identified as a crucial factor for re-endothelialization after stenting, thereby resulting in the prevention of stent thrombosis and neointimal hyperplasia. Because EPCs can be introduced by antibody–antigen interactions, the exploration of suitable antibody and the biocompatible surface modification technology including its immobilization are essential for developing an EPC-capturing stent.

In this study, we fabricated a biofunctional stent with EPC specificity by grafting a hydrophilic poly(ethylene glycol) (PEG) and consecutively immobilizing the antibody against vascular endothelial-cadherin (VE-cadherin) which is a specific EPC surface marker. We chose VE-cadherin as an ideal target because it is exclusively expressed on the late EPCs and regulates cellular processes such as proliferation.

Above all, the correlation between surface properties and protein

adsorption was investigated in terms of hydrophilicy and micro-roughness. From the quantitative fibrinogen adsorption assay, it was suggested that the hydrophilic and smooth surface was the best choice to reduce protein adsorption. When developing EPC-capturing stent, biocompatible surface is important because non-specific protein adsorption usually causes unfavorable responses and the adsorbed proteins interfere with the molecular recognition between antibody on the stent and EPCs in bloodstream.

Based on our correlation study, the surface of a stainless steel stent was sequentially modified by acid treatment, silanization and covalent attachment of polymers not only to improve biocompatibility but also to introduce functional groups on the stent surface. This polymer-grafted stent intactly immobilized anti-VE-cadherin antibodies through peptide coupling procedure. A variety of surface analysis methods such as AFM, AES, FE-SEM, and CLSM confirmed whether each step proceeded well as planned.

In cellular experiment, our EPC-capturing stent specifically captured the EPCs (96±7 vs. 15±3) whereas THP-1s, human acute monocytic leukemia cells, were not adsorbed, when compared to bare stainless steel as a control. Furthermore, we confirmed that the recruited EPCs immediately developed the endothelial cell layers on the surface-modified stent.

Through rabbit iliac artery study model, we compared the capability of bare stainless steel stent and our EPC-capturing stent with regard to re-endothelialization and neointimal hyperplasia. Over 90% of EPC-capturing stent was covered with endothelial cell within 3 days, whereas bare stainless steel stent was covered less than 10%. Neointimal area in stented vessel at 42 days was quite smaller in EPC-capturing stent than in bare stainless steel stent (0.95 ± 0.22 mm^2 vs. 1.34 ± 0.43 mm^2). These are totally due to high EPC specificity of the modified stent surface. In addition, immunohistochemical analysis revealed that our surface coating did not induce any further inflammation.

These positive *in vitro* and *in vivo* results will encourage the extensive application of biofunctional surface modification technology for a variety of medical devices.

Keywords: stent, surface modification, protein adsorption, endothelial progenitor cell, re-endothelialization, neointimal hyperplasia

Student Number: 2009-30265

Contents

List of Tables

List of Figures

List of Schemes

List of Abbreviations

AES	auger electron spectroscopy
AFM	atomic force microscopy
ATR	attenuated total reflectance
BMS	bare metal stent
CD31	cluster of differentiation 31
CD34	cluster of differentiation 34
CFSE	carboxyfluorescein succinimidyl ester
CLSM	confocal laser scanning microscopy
DES	drug-eluting stent
DIC	*N,N'*-diisopropylcarbodiimide
DMF	*N,N'*-dimethylformamide
DNA	deoxyribonucleic acid
DIEA	diisopropylethylamine
DMAP	4-(dimethylamino)pyridine
EDX	energy dispersive X-ray spectrometer
EGM-2MV	endothelial cell culture medium
EP	electropolished
EPC	endothelial progenitor cell
Fc	fragment, crystalizable
FITC	fluorescein isothiocyanate
FE-SEM	field-emission scanning electron spectroscopy
GPTS	3-glycidoxypropyltrimethoxysilane
HPLC	high performance liquid chromatography
IgG	Immunoglobin G
Jeffamine®	*O,O'*-Bis-(2-aminopropyl)polyethylene glycol
MC	methlyene chloride

NHS	*N*-hydroxysuccinimide
NMP	*N*-methylpyrrolidinone
PCNA	proliferating cell nuclear antigen
PDAM	polydopamine
PDMS	poly(dimethylsiloxane)
PECAM-1	platelet endothelial cell adhesion molecule-1
PEG	poly(ethylene glycol)
PPG	poly(propylene glycol)
PTCA	percutaneous transluminal coronary angioplasty
PTG	poly(tetrahydrofuran)
RAM11	mouse monoclonal anti-rabbit macrophage antibody
RMS	root mean square
SA	succinic anhydride
SMC	smooth muscle cell
SS	stainless steel
THP-1	human acute monocytic leukemia cell line
unEP	unelectropolished
VE-cadherin	vascular endothelial-cadherin
XPS	X-ray photoelectron spectroscopy

I. Introduction

I.1. General Introduction

Heart disease describes a variety of disorders and failures in conditions that can affect the heart. The most common type of this is coronary artery disease, also called coronary heart disease and cardiovascular disease. The word 'coronary' means crown and it is the name given to the arteries that circle the heart like a crown. The coronary arteries supply the heart muscle with oxygen and nutrients, similar with fuel pipe in a car.

Coronary artery disease develops when one or more of the coronary arteries that supply the blood to the heart become narrower than they used to be. This happens due to a buildup of cholesterol and other substances inside the wall of the blood vessel. When the coronary arteries which start out smooth and elastic, become narrow and rigid, blood flow to the heart is restricted. Then, heart becomes starved of oxygen and the vital nutrients it needs to pump properly. From this inadequacy, heart muscle tissue can be damaged and thus angina or a myocardial infarction can occur.

At present, coronary artery disease is ranked No.1 killer among all medical diseases in USA and No. 3 killer in Korea. While one in every 5 deaths in the USA occurs due to this disease, over fourteen million Americans are estimated to have active symptoms related to this precarious condition. From the OECD health reports, coronary artery diseases are the leading cause of mortality in almost all OECD countries. Considering a whole circulatory disease, it accounted for 35% of all deaths.

Recently, many technological advances to treat coronary artery diseases have been achieved and new devices for coronary interventions have been tested[1]. Previously, the bypass surgery was mainly performed. Herein, arteries or veins from elsewhere in the patient's body are grafted to the coronary arteries to bypass inside narrowing area and improve the blood supply to the coronary circulation. This surgery necessitates the usage of cardiopulmonary bypass with the heart stopped. It is not only dangerous but also painful for patients. Since the introduction of a catheter-based percutaneous transluminal coronary angioplasty[2] (PTCA) by Dr. Gruntzig in 1977, major progress has rapidly begun in the clinical practice. This minimally-invasive procedure leads to less patient trauma, faster recovery times and less expense. However, it raised a stiff problem, 30-40% re-narrowing ratio. In 1986, Puel and Sigwart deployed the first coronary stent in the narrowed vessel with balloon angioplasty[3]. Then, the stent was approved for use in USA by the FDA in 1994. This is innovative device to resolve a couple of complications derived from traditional PTCA[4]. Since then, cardiologists have the most commonly used stents to treat coronary artery diseases[5].

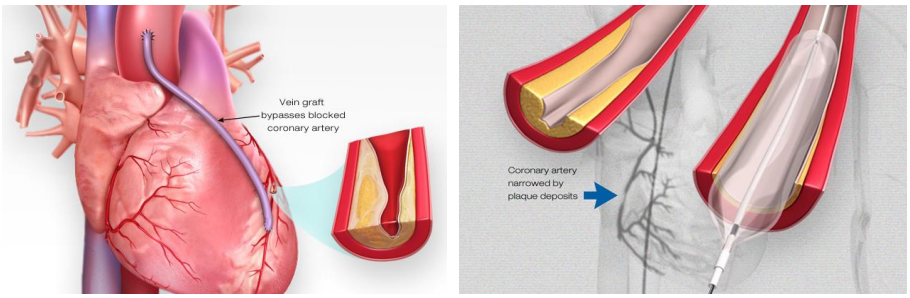

(a) (b)

Figure 1. Traditional coronary artery interventions; (a) bypass surgery, (b) balloon angioplasty.
Source: American Heart Association website (www.heart.org)

I.2. What Is a Stent?

A stent is a wire mesh tube support placed inside a coronary artery to keep the vessel open. It is small but strong enough to be inserted with a catheter to fit inside an artery to prop it open and prevent widened artery from collapsing. The stent exerts a continuous radial pressure on diseased coronary artery, resulting in a compression of atherosclerotic plaques, sealing of dissections and expansion of coronary vessel (**Figure 2**). In the years to come, this stent will be increasingly used for treating heart diseases due to its efficient operation and excellent clinical results[6].

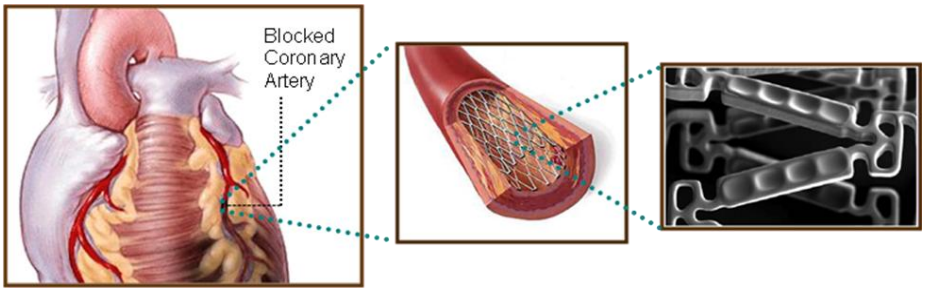

Figure 2. Schematic view of stenting to the blocked coronary artery.
Source: Bostonscientific website (www.bostonscientific.com)

One major difference between balloon angioplasty and stenting is that in angioplasty, the balloon which was inflated to push plaque is then removed, and nothing is left behind in the patient's vessel. On the contrary, a stent is permanently implanted in the patient's vessel.

Taking a look at the stenting procedure, a stent is mounted on a balloon catheter in a crimped or collapsed state before operation. Through a small

opening in a blood vessel of the patient's groin, arm or neck, a thin and flexible catheter with the stent is threaded. Then, the stent on the tip of catheter is moved to the narrow section of the artery. When the balloon is inflated, the stent expands or opens up and pushes itself against the inner wall of the coronary artery. This holds the artery open and restores inadequate blood flow even after the balloon is deflated and removed (**Figure 3**). During these procedures, special x-ray movies, angiograms, help the doctor position the catheter (**Figure 4**).

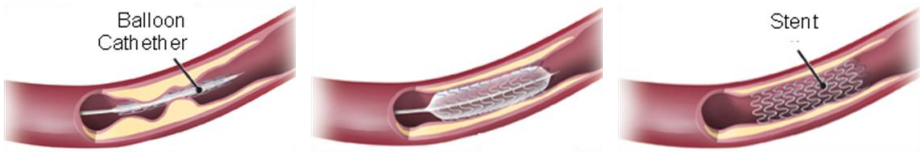

(a) (b) (c)

Figure 3. Procedures of stenting surgery; (a) stent insertion, (b) stent expansion by balloon inflation, (c) stent implantation. Source: University of Ottawa heart institute website (www.ottawaheart.ca)

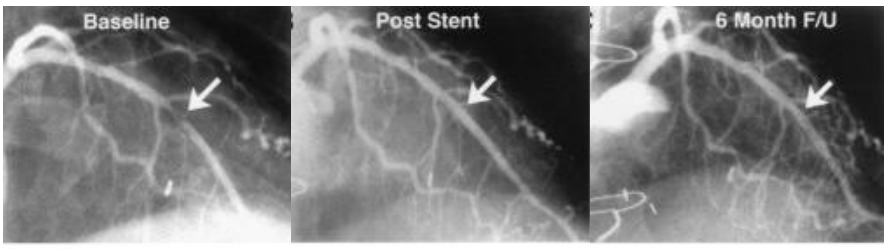

Figure 4. Angiograms of stenting surgery[7].

I.3. Stent Market

Due to aging population and rising obesity rate, coronary artery disease has increased, continually. Moreover, as the Asian diet pattern is becoming more westernized, coronary artery disease is recognized to be the main cause of death over the world in the future.

Accordingly, the stent market has grown rapidly and the stent is one of the biggest items in the field of medical device. From the Global Industry Analysts (GIA) report, the global market for coronary stents is forecasted to reach 9.8 billion dollars by the year 2017. Further, growing awareness and substantial clinical evidence supporting the efficacy, technological advancements drives high penetration levels, particularly in the affluent, developed markets. The future holds ample scope for development of the coronary stents market given the huge demand and the large number of high-profile innovations underway. Especially, untapped and developing markets of Asia and Latin America will propel rapid growth and expansion in this market. The worldwide stent procedures are expected to increase from 1,167,000 in 2000 to 3,200,000 in 2012.

Although the market size is huge, the global coronary stent market is largely dominated by a handful of international giant players. It is typical figure for high-tech industry. Key participants are Abbott, Boston Scientific, Medtronic and OrbusNeich. Recently, Johnson & Johnson, another major player, decided to exit the stent market due to the fierce competition.

Until 2004, bare metal stent accounted for most of the market. However,

since the first drug-eluting stent, sirolimus-eluting Cypher stent received FDA approval in 2003, drug-eluting stent segment has been driving the market, contributing 60-70% of global market. Now, drug-eluting stent is estimated that it is superior to bare metal stent in terms of safety and efficacy, showing statistically lower rates of major adverse cardiac events.

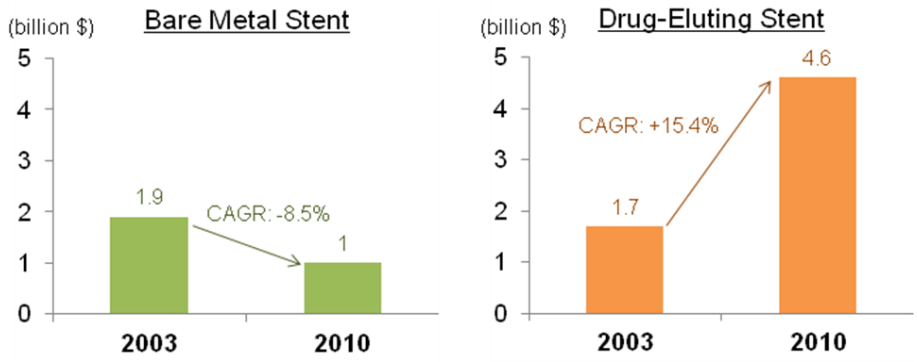

Figure 5. Global revenue of bare metal stent and drug-eluting stent.

As the technological advancement is getting accelerated ranging from material and geometric design to surface modification and drug, the market has been dynamically changed. Once a better device is launched, intense competition ensues and the new device usually dominates the majority of the market. Moreover, the interventional cardiologists are known to adopt new technologies rapidly.

As shown in the **Figure 6**, leadership in the coronary stent market shifted many times. For example, Boston Scientific which developed paclitaxel-eluting Taxus stent emerged as a strong player since 2004. Recently, everolimus-eluting Xyence V stent from Abbott is gaining popularity.

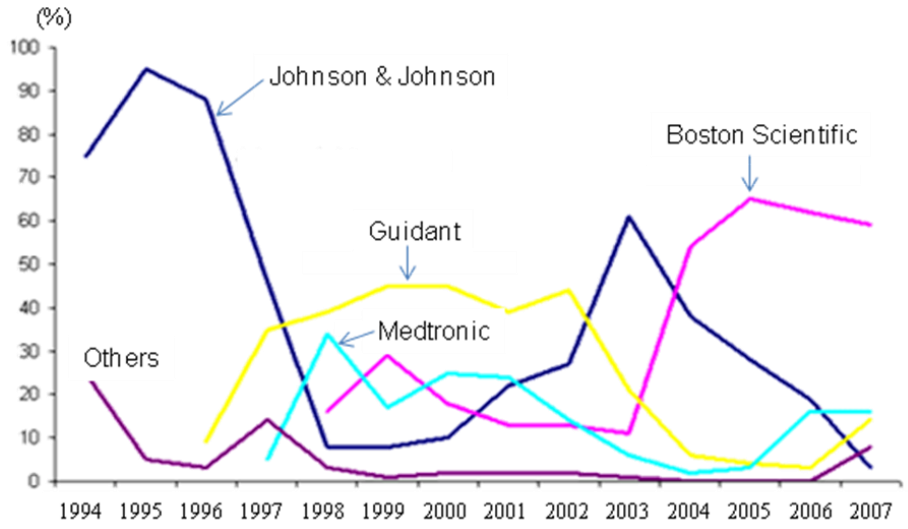

Figure 6. USA total stent market shares.

Source: Kim, J. *et, al*. Future of the coronary stent market.

I.4. Issues with the Stent

Although coronary artery stents have received widespread application, some significant limitations exist as ever[8,9]. Accordingly, various types of stents such as drug-eluting stent, bioactive stent, and biodegradable stent have been actively developed and they alleviated the related complications (**Table 1**). However, there are still plenty of rooms for improving the clinical performance in a field of respective limitations.

Table 1. Types of Coronary Artery Stents

Stent type	Description	Examples
Bare Metal Stent	Without any coating, the first-generation stent	Bx Velocity (J&J) Express2 (Medronic)
Drug-eluting Stent	Slowly releasing a drug to block cell proliferation	Taxus (Boston Scientific) Xience (Abbott) Endeavor (Medtronic)
Bioactive Stent	Initiating the body's natural healing processes	Genous (OrbusNeich)
Absorbable Stent	Completely biodegradable, typically polymer or magnesium-based	AMS (Biotronik) ABSORB (Abbott)

I.4.1. Restenosis

Restenosis means a re-narrowing of the stented blood vessel, leading to restricted blood flow (**Figure. 7**). It is the most common adverse event of stenting[10].

The failure mode of implantable vascular stents varies according to the final expanded diameter. While aortic stents, large diameter devices, are the most susceptible to corrosion that leads to degradation of mechanical integrity, coronary artery stents, small diameter and medium diameter stents, are prone to neointimal hyperplasia that leads to in-stent-restenosis. The vessel recoil and negative remodeling are not detected after stenting, different from balloon angioplasty[11]. Neointimal hyperplasia results from: (1) a foreign body response to the stent; and (2) a healing response to the injury caused by the stent implantation[12]. Factors that seem to influence the neointimal hyperplasia are genetic factors, local disease-related factors, stent delivery-related factors and stent-related factors.

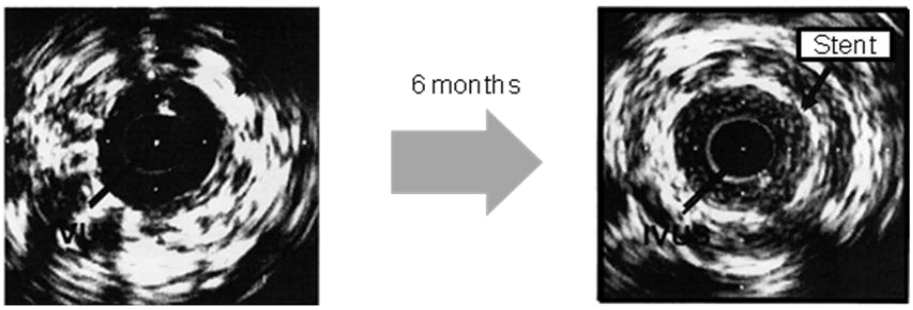

Figure 7. Diagram of in-stent-restenosis[13].

Examining it in more detail, this biological response consists of the following four phases[14].

① **Platelet Aggregation**: Immediately after stent placement, endothelial denudation and medial dissection are induced by the mechanical injury. This injury causes platelets aggregation and activation, initiating an inflammatory cascade.

② **Inflammatory Phase**: Over the next few days to weeks, a variety of inflammation-related cells gather at the injury site, secrete their own factors and induce the healing process.

③ **Proliferation Phase**: The inflammatory phase stimulates smooth muscle cells (SMCs) migration and proliferation. This is enabled by leukocytes cells releasing and activating tissue-digesting enzymes. SMCs migrate to the substrate for neointimal formation and thus form an overgrown, obstructing scar.

④ **Late Remodeling**: A neointimal layer is produced by proliferating SMCs and extracellular matrix. Inflammatory mediators and cellular elements contribute to trigger a complex event that modulates matrix production. As it develops, the blood flow is gradually reduced.

In-stent-restenosis has been the principal drawback of coronary angioplasty since its inception. It is commonly defined as lumen loss of over 50% caused following stent placement[15] (**Figure 8**). The in-stent-restenosis peaks at about the third month and reaches a plateau between the third and sixth months after stent implantation[16,17]. This complication occurs in about

20% of the procedures in a case of bare metal stent. In practice, out of 1 million patients who underwent stenting in 1999, in-stent-restenosis has occurred in about 250,000 patients[18]. Recently, after drug-eluting stents which effectively inhibit cellular proliferation were developed, the ratio of in-stent-restenosis was significantly reduced to less than 10%.

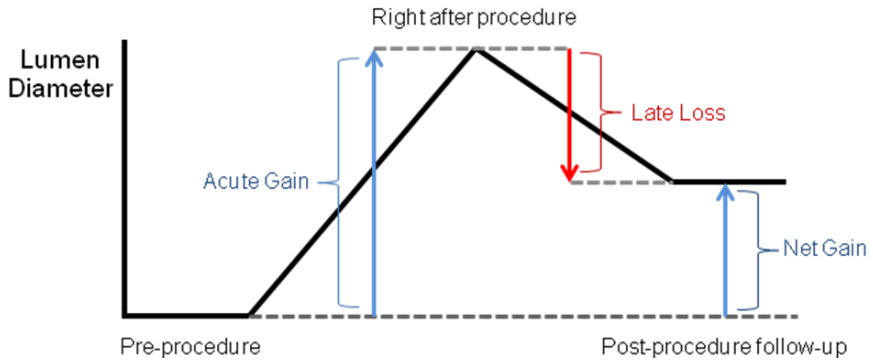

Figure 8. Conceptual graph of the lumen diameter loss through stenting.

I.4.2. Thrombosis

Thrombosis is the formation of a blood clot inside a blood vessel, which hampers the circulating flow of blood. When a blood vessel is injured, a blood clot is developed to prevent blood loss by using platelets and fibrin (**Figure 9**). Stent thrombosis is uncommon. However, it is serious and fatal because of its abruptness, whereas in-stent restenosis proceeds gradually.

All stents are foreign bodies in terms of the vessel wall and thus induce platelet adhesion and activation of the coagulation cascade. Furthermore, high-pressure implantation with noncompliant balloons leads to significant vascular injury, with exposure of thrombogenic molecules of the subintima and media to the bloodstream. As a result, potent platelet inhibition made the process feasible. However, the mechanism is not fully understood because it is complex and closely related the patient factors.

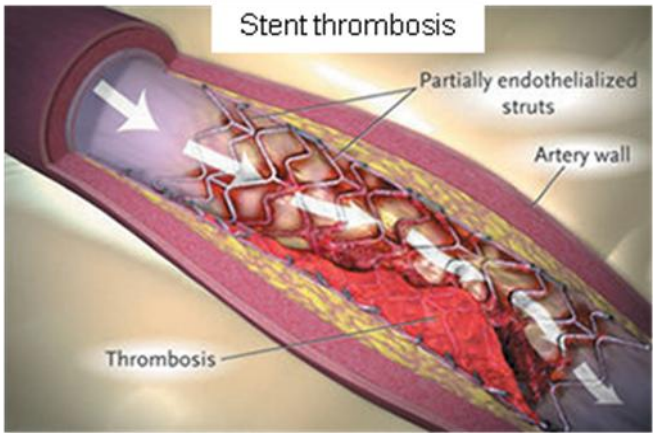

Figure 9. Diagram of stent thrombosis[19].

The advent of drug-eluting stent has largely solved the problem of restenosis[20,21,22,23,24]. However, thrombus problem still remains. Unfortunately, it is revealed that drug-eluting stent causes rapid total blockage of the artery more than bare metal stent, resulting in an acute myocardial infarction or even sudden death. Currently, the most significant issue in cardiology is about increased risks of late stent thrombosis when using drug-eluting stents[25].

A drug-eluting stent has successfully inhibited cell growth within the stented area. Drugs are responsible for preventing vascular smooth muscle cell proliferation and migration. As a result, they also impair re-endothelialization[26], as shown in **Figure 10**. The delayed vascular healing leaves the surface of the stent itself directly exposed to the blood flow for a very long period of time, a few months or years. When blood comes in direct contact with the surface of the stent, the clotting mechanism can be engaged, which can lead to thrombosis[27]. Therefore, after the interventions with drug-eluting stents, dual anti-platelet therapy combined with aspirin and clopidogrel should be continued for 12 months in order to reduce the risk of sudden thrombosis[28,29].

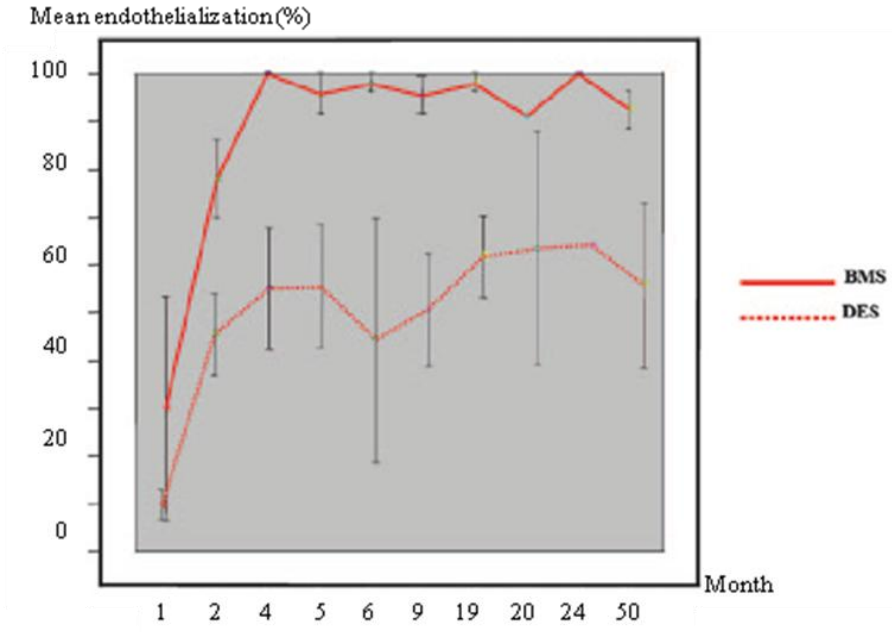

Figure 10. Comparison of re-endothelialization in BMS and DES[23].

Numerous reports have described the occurrence of acute (<1 day), subacute (<30 days), late (>30 days) and very late (>1 year) stent thrombosis after drug-eluting stent implantation[30]. Notably, many cardiologists have experienced very late stent thrombosis (~3 years after implantation and beyond) in a number of patients. It was not seen with bare metal stent. In a large analysis of >38,000 patients from 2 academic referral hospitals, anigiographically documented thrombosis was noted at 2.9% in drug-eluting stent. However, no patients with bare metal stent were included in this analysis[31].

I.4.3. Materials

Since stent's inception, 316L stainless steel has been widely used in developing coronary artery stents due to its good corrosion resistance and excellent mechanical property. Despite of these advantages, there are some problems derived from stainless steel such as low radio-opacity and surface bio-fouling. Therefore, new stent material to improve the performance has been consistently investigated.

Early in stent development, key characteristics were the ease with which a device could be tracked through to the target vessel and cross through lesions. These features were mainly affected by strut thickness, because thinner struts lead to more flexibility and reduce cross-sectional profiles. There was also a hypothesis that thinner struts would decrease restenosis rates. This led to the initial introduction of cobalt-chromium alloy-based stents. For example, Abbott developed Multi-Link Vision coronary stent, utilizing cobalt-chromium alloys. The L605 alloy (Co-20Cr-15W-10Ni) provided increased both of strength and X-ray attenuation than stainless steel, allowing for thinner struts[32]. The higher-strength alloys have also enabled novel stent designs such as the CoStar stent from Johnson & Johnson. It has its unique drug reservoirs within the stent struts[33]. This design would not have been possible with lower-strength materials. **Table 2** presents details of a series of coronary stents summarizing this trend through the use of higher-strength materials and composite structures.

Table 2. Strength and Strut Thickness for Stent Materials

Stent name	Material	0.2% Yield strength (MPa)	Strut thickness (㎛)
BX Velocity	316L SS	340	140
Express	316L SS	340	132
Driver	CoCr MP35N	415	91
Vision	CoCr L605	510	81

Recently, there has been significant interest in the field of biodegradable stents. The concept of biodegradable stent is that it works by restoring blood flow similar to a metallic stent, but then dissolves into the body, leaving behind a treated vessel. This is started from the fact that stent is indeed a foreign object within the vessel and thus its presence can be associated with the potential for inflammatory reactions, progressive neointimal formation and related thrombosis risks.

Several polymeric degradable stents have been extensively studied in clinical stage. For example, the BVS stent (Abbott, USA) is made from poly-L-lactic acid (PLLA). In the feasibility study from a very small patient population, the stent was only partially degraded at one-year follow-up[34]. This problem might be due to the long degradation times presumably to delay the rate at which any by-products are released. Igaki-Tamai stent (Kyoto Medical Planning, JP) showed that although some acute stent recoil occurred, follow-up practice at six months was satisfactory with initial hyperplasia[35]. It is comparable to bare metal stents. After 4 years, the stents were completely

degraded without further hyperplasia. In September 2012, the Abbott officially launched the world's first biodegradable stent across Europe and parts of Asia Pacific and Latin America, not including USA. However, despite of extensive researches, there is doubt that biodegradable stent will replace drug-eluting stent.

As another promising candidate, attention is paid to magnesium alloy stents. Magnesium has the advantage of corroding easily and being an essential element in the biological system. These make magnesium alloy a suitable material for biodegradable stent development. In the first animal study, the AE21 magnesium alloy that contained 2% aluminium and 1% rare earths (Ce, Pr, Nd) was utilized. Follow-up at 56 days showed strut material to be still alive and extrapolation suggested that it would have been fully degraded at 89 days[36]. This was much faster than expected and this rapidness is controversial today. Therefore, there is a desire to slow it down, ensuring that the scaffolding function of the stent remains for longer[37].

Table 3. Various Biodegradable Stents

Stent name	Company	Material
BVS	Abbott	Poly-lactic acid
IDEAL	Bioabsorbable Therapeutics	Polyanhydride ester
AMS	Biotronik	Magnesium alloy
REVA MR	REVE Medical	Tyrosine-derived polycarbonate

I.4.4. Surface Modification

Biological reactions are frequently considered to occur in a solution phase, for instance, as the reaction of a soluble enzyme with a substrate. In fact, however, most of the biological reactions occur, not in a solution but at the interfaces. The reactions around a stent are occurred at the surface as well.

Figure 11. Scanning electron microscopy (SEM) image of myoblast cell interacting with a synthetic surface[38].

When stents are placed in a coronary artery, their surfaces come into direct contact with host tissue or body fluid[39,40]. Its deployment causes vascular injury and the denudation of the endothelial layer. In addition, the stent surface itself can result in hypersensitivity reactions. These biological event cascades begin with platelet and leukocyte adsorption on stent surface, followed by smooth muscle cell migration, proliferation, production of extra cellular matrix, and finally formation of neointimal hyperplasia[41,42]. Therefore, the physicochemical properties of the stent surface can alter the clinical results. If the biological responses towards the implanted stent are unfavorable and not specific, the stent will be markedly disturbed to perform its

function[43,44,45,46,47]. From this point of view, proper surface modification is of great importance to overcome the stent-related problems.

In the early stage, a wide variety of inorganic coatings were explored to improve biocompatibility with its vascular environment. For example, gold coating was examined because gold is known to have little tissue reaction. However, gold-coated stainless steel stents have been associated with platelet activation and more neointimal formation. Kastrati, *et al.* revealed that thrombosis occurred in 2.5% of cases, and also restenosis in 49.7% of gold-coated stent patients[48]. These were considerably negative results, compared to 0.8% and 38.1% in the bare stainless steel stent group, respectively. In addition to this, silicon carbide coating was tried but did not show any significant improvement[49,50].

While inorganic coatings have limited success, polymer-based surface modification starts to be explored.

Heparin-coated stent was developed because heparin reduces platelet adhesion and coagulation. Some studies showed the favorable effects of heparin-coated Palmaz-Schatz stents in patients with both stable and unstable angina pectoris. However, in randomized trials of heparin-coated vs. uncoated Jostent (Jomed International AB, Sweden), stent thrombosis was not different between two groups (1.9% vs. 1.3%) and restenosis rates were also similar (33.1% vs. 30.3%)[51].

The interesting approach for surface modification was the use of phosphorylcholine (PC)-based coating to mimic the phospholipids on the outer membrane of red blood cells[52]. This coating is biocompatible and non-allergic and also elicits less adverse inflammatory response. However, it also

shows no better clinical results than bare stainless steel stents, when used on the BiodivYsio stent (Biocompatibles, UK). While safety and reduced thrombogenicity was demonstrated, the benefit in terms of restenosis rates was not evident[53]. This coating technology has been used as a drug reservoir for drug-eluting stent, as shown in **Figure 12**[54].

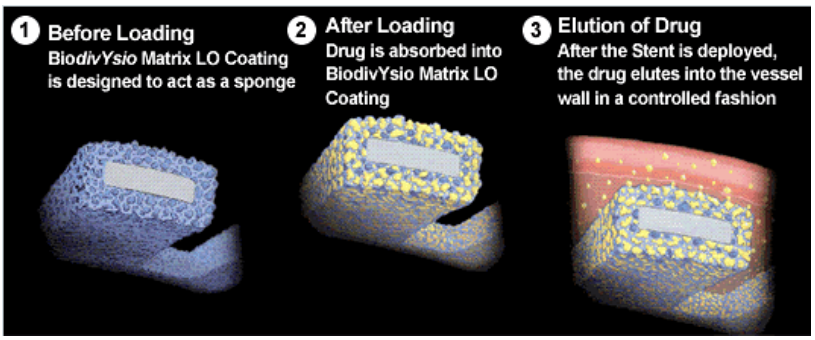

Figure 12. Phosphorylcholine-coated stent system of Biocompatibles.
Source: Biocompatibles website (www.biocompatibles.com)

Recently, a mussel adhesive protein-inspired polydopamine (PDAM) coating was suggested as another biomimetic approach. This features the cellular specificity, different from previous bio-inert surface coating. Yang, *et al*. investigated the polydopamine-based surface modification on stainless steel stents and the response of cells of the blood vessel wall, endothelial cell, and smooth muscle cell[55]. They found that the PDAM-modified surface remarkably enhanced endothelial cell adhesion, proliferation, and migration, release of nitric oxide, and secretion of prostaglandin I_2. On the other hand, the adhesion and proliferation of smooth muscle cell was inhibited on this surface. It is expected that PDAM coating technology may be able to address issues related with restenosis and thrombosis. However, clinical performance for human and animal was not yet tested.

I.4.5. Drug-eluting Stent

Since the late 1990's technologically innovative efforts have been paid to develop drug-eluting stent (DES) with improved performances. It is coated with a pharmacological drug, which allows drug elution into the vessel wall for a couple of weeks after stent implantation. **Table 4** summarizes a variety of conventional drug-eluting stents.

Table 4. Classification of Drug-eluting Stents

Type	Drug	Way of Action
Anti-coagulants	Heparin	Anti-thrombotic and possibly direct inhibition of SMC proliferation
Anti-platelet	Sodium nitroprusside	NO donor
	Abciximab	BP IIb/IIIa inhibitor
Anti-proliferation	Angiopeptin	Inhibitor of SMC proliferation
	Paclitaxel	Microtubular inhibitor
	Dexamethasone	Anti-inflammation
Immunosuppressant	Sirolimus(Rapamycin)	Immunosuppressant and anti-proliferative
	Everolimus	Immunosuppressant and anti-proliferative

In 2002-2003, the field of interventional cardiology entered a new era with the advent of the first drug-eluting stent. These stents were quickly embraced by cardiologists, because it has dramatically reduced the incidence of restenosis.

Each drug-eluting stent comprises three components: stent platform, the active drug, and a drug carrier matrix which can control release kinetics. For example, the sirolimus-eluting Cypher stent (Johnson & Johnson, USA) consists of a stainless steel platform coated with a permanent polymer (polyethylene-co-vinyl acetate [PEVA] and poly-n-butyl methacrylate [PBMA]) containing sirolimus 140 mcg/cm^2, 80% of which is released in 30 days[56]. Sirolimus is known to be a naturally occurring macrolide, a potent immunosuppressant. It binds to FK506-binding protein 12 (FKBP 12) and subsequently the mammalian target of rapamycin (mTOR) and eventually blocks the cell cycle, inhibiting the transition from the G1 to S phase[57]. It leads to prevention of smooth muscle cell migration and proliferation as shown in **Figure 13**. The paclitaxel-eluting Taxus stent (Boston Scientific, USA) also incorporates a stainless steel platform with a robust polymer coating (polystyrene-b-isubutylene-b-styrene [SIBS]) combined with 1 mcg/mm^2 paclitaxel[58]. The release profile is biphasic, with a 48 hr early burst followed by low-level release for 2 weeks[59]. Paclitaxel is an antimitotic microtubule inhibitor, which suppresses cell division in the G0/G1 and G2/M phases, resulting in disruption of smooth muscle cell migration and proliferation. The everolimus-eluting Xience V stent (Abbott, USA) is made of a cobalt-chrome platform with a synthetic polymer (poly-n-butyl-methacrylate [PBMA] and polyvinylidenefluoro-hexafluoropropylene [PVDF-HFP]) and 100 mcg/cm^2 everolimus, an analogue of sirolimus[60]. The zotarolimus-eluting Endeavor stent (Medtronic, USA) is also cobalt-chrome platform loaded with a polymerized phosphorylcholine and a zotarolimus, an

analogue of sirolimus[61,62,63].

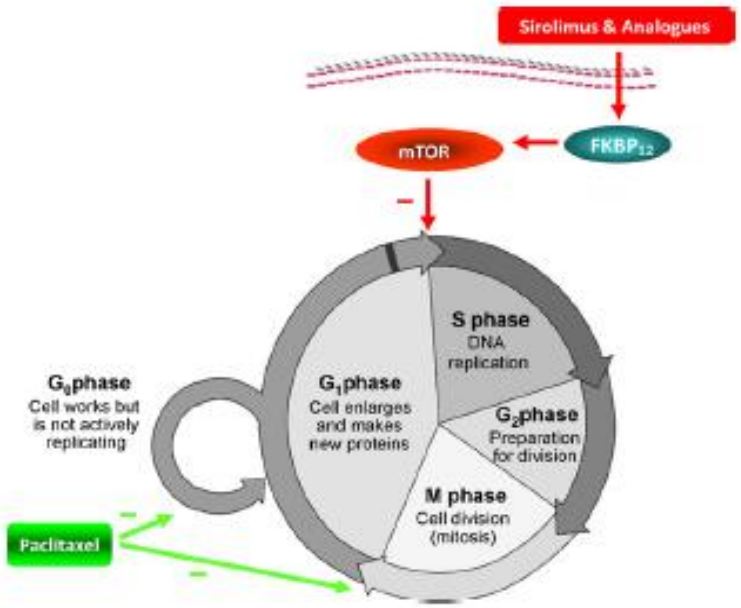

Figure 13. Effects of sirolimus and paclitaxel on the cell cycle[64].

Despite the beneficial effects of drug-eluting stent on restenosis and repeat revascularization, as I mentioned in I.4.2., worrisome data on late stent thrombosis after drug-eluting stent implantation have recently emerged. Antiproliferative drugs, eluted from the stents, interfere with the natural vascular healing process and delay endothelial coverage over the stenting area due to its own cytotoxicity, thereby inducing stent thrombosis[65,66].

Therefore, a wide variety of research including new drug, new coating, and new concept are proceeding. An alternative approach to concentrate on natural healing has been investigated as opposed concept to drug-eluting stent. It is the Endothelial Progenitor Cell (EPC)-capturing stent[67,68,69].

I.5. EPC-capturing Stent

The EPC-capturing stent is an innovative solution that uses the Endothelial Progenitor Cell (EPC) ability to migrate to injured arterial segments for healing. EPC is an immature cell originated from the bone marrow. Its character was initially suggested in 1997 by Asahara, *et al*[70]. EPC is capable of migrating, proliferating and differentiating into endothelial cells. Since the discovery of EPC, several studies have demonstrated that EPCs play an essential role in postnatal vasculogenesis as well as in the vascular repair process[71,72].

The EPC-capturing stent consists of metal stent platform, polymer matrix, and EPC-capturing ligand such as antibody and aptamer. The major difference between EPC-capturing stent and drug-eluting stent is the feature of loaded molecules and their coupling method. The ligand of EPC-capturing stent should not be released, on the contrary to drug-eluting stent.

As soon as stent is inserted, EPC-specific targets on the stent will attract circulating EPCs, which are expected to develop into mature functional endothelium (**Figure 14**). This healing-based strategy aims to lower the risk of restenosis and stent thrombosis, as well as obviate prolonged dual antiplatelet therapy, altogether. Many researchers and cardiologists evaluate this EPC-capturing stent as a fascinating approach to rapidly create an *in vivo* endothelialization on the stented sites[73,74]. However, its effectiveness, compared with bare metal stents and drug-eluting stents, could not be ascertained owing to rare commercialization and unsatisfactory clinical data.

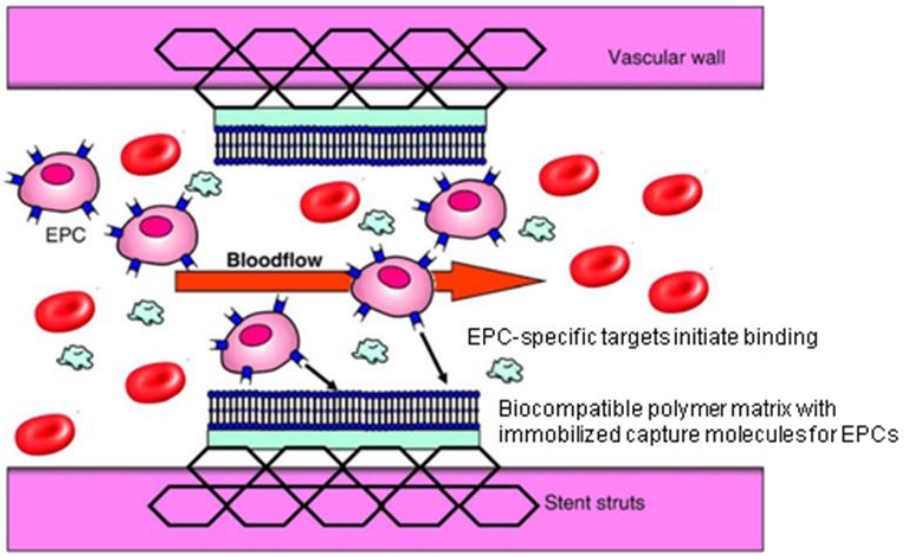

Figure 14. Schematic representation of EPC-capturing stent[75].

OrbusNeich commercialized EPC-capturing stent, bio-engineered Genous R stent™, for the first time in the world (**Figure 15**). According to OrbusNeich's patents, Genous R stent consists of polymer matrix and anti-CD34-antibody. The matrix may be composed of polyurethane, cellulose, collagen, and so on. The stent surface is coated by dipping or spraying with a liquid solution of the matrix and its thickness is less than 100 μm[76].

Unlike drug-eluting stents, late stent thrombosis does not seem to be a concern for this stent, despite short treatment with just 1-month dual anti-platelet therapy. Several single-arm clinical studies revealed that Genous R stent was safe and feasible for the treatment of coronary artery disease[77]. On the other hand, the late lumen loss results with this stent appear to be similar to the conventional bare metal stent and worse than the drug-eluting stent. For example, recently, 2 years follow-up randomized controlled study compared Genous R stent with paclitaxel-eluting stent. In this study from patients with

high risk lesion of restenosis, the Genous R stent demonstrated not only higher late lumen loss at 12 month (1.14 ± 0.64 mm vs. 0.55 ± 0.61 mm) but also higher rates of target vessel failure (20.4% vs. 15.8%) than paclitaxel-eluting stent[78,79]. Furthermore, disappointing results were continually reported by other randomized controlled study where Genous R stent was compared with bare cobalt-chrome stent in the treatment of acute ST-elevation myocardial infarction. In this trial, the rate of major adverse cardiac events and target lesion revascularization at 6 month was much higher for Genous R stent group (24% vs. 10%). The stent thrombosis rate at 6 month also came to 6% in Genous R stent group, while 0% in bare cobalt-chrome stent group[80].

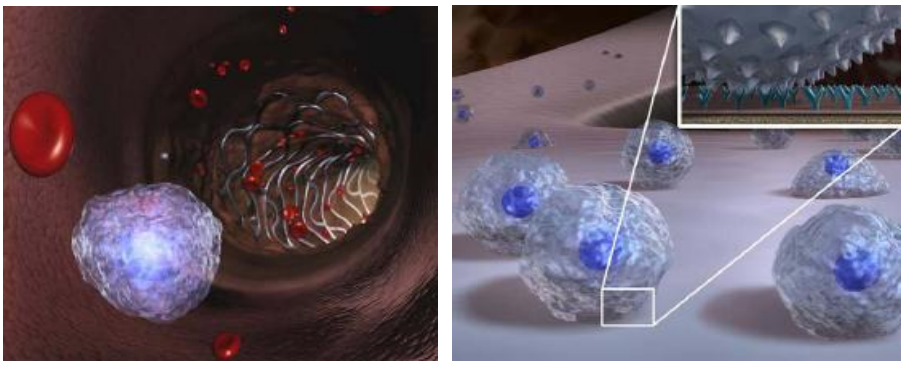

(a) (b)

Figure 15. Depiction of EPC capture onto the Genous R stent surface;
(a) EPCs and platelets approaching the implanted stent,
(b) EPCs captured by anti-CD34 antibody on the stent.
Source: OrbusNeich website (www.orbusneich.com)

Therefore, doubts about the success of the Genous R stent have been raised. Many researchers have pointed out the poor specificity of Genous R stent surface, especially anti-CD34 antibody. As only 0.4 ± 0.2% out of CD34-positive population is EPC, CD34-positive cells are able to differentiate into various kinds of cells such as smooth muscle cells, monocytes, and macrophages in addition to endothelial cells. Even platelet is able to express CD34[81]. In spite of the brilliant concept, the commercialized EPC-capturing stent has not solved both of restenosis and thrombosis, definitely (**Figure 16)**. This field needs much more technological improvements[82,83].

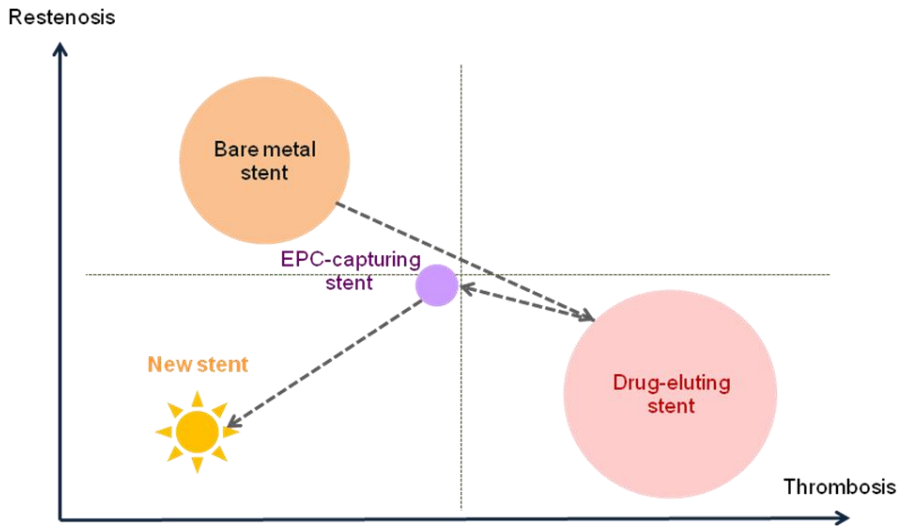

Figure 16. Current status of stent technology; the area of the each circle is proportional to its market size.

I.6. Research Objectives

In order to develop new EPC-capturing stent, it is critically important to endow the stent surface with high EPC specifity. For this, specific EPC-capture ligand and sophisticated coating technology are required. Unfortunately, compared to other materials such as titanium[84,85], gold[86,87], and silicon[88,89,90], research on the surface modification of stainless steel is rare, because it is difficult to functionalize its surface.

Firstly, we analyzed the influence of the surface roughness and hydrophilicity to protein adsorption, because protein adsorption on the stent surface is the first event of bio-fouling when stenting. An electropolishing method was employed to control the surface roughness. As electropolishing is a non-contact and simple method, it is compatible with sophisticated stents than other mechanical treatments. To control the surface hydrophilicity/hydrophobicity, various polymers such as hydrophilic poly(ethylene glycol) (PEG), meta-hydrophilic poly(tetrahydrofuran) (PTG), meta-hydrophilic poly(propylene glycol) (PPG) and hydrophobic poly(dimethylsiloxane) (PDMS) were grafted. Following these surface modifications, we investigated the dependency of surface properties on protein adsorption by the fluorescence-tagged fibrinogen assay.

Based on this correlation study between surface properties and protein adsorption, we tried to fabricate EPC-capturing stent that can selectively interact with EPC at the stent/biological interface. For the robustness of surface modification, silanization and polymer 'grafting-to' method was utilized. To covalently bridge dissimilar materials such as a stainless steel stent and a polymer, stent surface was previously silanized[91]. Then, we grafted

hydrophilic poly(ethylene glycol) (PEG) polymer onto the silanized stainless steel stent surface to prevent non-specific biological interactions. After this, the anti-vascular endothelial-cadherin (VE-cadherin) antibody[92] was coupled to the polymer-grafted stent. We chose this ligand, because VE-cadherin is specifically expressed at the surface of late EPCs and fulfills important functions such as cellular proliferation and intracellular signaling[93].

To demonstrate biological specificity, the EPC and THP-1 (human acute monocytic leukemia cell line) adsorption assay were simultaneously conducted for bare metal stent (BMS) and our EPC-capturing stent. The proliferation of EPCs on the fully surface-modified stent was also investigated to confirm the immediate re-endothelialization after capturing EPCs. Furthermore, through a comparative paired rabbit's iliac artery stenting surgery, we evaluated whether our EPC-capturing stent might accelerate endothlialization and reduce neointimal formation, based on the EPC specificity at the surface. Concurrently, histomorphometic and immunohistochemical analyses were performed as well.

II. Experiments

II.1. General

II.1.1. Materials

AISI type 316L stainless steel plates with a thickness of 500 μm were purchased from Goodfellow Ltd. of Cambridge, UK. All the plates were cleaned ultrasonically for 10 min in distilled water and acetone. Then, the stainless steel plates were cut into rectangles, 10 mm × 15 mm in size.

316L stainless steel stents were purchased from Humed, Korea. The diameter and the length of stents were 3 mm and 15 mm, respectively. The design was wave-like cell pattern as shown in **Figure 17**. All stents were electropolished in advance and cleaned ultrasonically for 10 min in distilled water and acetone.

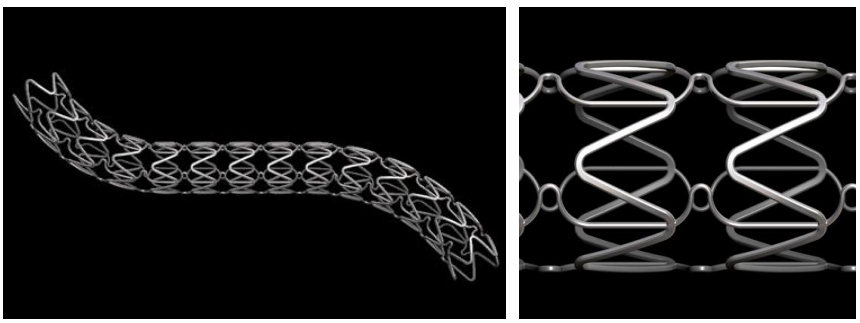

Figure 17. Design of the Humed stent.
Source: Humed website (www.humed.co.kr)

3-Glycidoxypropyltrimethoxysilane (GPTS), *N*,*N*-diisopropylethylamine (DIEA), 4-*N*,*N*-dimethylaminopyridine (DMAP) and fluorescein isothiocyanate (FITC) were obtained from Aldrich and used as received. Succinic anhydride (SA) and *N*-hydroxysuccinimide (NHS) were purchased from Fluka. *O*,*O*'-Bis(aminopropyl)polyethylene glycol (PEG, Mn=1,500 g/mol) was purchased from Fluka and the other polymers, polypropylene glycol bis(2-aminopropyl ether) (PPG, Mn=2,000 g/mol), polytetrahydrofuran bis(3-aminopropyl) terminated (PTG, Mn=1,100 g/mol), polydimethylsiloxane bis(3-aminopropyl) terminated (PDMS, Mn=2,500 g/mol) were purchased from Aldrich. *N*,*N*'-diisopropylcarbodiimide (DIC) was purchased from TCI. All other chemicals were analytical grades and used without purification. Tetramethylrhodamine protein labeling kit was purchased from Molecular Probe and human plasma fibrinogen was obtained from Sigma. Mouse monoclonal antibodies, RAM 11 and PCNA, were purchased as a commercial product from Dako and Santa Cruz Biotech, respectively.

II.1.2. Instruments

Static water contact angle goniometry (SEO, Phoenix 300), AFM (NanoScope IIIa, Digital Instrument), AES (Scanning Auger Nanoprobe PHI-700, Ulvac Inc.), FE-SEM (JSM-6700F, JEOL), EDX(JSM-6700F, JEOL), and CLSM (LSM 5 Pascal, Zeiss) were used for surface characterization and biological assay of stainless steel plates as well as stents.

Contact Angle Goniometry

Static contact angle was measured on sessile drops by taking the tangent to the drop on various stainless steel surfaces. This was measured only with stainless steel plates, because it is impossible to calculate the angle on the stent struts. Prior to contact angle measurement, each stainless steel plate was fully dried in a vacuum oven for at least 24 hr to exclude the effect of the washing solvent. Five contact angle measurements were performed within 30 sec after drop formation, and the results were averaged.

Atomic Force Microscopy (AFM)

The bare, silanized and polymer-grafted stainless steel plates and stents were imaged by AFM with tapping mode to detect changes in surface topography as surface modification reactions proceeded. Concurrently, the surface micro-roughness was quantified for each surface-modified sample. Micro-roughness analysis was performed at three random sites and the analyzed data were averaged. The scale of scanning images was 5 μm × 5 μm and the z value was 100 nm.

Auger Electron Spectroscopy (AES)

Instead of X-ray photoelectron spectroscopy, AES was employed for the sophisticated stent characterization due to its high spatial resolution. AES data were recorded using an electron beam source run at 5 kV and 10 nA. The spectra data were collected at take-off angles of 30°. The atomic ratios were quantitatively determined from each peak area with the corresponding elemental sensitivity factor. With focused ion etching, the depth profiles of the bare, silanized, and polymer-grafted stent surfaces were obtained for the

elemental types C, Si, Fe, and Cr, as they are the essential components for each sample.

Field Emission-Scanning Electron Microscopy (FE-SEM)

The morphology of the polymer-grafted and the antibody-conjugated stent surface was observed on a FE-SEM and comparatively analyzed to confirm whether the antibody was immobilized on the polymer layers. In addition to this, the endothelialization on the surface-modified stent was observed in detail by FE-SEM.

Energy Dispersive X-ray spectrometer (EDX)

Concurrently with FE-SEM imaging, elemental spectra were recorded on EDX profiles for the polymer-grafted and the antibody-conjugated stent. The atomic ratio of C, O, Fe, and Cr were calculated after normalization. The other compositions such as Na, Cl, and Ni are not included as they exist in trace amount. Measurement of each spectrum was repeated at three times and averaged.

Confocal Laser Scanning Microscopy (CLSM)

The fibrinogen adsorption on the stainless steel plates was analyzed by CLSM, after rhodamine tagging. The scale of the detection images was 930 μm × 930 μm and the detected fluorescence intensity was averaged. The amine group of the polymer-grafted stent surface was detected by CLSM after FITC conjugation.

II.2. Biocompatibility Study

II.2.1. Electropolishing

To smoothen stainless steel plates in an electrolytic bath, a glass container (250 mL) was prepared. The stainless steel sample was linked to an anode and a stainless steel reference was linked to a cathode. The distance between the sample and the reference was 10 mm. In terms of the electrolyte conditions, we chose a solution of phosphoric acid, glycerol and water (34:47:19, weight %). The electropolishing time and current are 3 min and 1 A/cm^2, respectively. The settings of these two parameters are critical for obtaining consistent surface roughness. The electropolished stainless steel was rinsed copiously with deionized water and acetone.

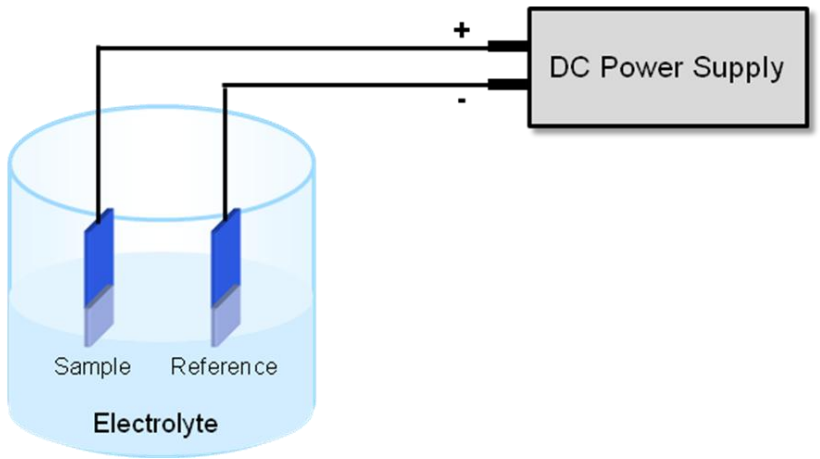

Figure 18. Diagram of electropolishing system.

II.2.2. Acid Treatment

The stainless steel plates were acid-treated using piranha solution composed of H_2SO_4 and H_2O_2 (4:1, v/v) for 1 hr to remove any contaminants and to expose the reactive hydroxyl groups on the surface. The acid-treated stainless steels were cleaned by ultrasonication in deionized water, ethanol and acetone for 10 min in a sequential manner, followed by nitrogen blowing and used for silanization, immediately.

II.2.3. Silanization

Silanization of acid-treated stainless steel plates was performed with epoxy-functionalized silane (GPTS) in a 10% (v/v) GPTS/toluene solution at 55 °C for 48 hr. After the coupling reaction, ultrasonication in toluene and MC was performed for 5 min (×2) each to eliminate the non-covalently adsorbed silane compounds. The silanized plates were then dried gently under a nitrogen gas stream and thermally cured in an oven at 70 °C for 3 hr. Prior to curing, purified argon gas was purged into the stainless steel plates containing vials to exclude the possibility of air oxidation.

II.2.4. Polymer Grafting

To control the hydrophilicity/hydrophobicity of stainless steel surface, four kinds of polymers were grafted; hydrophilic poly(ethylene glycol) (PEG), meta-hydrophilic poly(tetrahydrofuran) (PTG), meta-hydrophilic poly(propylene glycol) (PPG) and hydrophobic poly(dimethylsiloxane) (PDMS).

As all the polymers contained diamino group, the epoxy-functionalized stainless steel surface could be reacted straightforwardly with these polymers in a basic condition. The grafting of the PEG, PTG, PPG polymers was carried out in a 10 mM of NMP solution, with 6 equivalent of DIEA. In the case of PDMS grafting, the same protocol was used, but toluene instead NMP was used as a solvent. Polymer grafting process was performed in a shaking incubator at 50 °C for 24 hr. After this, to eliminate any ungrafted polymers, ultrasonication was carried out in the grafting solvent and MC for 5 min (×2), respectively. The polymer-grafted stainless steels were dried gently by nitrogen purge and then stored in a vacuum oven until required.

II.2.5. Fibrinogen Adsorption Assay

Prior to protein adsorption, the aminated polymer-grafted stainless steel surfaces were capped by acetylation, in order to exclude any electrostatic interaction between the amino groups on the stainless steel surface and the proteins. Anhydrous MC (20 mL) and acetic anhydride (2 mL) were mixed,

and then 4-*N*,*N*-dimethylaminopyridine (DMAP) (1.0 mg) was added to the solution. The polymer-grafted stainless steel plates were incubated in the capping solution at 30 °C for 24 hr. After the capping, each sample was ultrasonicated for 5 min (×2) in MC and dried by nitrogen.

We used a fluorescence detection method to quantify the amount of adsorbed fibrinogen, due to its simplicity and high sensitivity. For fluorescence detection, rhodamine succinimidyl ester was coupled to the fibrinogen via protein labeling kit protocol. The degree of labeling of the fluorescence dye was estimated to be 4-5 molecules per fibrinogen.

Rhodamine-tagged human plasma fibrinogen was dissolved in a 50 mM phosphate buffer (pH=7.4) to provide a final concentration of 0.5 mg/mL. For all of the surface-modified stainless steel plates, fibrinogen adsorption was allowed to proceed in a shaking incubator for 2 hr at 37 °C. Upon completion of a fibrinogen adsorption, all of the stainless steel samples were thoroughly rinsed with phosphate buffer (×10) to remove any non-adsorbed proteins. Subsequently, they were washed with copious deionized water (×5) to remove the buffer salts. The final samples were dried gently with nitrogen gas and immediately analyzed by means of CLSM.

II.3. Preparation of EPC-capturing Stent

II.3.1. Acid Treatment

All stents were previously electropolished by supplier, Humed. The electropolished stainless steel stents were acid-treated using a piranha solution composed of H_2SO_4 and H_2O_2 (4:1, v/v) for 1 hr to remove any contaminants and expose the reactive hydroxyl groups on their surface. The acid-treated stents were ultrasonically cleaned in deionized water, ethanol and acetone for 10 min in a sequential manner, followed by drying with a nitrogen stream, and then immediately subjected to silanization.

II.3.2. Silanization

The acid-treated stents were silanized with epoxy-functionalized silane (GPTS) in a 10% (v/v) GPTS/toluene solution at 55 °C for 48 hr. Subsequently, ultrasonication in toluene and MC was performed for 5 min (×2) to eliminate the non-covalently adsorbed silane compounds. The silanized stents were then dried gently under a nitrogen gas stream and thermally cured in an oven at 70 °C for 3 hr. Prior to curing, purified argon gas was purged into the stents containing vials to exclude the possibility of air oxidation.

II.3.3. Polymer Grafting onto the Silanized Stent

PEG Grafting

PEG grafting was carried out on the epoxy-silanized stent surface in a 10 mM Jeffamine® 1500/NMP solution, into which six equivalents of DIEA to Jeffamine® were added. Because the used Jeffamine® contained two amino groups, the epoxy-functionalized stainless steel surface could be reacted straightforwardly with Jeffamine® under basic conditions. Polymer grafting proceeded in a shaking incubator at 50 °C for 24 hr. Ultasonication was carried out sequentially in NMP and MC for 5 min (×2) to eliminate the ungrafted polymer. The resulting stainless steel stent was dried gently under a nitrogen gas stream and stored in a vacuum oven until required.

Detection of Functional Groups on the Stent

The stainless steel stents were amine-terminated as a result of PEG grafting, because the PEG contained two amino groups. Thus, fluorescein isothiocyanate (FITC) was reacted with the aminated surface and the resulting FITC-coupled stent surface showed stronger fluorescence than the bare metal stent surface. FITC coupling reactions on the bare and polymer-grafted stent surface were performed in a 4 mM FITC/NMP solution at 30 °C for 1 hr. After this, the two types of stents were ultrasonicated for 10 min in NMP and MC, sequentially, to remove physically-adsorbed FITC, and then fluorescence intensity was measured immediately by means of confocal laser scanning microscope (**Scheme 1**).

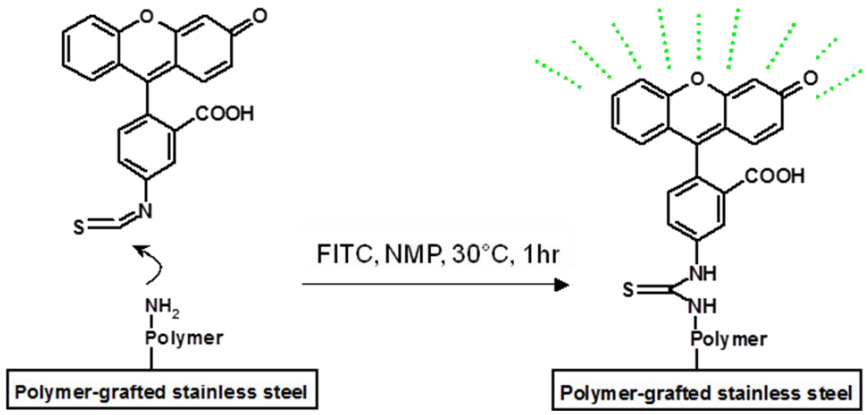

Scheme 1. Fluorescein probe (FITC) conjugation to the aminated stainless steel surface.

II.3.4. Antibody Immobilization on the PEG-grafted Stent

Antibody Production

Since large amounts of antibodies were necessary to make the antibody-coated stents, we requested an antibody-manufacturing specialty company (AbFrontier, Korea) to produce our antibody. We chose an extracellular domain of human VE-cadherin protein as the antigen for the antibody production, instead of VE-cadherin whole protein. DNA sequence of the antigen was cloned in circular form, which was transfected to *Escherichia. Coli (E. coli)*. After the purification, VE-cadherin injected into rabbits, host, for immunization. After 10 weeks, rabbits were harvested and polyclonal anti-human VE-cadherin antibodies were isolated from the rabbit serum by protein A/G column and antigen-specific affinity chromatography.

```
   1 ATGCAGAGGC TCATGATGCT CCTCGCCACA TCGGGCGCCT GCCTGGGCCT GCTGGCAGTG
  61 GCAGCAGTGG CAGCAGCAGG TGCTAACCCT GCCCAACGGG ACACCCACAG CCTGCTGCCC
 121 ACCCACCGGC GCCAAAAGAG AGATTGGATT TGGAACCAGA TGCACATTGA TGAAGAGAAA
 181 AACACCTCAC TTCCCCATCA TGTAGGCAAG ATCAAGTCAA GCGTGAGTCG CAAGAATGCC
 241 AAGTACCTGC TCAAAGGAGA ATATGTGGGC AAGGTCTTCC GGGTCGATGC AGAGACAGGA
 301 GACGTGTTCG CCATTGAGAG GCTGGACCGG GAGAATATCT CAGAGTACCA CCTCACTGCT
 361 GTCATTGTGG ACAAGGACAC TGGCGAAAAC CTGGAGACTC CTTCCAGCTT CACCATCAAA
 421 GTTCATGACG TGAACGACAA CTGGCCTGTG TTCACGCATC GGTTGTTCAA TGCGTCCGTG
 481 CCTGAGTCGT CGGCTGTGGG GACCTCAGTC ATCTCTGTGA CAGCAGTGGA TGCAGACGAC
 541 CCCACTGTGG GAGACCACGC CTCTGTCATG TACCAAATCC TGAAGGGGAA AGAGTATTTT
 601 GCCATCGATA ATTCTGGACG TATTATCACA ATAACGAAAA GCTTGGACCG AGAGAAGCAG
 661 GCCAGGTATG AGATCGTGGT GGAAGCGCGA GATGCCCAGG GCCTCCGGGG GGACTCGGGC
 721 ACGGCCACCG TGCTGGTCAC TCTGCAAGAC ATCAATGACA ACTTCCCCTT CTTCACCCAG
 781 ACCAAGTACA CATTTGTCGT GCCTGAAGAC ACCCGTGTGG GCACCTCTGT GGGCTCTCTG
 841 TTTGTTGAGG ACCCAGATGA GCCCCAGAAC CGGATGACCA AGTACAGCAT CTTGCGGGGC
 901 GACTACCAGG ACGCTTTCAC CATTGAGACA AACCCCGCCC ACAACGAGGG CATCATCAAG
 961 CCCATGAAGC CTCTGGATTA TGAATACATC CAGCAATACA GCTTCATCGT CGAGGCCACA
1021 GACCCCACCA TCGACCTCCG ATACATGAGC CCTCCCGCGG GAAACAGAGC CCAGGTCATT
1081 ATCAACATCA CAGATGTGGA CGAGCCCCCC ATTTTCCAGC AGCCTTTCTA CCACTTCCAG
1141 CTGAAGGAAA ACCAGAAGAA GCCTCTGATT GGCACAGTGC TGGCCATGGA CCCTGATGCG
1201 GCTAGGCATA GCATTGGATA CTCCATCCGC AGGACCAGTG ACAAGGGCCA GTTCTTCCGA
1261 GTCACAAAAA AGGGGGACAT TTACAATGAG AAAGAACTGG ACAGAGAAGT CTACCCCTGG
1321 TATAACCTGA CTGTGGAGGC CAAAGAACTG GATTCCACTG GAACCCCCAC AGGAAAAGAA
1381 TCCATTGTGC AAGTCCACAT TGAAGTTTTG GATGAGAATG ACAATGCCCC GGAGTTTGCC
1441 AAGCCCTACC AGCCCAAAGT GTGTGAGAAC GCTGTCCATG GCCAGCTGGT CCTGCAGATC
1501 TCCGCAATAG ACAAGGACAT AACACCACGA AACGTGAAGT TCAAATTCAT CTTGAATACT
1561 GAGAACAACT TTACCCTCAC GGATAATCAC GATAACACGG CCAACATCAC AGTCAAGTAT
1621 GGGCAGTTTG ACCGGGAGCA TACCAAGGTC CACTTCCTAC CCGTGGTCAT CTCAGACAAT
1681 GGGATGCCAA GTCGCACGGG CACCAGCACG CTGACCGTGG CCGTGTGCAA GTGCAACGAG
1741 CAGGGCGAGT TCACCTTCTG CGAGGATATG GCCGCCCAGG TGGGCGTGAG CATCCAGGCA
1801 GTGGTAGCCA TCTTACTCTG CATCCTCACC ATCACAGTGA TCACCCTGCT CATCTTCCTG
1861 CGGCGGCGGC TCCGGAAGCA GGCCCGCGCG CACGGCAAGA GCGTGCCGGA GATCCACGAG
1921 CAGCTGGTCA CCTACGACGA GGAGGGCGGC GGCGAGATGG ACACCACCAG CTACGATGTG
1981 TCGGTGCTCA ACTCGGTGCG CCGCGGCGGG GCCAAGCCCC CGCGGCCCGC GCTGGACGCC
2041 CGGCCTTCCC TCTATGCGCA GGTGCAGAAG CCACCGAGGC ACGCGCCTGG GGCACACGGA
2101 GGGCCCGGGG AGATGGCAGC CATGATCGAG GTGAAGAAGG ACGAGGCGGA CCACGACGGC
2161 GACGGCCCCC CCTACGACAC GCTGCACATC TACGGCTACG AGGGCTCCGA GTCCATAGCC
2221 GAGTCCCTCA GCTCCCTGGG CACCGACTCA TCCGACTCTG ACGTGGATTA CGACTTCCTT
2281 AACGACTGGG GACCCAGGTT TAAGATGCTG GCTGAGCTGT ACGGCTCGGA CCCCCGGGAG
2341 GAGCTGCTGT ATTAG
```

Figure 19. Nucleotide sequence of VE-cadherin. Extracelluar domain of VE-cadherin was presented in red character.

Antibody Immobilization

The exposed amine groups on the stent were changed to carboxylic groups by succinylation to covalently couple the anti-VE-cadherin antibody. A mixture of succinic anhydride (10 mM) and *N,N'*-diisopropylethylamine (20

mM) in NMP (3 mL) was reacted to the amino groups of PEG on the stent for 3 hr at room temperature. After the succinylation, the stent was washed by unltrasonication in NMP and MC for 5 min (×2), and then fully dried with nitrogen gas. In the following step, we activated the carboxyl groups *via* coupling with *N*-hydroxysuccinimide (NHS) (20 mM) by *N,N'*-diisopropylcarbodiimide (DIC) (10 mM) in DMF (3 mL) for 2 hr at room temperature. This was also washed by ultrasonication in DMF and MC for 5 min (×2) each, and then dried with nitrogen gas blowing.

Right after the surface activation, anti-VE-cadherin antibody (100 ug/mL) in phosphate buffered saline (pH=7.4) was straightforwardly immobilized on the surface-activated stents for 24 hr at room temperature. Ultrasonication was carried out in phosphate buffer (pH=7.4) and deionized water for 5 min (×2) to eliminate uncoupled antibody.

Detection of Antibody on the Stent

To analyze the antibody-conjugated surface after stent deployment, stents were mounted onto a delivery catheter, passed through a guiding catheter, and subsequently expanded in phosphate-buffered saline. Then, we performed immunofluorescent staining of anti-VE-cadherin antibodies with anti-rabbit IgG antibodies (1:500, Alexa Fluor 555 Conjugate, Cell Signaling Technology, UK) to confirm the antibody coating on the stent surface. Additionally, after full expansion of the stents, SEM images were pictured to evaluate the integrity of antibody-coated surface at macro level.

II.4. Biological Characterization of EPC-capturing Stent

II.4.1. Human EPC Culture

All experiments dealing with humans or human products were performed with informed consent and approved by the Institutional Review Board of Seoul National University Hospital. Peripheral blood (50 mL) was obtained from healthy donors with informed consent.

The mononuclear cells were fractionated from other components of peripheral blood by centrifugation on Histopaque 1077 (Sigma, St. Louis, MO) gradients according to the manufacturer's instructions. The isolated mononuclear cells were resuspended in the EGM-2 Bullet Kit system (EGM-2 MV, Clonetics, San Diego, CA, USA) consisting of endothelial basal medium, vascular endothelial growth factor, human endothelial growth factor, human fibroblast growth factor-B, insulin-like growth factor-1, ascorbic acid, heparin, and 5% fetal bovine serum. Mononuclear cells were seeded at a density of 1×10^7 per well on 2% gelatin-coated six-well plates and incubated in a humidified 5% CO_2 incubator at 37℃. First media was changed approximately 6 days after plating and thereafter every 3 days. Late authentic EPC appeared at least 2 weeks after plating as colonies that consisted of cells with different morphology appeared from early myeloid EPCs. In this experiment, we used late EPC grown to confluence that showed a cobblestone-like monolayer.

II.4.2. *In vitro* Assay for EPC-capture and Endothelialization

Head to Head Comparison for EPC Specificity

The EPC specificity of our surface-modified stents was evaluated with a EPC-capturing assay and the result was compared with that of BMS. We harvested late EPC grown to confluence and labeled them with carboxyfluorescein succinimidyl ester (CFSE, 1:500, Sigma-Aldrich) as instructed by the manufacturer.

Late EPC suspensions were prepared at 10^5 cells/mL in EGM-2MV media. Stents were submerged into separate tubes and filled with 2 mL of CFSE-tagged late EPC suspension. The reaction was performed in a gentle shaker for 30 min at 37℃ to analyze the adhesion of EPCs on the surface of the stent strut in a dynamic moving state. The number of late EPCs firmly attached to the stent struts was counted using a digital image-analysis system (Image Pro version 4.5, MediaCybernetics, Silver Spring, MD, USA).

We also tested EPC-capturing specificity of our anti-VE-cadherin antibody-coated stents by comparing with THP-1 adsorption assay. THP-1 cells are derived from the peripheral blood of patients with acute monocytic leukemia, and these cells have Fc and C3b receptors but lack surface and cytoplasmic immunoglobulins. Thus, we used THP-1 cells to evaluate non-specific binding of monocytes to our EPC-capturing stents. THP-1 cells were tagged with cell stalker (1:500, Biterials, Korea) and the adsorption of THP-1 cells on the stent surface was estimated by the same method described above.

Endothelialization on Stent Surface

To investigate the possibility of endothelialization, the morphology of a single EPC on the antibody-conjugated stent was observed by FE-SEM in detail, after captured. The image during the endothelialization was pictured at 2 hr after EPC-capturing test.

To confirm the growth and endothelialization of late EPCs on the stent surface *in vitro*, antibody-conjugated stents were reacted with late EPC suspensions as described in II.4.2. Captured EPCs were labeled with DiO solution (1:200, Molecular Probes, Eugene, OR, USA) and cultured in EGM-2MV media for 48 hr. After cell attachment, immunofluorescence imaging was performed at 1 hr and 48 hr, respectively.

II.4.3. Animal Care and Stent Implantation

All animal experiments were performed after receiving approval from the Institutional Animal Care and Use Committee (IACUC) of the Clinical Research Institute in Seoul National University Hospital and complied with the National Research Council's Guidelines for the Care and Use of Laboratory Animals.

Male New Zealand White rabbits with 3.0-3.5 kg weight (Yonam Laboratory Animals, KR) were fed with a 1% cholesterol diet (Oriental East, KR) from at least 2 weeks before stent implantation[94]. After these pre-treatments, stent was deployed on bilateral iliac arteries via right common carotid artery. Also, they were received aspirin of 2 mg/kg from the day of

stenting.

II.4.4. *In vivo* Assay for Animal Stenting

Figure 20 showed overall schedule for animal experiments including imaging and biochemical assay.

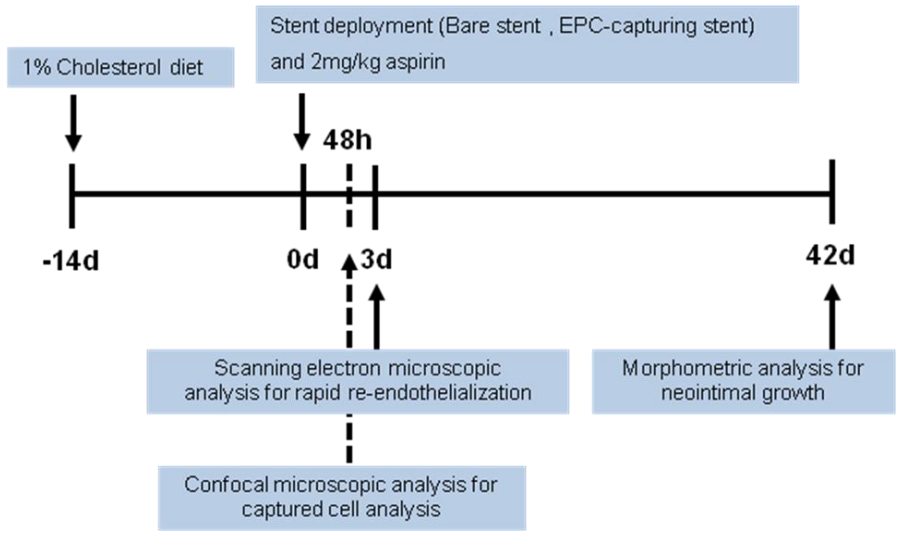

Figure 20. Schematic diagram of animal experiment.

SEM and CLSM Examination

To evaluate re-endothelialization and neointimal hyperplasia after stenting, we implanted 12 BMS and 12 EPC-capturing stents in the right and left iliac arteries, respectively, in 12 rabbits. Three days after stenting, two

rabbits were harvested and their stents were dissected longitudinally to evaluate the luminal surface as en-face, fixed in 2.5% glutaraldehyde, and imaged by SEM for evaluation of re-endothelialization. We also harvested the stented rabbit arteries at 48 hr after stent deployment, when the surface is not fully re-endothelialized. Then, the cells attached on the BMS and EPC-capturing stents were stained with CD31/PECAM-1 and analyzed by CLSM.

Neointimal Hyperplasia Measurement

At 42 days, 10 rabbits were harvested. The stented iliac arteries were removed and fixed in 10% buffered formalin with perfusion fixation. Cautious care needed to be taken when manipulating the stented vessels. They were embedded in resin and cut with tungsten blade. The degree of neointimal growth was analyzed in the sections stained with hematoxylin and eosin. Morphometric analysis was performed with a computerized digital image-analysis system (Image-Pro Plus version 4.5, MediaCybernetics, Silver Spring, Maryland). Cross-sectional images of stented rabbit iliac arteries were loaded onto Image-Pro Plus® and neointimal areas are measured by the observer who was blinded to treatment. Outer struts margin and inner luminal surface were traced manually, and two areas were calculated automatically (**Figure 21**).

Neointimal area = Outer area (PG 1) – Inner area (PG 2)

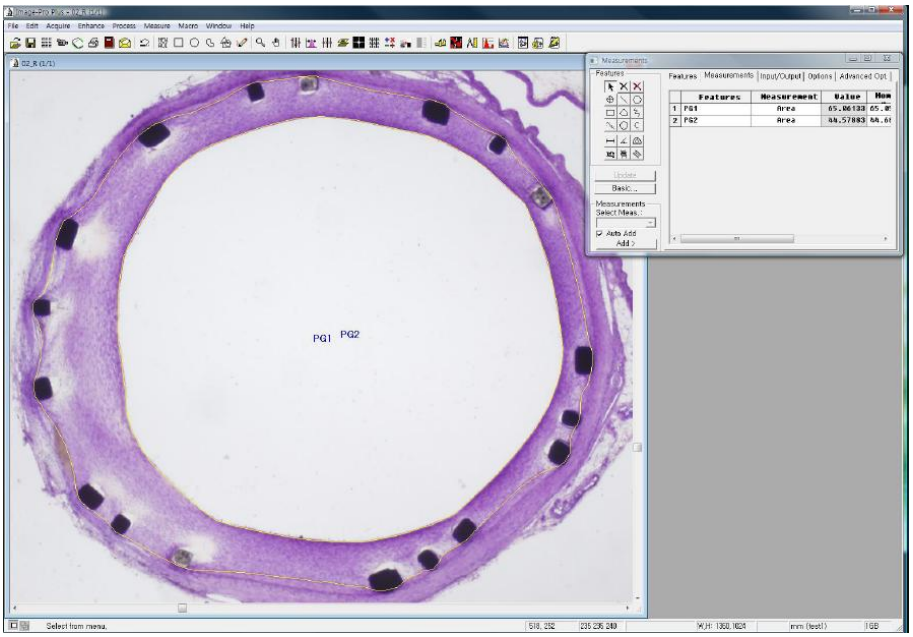

Figure 21. Digital image analysis program for measuring neointimal area.

Immunohistochemical Analysis

After 42 days, we investigated cellular status of neointima to concretely confirm the performance of our surface-modified stent. Immunohistochemical staining was used to assess the infiltration of inflammatory cells to neointimal with the same samples. In addition to this, the level of endothelial proliferation around stent struts was analyzed. We used a mouse monoclonal antibody against rabbit macrophage (RAM11) for macrophage detection and also used proliferating cell nuclear antigen (PCNA) as a proliferation marker.

III. Results and Discussion

III.1. Correlation between Surface Properties and Protein Adsorption

III.1.1. Surface Modification and Characterization

Surface Modification of Stainless Steel Plates

The overall surface modification scheme for stainless steel plates and their film structures are presented in **Scheme 2**.

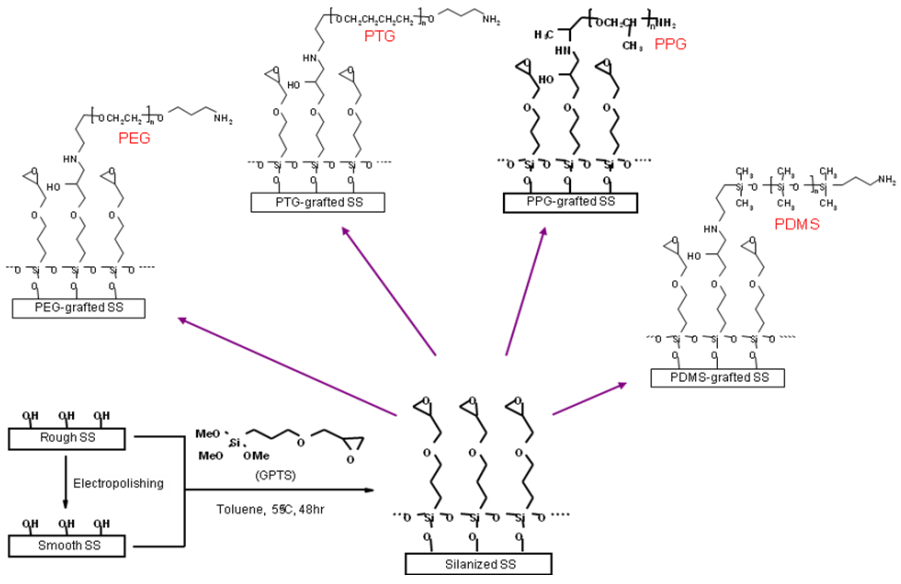

Scheme 2. Surface modification procedure of stainless steel plates.

Generally, the bare stainless steel surface is very hydrophobic and rough. To investigate the relationship between surface properties and protein adsorption, we modified bare stainless steel plates via electropolishing and various polymers grafting.

For further application to stent development, we designed a novel polymer grafting approach using silanization process. Silane coupling agents are well-known chemicals that bridge inorganic materials and polymer.

$$R\text{-}Si\text{-}(OR')_3$$

However, unlike silicone-based materials, stainless steel does not have sufficient oxide layer and thus silane film on the stainless steel is unstable. Therefore, the crosslinking by thermal curing is critically important to stabilize the silane film. Herein, we applied the optimized experimental protocol of silanization and polymer attachment in previous research[95].

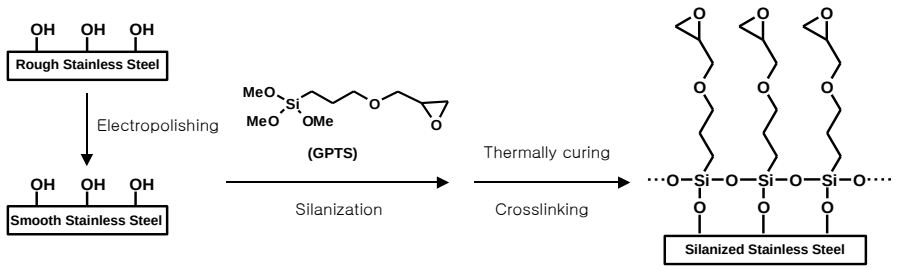

Scheme 3. Silanization on the stainless steel.

Hydrophilicity Analysis

The contact angle data of the surface-modified stainless steel plates were summarized in **Table 5**. The water contact angle data provides direct evidence of the change in surface hydrophilicity by surface modification. The bare stainless steel surface is very hydrophobic and the contact angle was as high as 79°. However, after acid-treatment, the hydrophobic bare stainless steel surface became highly hydrophilic, exhibited a contact angle of less than 10°. This means that hydroxyl groups were exposed on the surface by acid treatment so that silanization reaction was possible. Through silanization with GPTS, the alkyl epoxide groups were introduced. Accordingly, the contact angle was increased drastically from <10° to 61° as hydrocarbon layer was added. Then, we grafted various polymers on the silanized surfaces. At this moment, the surface hydrophilicities were changed as shown in **Figure 22**. Depending on the kind of polymers grafted on the surface, contact angles were either decreased or increased, with the change in contact angle ranging from 46° to 70°. As we expected, the PEG, PTG, PPG, PDMS polymers showed different hydrophilicty according to their structure of repeating unit. Based on this data, we concluded that the polymers were successfully grafted on the stainless steel surfaces and that the surface hydrophilicity could be readily controlled by polymer grafting. Both the rough (unelectropolished) and the smoothened (electropolished) surfaces yielded similar contact angle data after polymer grafting, indicating that the surface modification reaction proceeded in a similar manner, regardless of the surface roughness.

Table 5. Contact Angles of Surface-modified Stainless Steels

Sample	Contact angle (°)
Bare stainless steel	78.8±1.9°
Acid-treated stainless steel	<10°
GPTS-silanized stainless steel	61.4±4.2°
PEG-grafted stainless steel	46.0±4.0° (45.8±3.8°)[a]
PTG-grafted stainless steel	52.6±4.3° (52.2±4.2°)[a]
PPG-grafted stainless steel	54.0±4.2° (53.4±4.4°)[a]
PDMS-grafted stainless steel	70.6±4.2° (69.0±5.2°)[a]

[a] Data in parenthesis are contact angle on unelectropolished stainless steel surfaces.

(a) (b) (c) (d)

Figure 22. Water droplet images of the surface-modified stainless steel plates; (a) PEG-grafted surface, (b) PTG-grafted surface, (c) PPG-grafted surface, (d) PDMS-grafted surface.

Micro-Roughness Analysis

To investigate the surface-modified stainless steel and analyze surface micro-roughness, we used AFM after each modification step. The surface topography and micro-roughness were shown in **Figure 23** and summarized in **Table 6**, respectively. Firstly, many of the valleys and hills were observed in bare stainless steel plates. However, they were clearly disappeared after electropolishing. Accordingly, the root-mean-square (RMS) roughness was significantly decreased from 116.4 nm to 1.4 nm. After silanization and polymer grafting on the electropolished stainless steels, some protrusions and many tiny peaks were detected and the RMS data increased slightly from 1.4 nm to approximately 6-10 nm. Depending upon the polymer structure, the surface topography and RMS were slightly different. These results indicate that the polymers were well grafted, and that the polymer-grafted surfaces were of brush type. If it is not a brush type, but an entangled type, RMS should decrease after the polymer grafting[98]. In the unelectropolished case, no major differences in surface structure were observed before and after polymer grafting, because the polymer grafting effect on the RMS roughness seemed to be too small, comparing to its own one.

Four kinds of polymers were grafted on the unelectropolished and the electropolished surface, thereby providing eight samples that possess various surface properties in terms of micro-roughness and hydrophilicity.

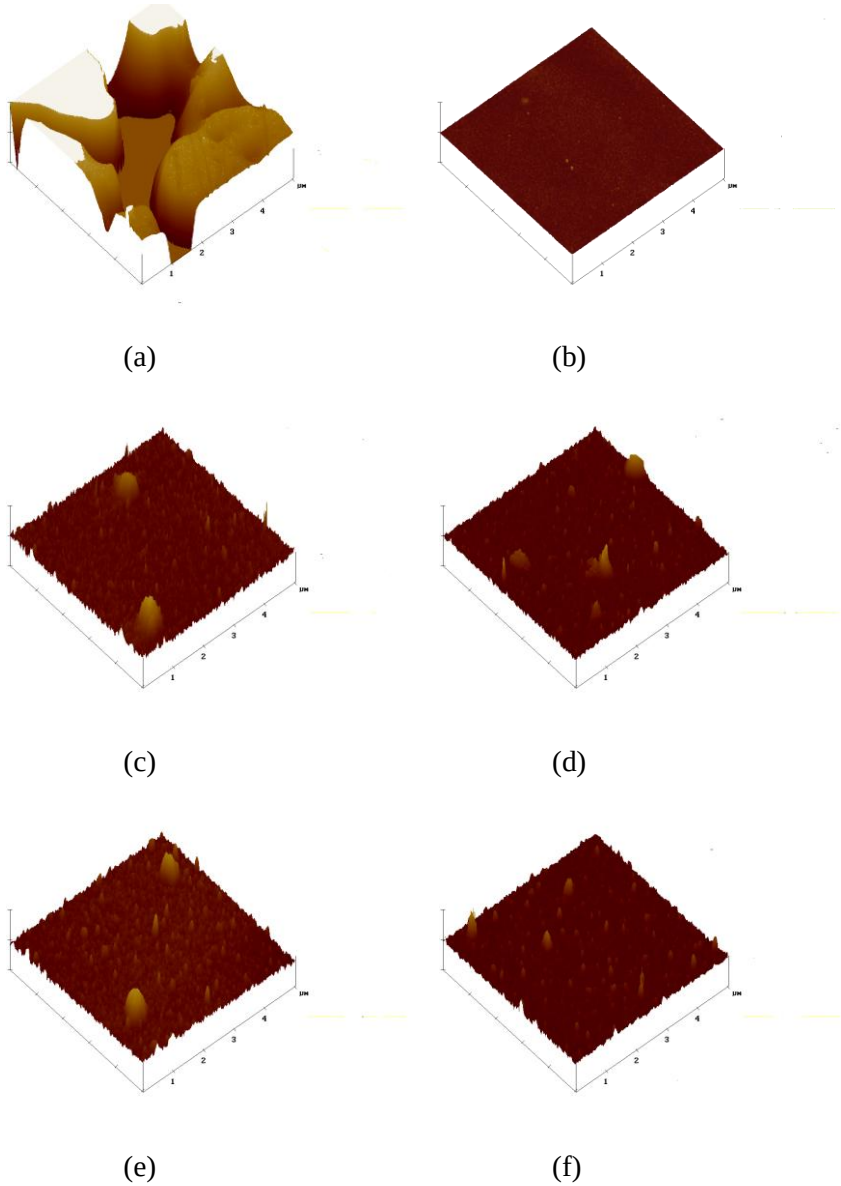

Figure 23. Atomic force microscopy (AFM) images of the surface-modified stainless steel plates (5μm×5μm, z=100nm); (a) bare surface, (b) EP surface, (c) EP/PEG surface, (d) EP/PTG surface, (e) EP/PPG surface, (f) EP/PDMS surface.

Table 6. Surface Roughness of Surface-modified Stainless Steels

Sample	Micro-roughness (RMS) (nm)
Bare stainless steel	116.4±26.3
Electropolished stainless steel	1.4±0.4
GPTS-silanized stainless steel	11.4±2.1
PEG-grafted stainless steel	10.6±0.3 (122.5±11.0) [a]
PTG-grafted stainless steel	9.0±2.3 (99.8±12.1) [a]
PPG-grafted stainless steel	8.6±1.0 (110.9±16.6) [a]
PDMS-grafted stainless steel	5.6±0.5 (119.8±13.0) [a]

[a] Data in parenthesis are RMS data on unelectropolished stainless steel surfaces.

III.1.2. Fibrinogen Adsorption Assay

Protein adsorption on a biomaterial surface occurs first in a mixture of biological solutions[96]. Those interactions are the overall result of complex cooperation, competition and interference between the biomolecules and the biomaterial[97,98]. Because handling all of the mixed biological solutions and then isolating the individual reactions are very difficult, we chose fibrinogen adsorption assay as a biocompatibility evaluation model of the surface-modified stainless steels.

Quantification of the Adsorbed Fibrinogen

Fibrinogen is a biochemical marker in biological cascade such as thrombosis and occasionally used as a standard to evaluate the biocompatibility of material[99,100]. The amount of adsorbed fibrinogens was probed by surface fluorescence measurements. First of all, all of the surface-modified stainless steels showed considerably lower fibrinogen adsorption, when compared to bare stainless steel taken as a control. In **Figure 24**, we presented the most and the least fluorescence images as representative examples. Furthermore, we found that the fluorescence intensity of fibrinogen adsorbed on the surface-modified stainless steel plates were 72-81% lower than those on the bare stainless steel plates (**Figure 25)**. This result is presumably due to the configurational entropy repulsion of the grafted polymers, preventing the protein from approaching the surfaces. The polymers used in this experiment are composed of simple linear chains and are very flexible. The entropy penalty associated with the compression and penetration of protein into the flexible polymer chains makes the polymer-grafted surface protein-resistant.

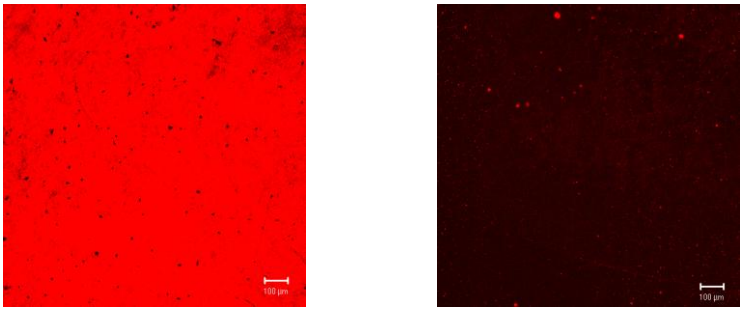

(a) (b)

Figure 24. Confocal fluorescence microscopy images of rhodamine -fibrinogen adsorbed on (a) bare stainless steel and (b) EP/PEG stainless steel.

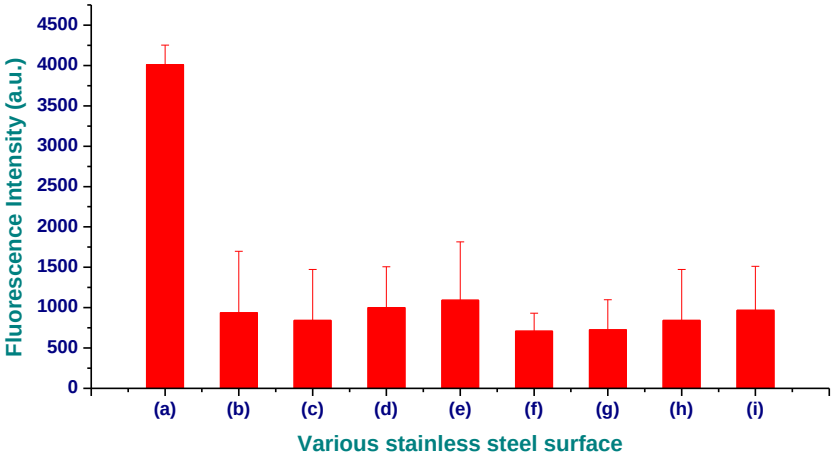

Figure 25. Fluorescence intensities of rhodamine-fibrinogen adsorbed on the surface-modified stainless steels; (a) bare surface, (b) bare/PEG surface, (c) bare/PTG surface, (d) bare/PPG surface, (e) bare/PDMS surface, (f) EP/PEG surface, (g) EP/PTG surface, (h) EP/PPG surface, (i) EP/PDMS surface.

To isolate the effects of micro-roughness and hydrophilicity on the protein adsorption from other factors, the entropy effect of polymers and terminal group effect were removed. For this, the terminal amine groups of grafted polymers were capped by acetylation. After capping, in spite of FITC reaction, the capped surface showed no fluorescence, which indicated that complete capping was achieved. Secondly, the molecular weight of each polymer was carefully selected by considering the repeating unit and the polymer structures were a linear type. Based on this, the approximate lengths of fully extended polymers are ~122 Å for PEG, ~90 Å for PTG, ~124 Å for PPG and ~109 Å for PDMS. The entropy effect inferred from these polymer chain lengths is supposed to be similar.

The fluorescence images by CLSM were systemically analyzed in order to investigate the correlation between the surface properties and the protein adsorption. These results are summarized in **Figure 26, 27**.

The data shown in **Figure 26** indicate that the protein adsorption is closely related to the surface hydrophilicity. On the PDMS-grafted hydrophobic surface, fibrinogen molecules were adsorbed in larger amounts than on less hydrophobic (PEG, PTG, PPG) surfaces. Comparing to the PEG-grafted surface, which is the most hydrophilic, about 30% more fibrinogen adsorption occurred on the PDMS-grafted surface. Previously, it has been reported that water molecules existed between the proteins and the surface can take part in reducing protein-substrate attraction[101]. As water contents on hydrophilic surface are increased, we can conclude that the result in **Figure 26** is consistent with the previous reports[102].

Figure 27 demonstrates that there is a correlation between the protein adsorption and the surface micro-roughness as well. Although its correlation

is weaker than that of the surface hydrophilicity, we found that rough surfaces consistently resulted in more protein adsorption, irrespective of polymer types. Approximately, the protein adsorptions on the electropolished/polymer-grafted surfaces were decreased by 4-9%, compared to those on the unelectropolished/polymer-grafted surfaces. The surface area should be also decreased by electropolishing, but we judged that this could not account for the 4-9% reduction of non-specific protein adsorption.

According to the previous reports on surface texture, thrombogenicity is usually higher for rougher surfaces. Sprague *et al*. revealed that the grooved surface increased the migration of cells over smooth one[103]. From this, we can conclude that the electropolishing gave rise to a decrease in not only the number of fibrinogen binding sites but also interactive force, which in turn led to less fibrinogen adsorption. Therefore, the surface roughness needs to be taken into consideration as an important parameter of stent performance.

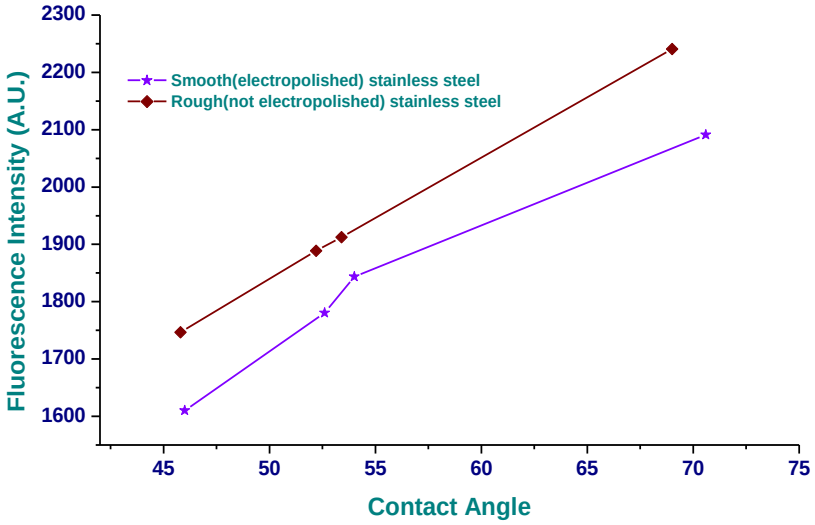

Figure 26. The amount of adsorbed fibrinogen vs. surface hydrophilicity.

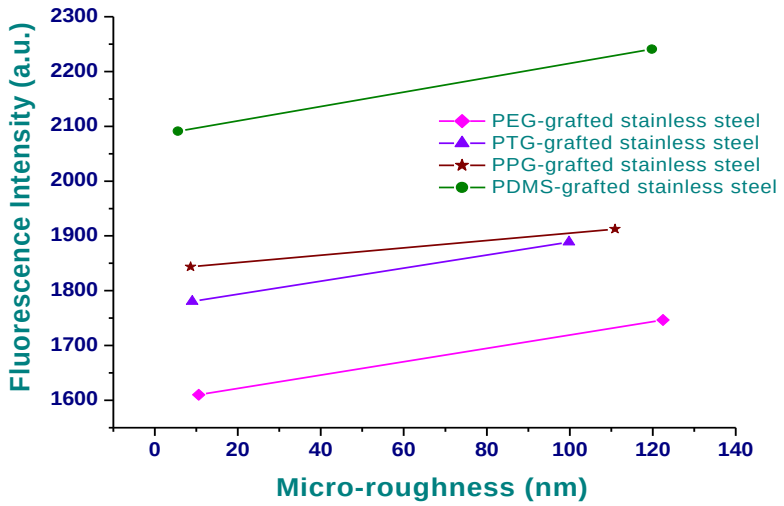

Figure 27. The amount of adsorbed fibrinogen vs. surface micro-roughness.

Contribution Ratio of Surface Factors for Biocompatibility

The big difference of fluorescence intensity (ca. 81%) was observed between bare stainless steel plate and EP/PEG-grafted stainless steel plate. A number of experimental reports and theoretical considerations suggest that a brush-like PEG layer is excellent for preventing protein adsorption[104,105]. These PEG effects include: (1) the low interfacial energy between biological fluids and the hydrophilic PEG layer enhances resistance to protein adsorption, (2) the large excluded volume and configurational entropy repulsion inhibit the protein from approaching the surfaces, and (3) the repulsion force created by favorable water-PEG interactions surpasses the attractive forces of the proteins with the surfaces.

Based on the data of fibrinogen adsorption on the EP/PEG-grafted surface, we attempted to analyze this protein repellent effect in detail. Overall, there are largely 3 contributing factors such as configurational entropy, hydrophilicity, and micro-roughness. According to our calculation based on the correlation between surface properties and protein adsorption, the contributing ratios of configurational entropy, hydrophilicity, and micro-roughness were 58%, 36%, and 6%, respectively (**Figure 28**). If a brush-type polymer is grafted, the surface could block non-specific protein adsorption, as nearly half amount. Hydrophilicity and micro-roughness also influence the protein adsorption but the portions are projected to be smaller than configurational entropy.

Putting these results together, we can conclude that if the surface is more hydrophilic, smoother, and grafted with more polymer, the less protein adsorption occurs on the surface. The electropolished and PEG-grafted surface is the ideal surface for inhibiting protein adsorption, whereas the

rough and hydrophobic surface, namely bare stainless steel is the worst one. Therefore, we fabricated a novel EPC-capturing stent, based on this conclusion.

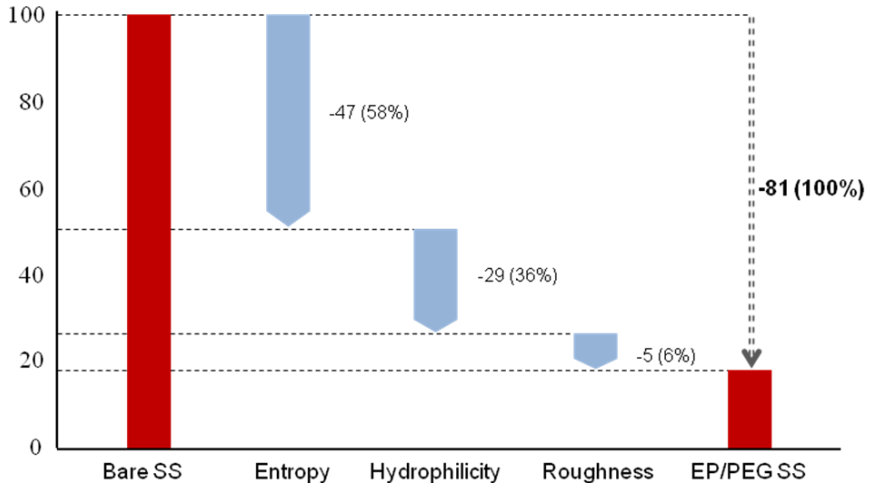

Figure 28. The contribution of surface factors for prohibiting non-specific protein adsorption.

[a] Data in parenthesis is respective proportion against a whole reduction.

III.2. Fabrication of EPC-capturing Stent and Characterization

The stent coating provided by surface modification should remain stable for a long period of time in spite of harsh environmental conditions such as fast blood flow, high salt concentration, and dynamic motion inside coronary artery. If polymer layers and bioligand are non-covalently attached to the metal stent, they can desorb due to weak interactions with the surface and cause unfavorable reactions. Cells and proteins in bloodstream can readily displace the physically-adsorbed polymers from the surface. Along the lines of fabricating the efficient, robust, and reliable EPC-capturing stent, we approached surface modification via chemical bonding.

In this study, we developed the smooth and PEG-grafted stent to make the surface biocompatible according to the aforementioned description. On this surface, VE-cadherin antibody as an EPC-capturing ligand was immobilized (**Figure 29**).

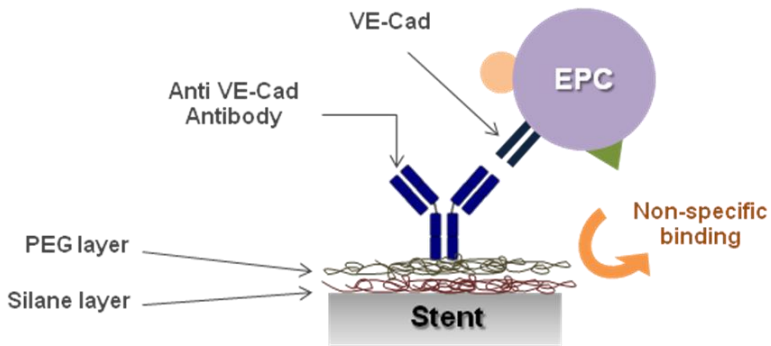

Figure 29. Graphical concept of our EPC-capturing stent.

The stepwise process for fabricating the EPC-capturing stent by antibody immobilization onto PEG-grafted surface is illustrated in **Scheme 4**.

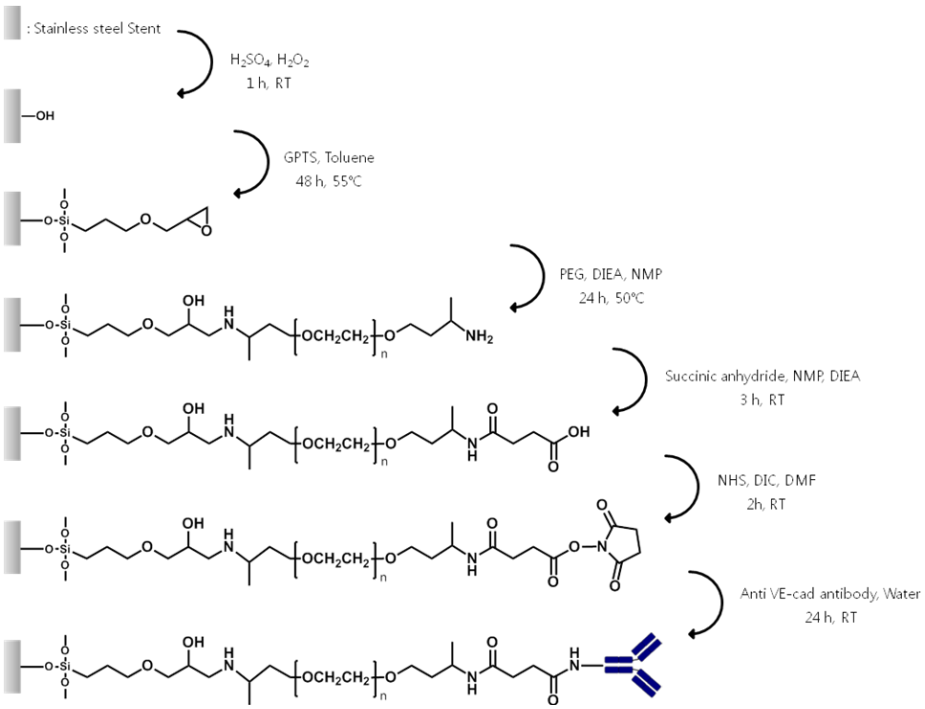

Scheme 4. The illustration of anti-vascular endothelial-cadherin (VE-cadherin) antibody immobilization on the silanized and polymer-grafted stainless steel stent.

III.2.1. Silanization and PEG Grafting

In this case, we skipped the electropolishing step, because we purchased electropolished stents. The bare hydrophobic stainless steel stent surface was changed to a highly hydrophilic one by acid treatment, causing hydroxyl groups to become exposed on the surface. Right after, acid-treated stent was silanized by GPTS as an organosilane coupling agent, which introduced an epoxide group on surface.

As a PEG polymer could effectively reduce nonspecific proteins binding, the Jeffamine® (M.W. 1,500) polymer, which has a PEG unit, was grafted to the epoxide group-introduced stent. We have already confirmed that the surface hydrophilicity of stainless steel, the bulk material of stents, was effectively enhanced by PEG polymer grafting through the comparison of the contact angles between a bare stainless steel plate (78.8±1.9°) and a Jeffamine®-grafted stainless steel plate (46.0±4.0°) as shown in **Figure 30**[106]. Based on this, the epoxy-functionalized stent reacted straightforwardly with the amine groups of the PEG polymer under basic conditions. Another free amine group of the grafted PEG polymers was applied for anti-VE-cadherin antibody coupling after the proper activation steps.

(a) (b)

Figure 30. Contact angle images of (a) bare stainless steel surface and (b) PEG-grafted stainless steel surface.

Morphological Analysis

Each surface modification step for bare, silanized, and PEG-grafted stents was followed by AFM analysis to observe the surface topography and roughness (**Figure 31**). Bare stainless steel stents had very smooth surfaces in the nanometer scale due to the electropolishing process[107]. Their surfaces became gradually roughened by silanization and the PEG-grafting steps. After the silanization step, many tiny peaks were newly detected on the smooth surface of the stent. Thicker and higher peaks were observed after PEG-grafting due to the polymer volume. Accordingly, the root-mean-square, degree of surface roughness, increased as the surface modifications proceeded from a bare stent (1.074) to a silanized stent (1.295) and then to a PEG-grafted stent (3.655). In this regard, RMS increment after PEG grafting indicates that the polymer layer on stent is same brush type as on stainless steel plates.

Besides, it was also demonstrated that all the topography is very uniform and thin over the scan area. Based on these results, we can conclude that each surface modification step proceeded without any defect spots.

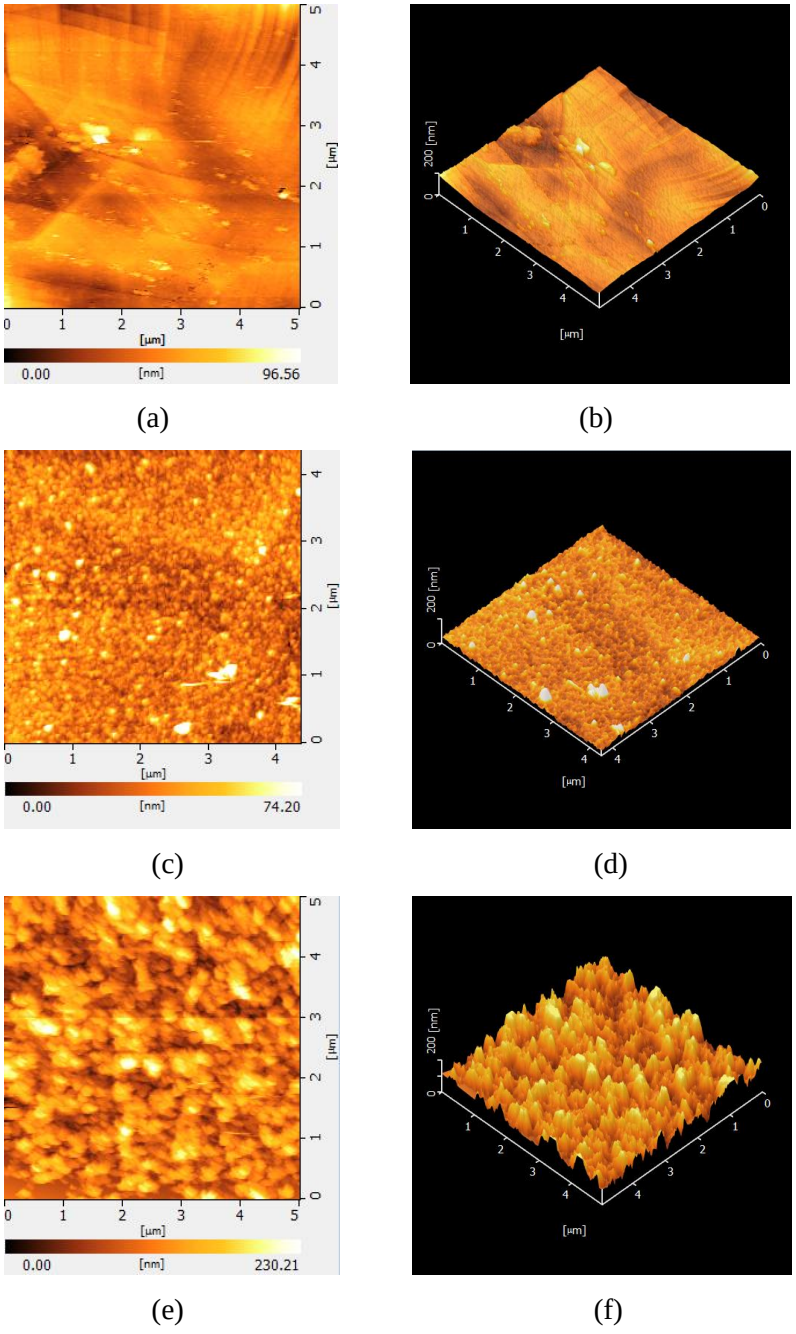

(a) (b)

(c) (d)

(e) (f)

Figure 31. Atomic force microscopy (AFM) images of bare stent (a, b), silanized stent (c, d), and polymer-grafted stent (e, f).

Compositional Analysis

The surface-modified stents were further analyzed by AES depth profiling analysis to observe any change in elemental composition with depth from the surface[108] as shown in **Figure 32**. At first, **Figure 32** shows a very thin carbon layer due to the carbon contamination on the surface. Except for the carbon contamination, iron was observed as the most abundant element on the bare stent surface (**Figure 32a**), as expected. In **Figure 32b**, silanization dramatically increased carbon and silicon contents, which obviously indicates that silanization on stainless steel stent was successful. The thickness of this organosilane layer was expected to be around 3 nm. Examining the signals at the start time, **Figure 32c**, obtained from PEG-grafted stent, showed more carbon content (60% vs. 41%) and less content of silicon (18% vs. 22%) than the ones from silanized stent (**Figure 32b**). It is attributed to the somewhat thick polymer layer of which backbone is [-O-CH_2-CH_2], thereby shielding silicon signal. Moreover, carbon content decreased with depth as the surface etching proceeded, whereas iron and chrome contents became higher on the etched surface than those in the grafted layer. This result indicates that the PEG polymer was thoroughly grafted. In addition to this, it took longer time to observe the iron content than the silanized stent surface, which also proved the polymer grafting.

In the depth profile analysis of PEG-grafted stent, the composition of carbon, silicon, iron, and chrome were not changed until approximately 12 nm. It means that the surface-modified stent had approximately 12 nm polymer layers on the stainless steel stent surface.

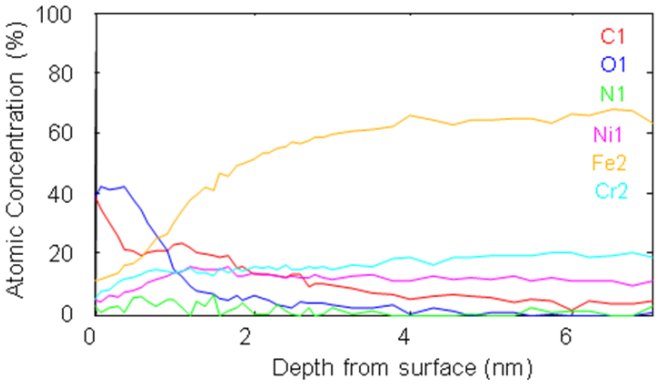

(a)

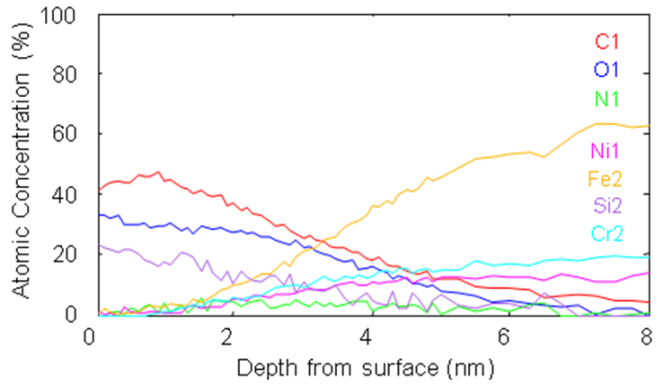

(b)

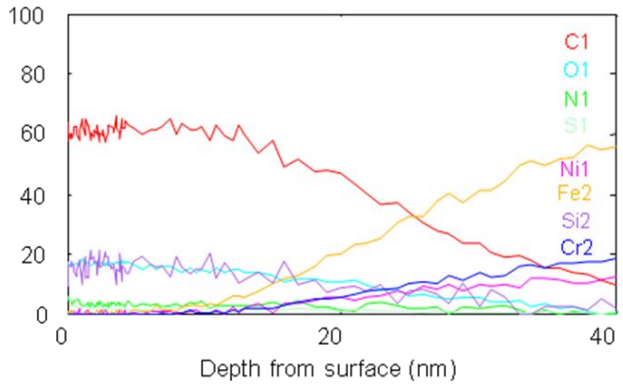

(c)

Figure 32. Auger electron spectroscopy (AES) depth profile spectra of (a) bare stent, (b) silanized stent, and (c) polymer-grafted stent.

Analysis of Amino Group Distributions on the Stent Surface

To analyze the functional group distributions, FITC was conjugated under basic conditions, to the free amino group of the PEG polymer on the stent surface. The entire PEG-grafted stents exhibited uniform and obvious fluorescence over the scan area on CLSM analysis (**Figure 33b**). However, BMS did not show any strong fluorescence intensity as shown in **Figure 33a**, because there was no functional group which could react with FITC.

These results indicate that the bare stent surface was homogeneously modified with the Jeffamine® polymer which has amino groups. Additionally, we can also confirm that the activity of the amino group was well-preserved; thus, the polymer-grafted surface could be directly used for antibody immobilization.

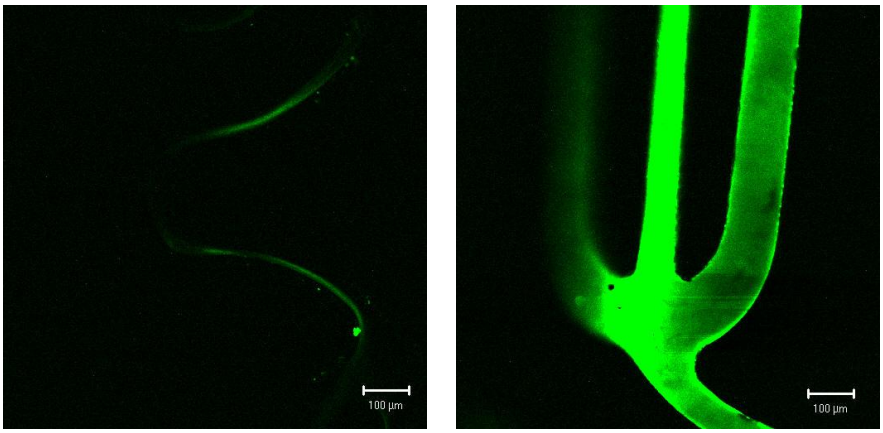

(a) (b)

Figure 33. Confocal laser scanning microscopy (CLSM) images of (a) FITC-treated bare stent and (b) FITC-treated polymer-grafted stent.

III.2.2. Antibody Immobilization

The anti-VE-cadherin antibody was immobilized to the polymer-grafted stent as the final modification step. We employed the peptide bond formation protocol because the antibody contained amino groups on its surface.

To immobilize the anti-VE-cadherin antibody, the exposed amino groups on the stent were modified and activated. Firstly, the free amine group of the PEG polymer on the stent was reacted with succinic anhydride to introduce carboxyl group onto the stent, and then the carboxyl group was activated by DIC and NHS. Herein, *N*-hydroxysuccinimide ester was selected as an activator, because its by-product after peptide coupling is water-soluble and thus suitable for coupling an antibody[109]. The activated carboxyl group could react easily with the free amino group of the antibody. In conclusion, we successfully introduced the anti-VE-cadherin antibody to the surface-activated stent as shown in **Scheme 5**.

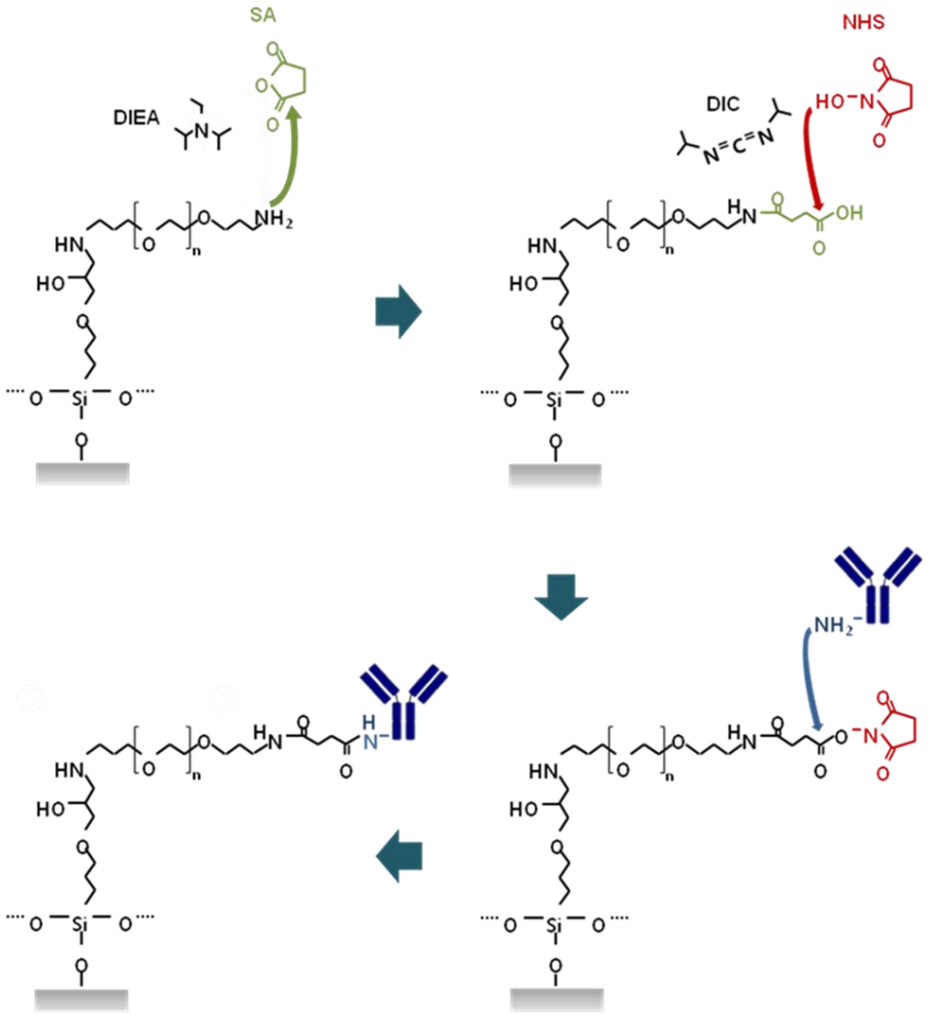

Scheme 5. Antibody coupling via peptide bond formation.

Topographical Analysis

The antibody immobilization step was confirmed by FE-SEM, EDX, and CLSM-based immunoassay using fluorescence dye-conjugated secondary antibody. As expected, dramatic changes in the surface topography of the polymer-grafted stent and antibody-immobilized stent were observed on the FE-SEM images (**Figure 34**). After the antibody immobilization, a large number of bulges in the size range of 100~150 nm appeared homogeneously.

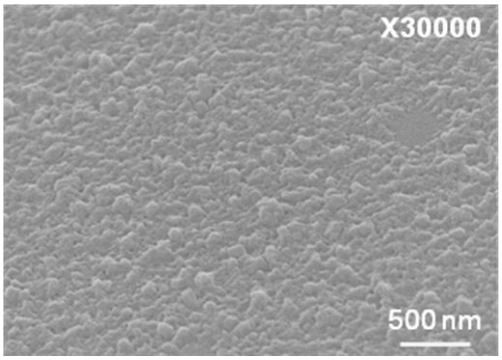

(a)

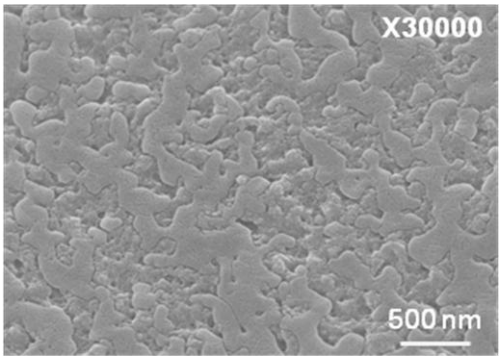

(b)

Figure 34. Field-emission scanning electron microscopy (FE-SEM) images of (a) PEG-grafted stent and (b) anti-vascular endothelial-cadherin antibody-coated stent.

Compositional Analysis

Slight changes of atomic composition were also observed in the EDX analysis (**Table 7**). Carbon and oxygen contents increased after anti-VE-cadherin antibody immobilization, when compared with the PEG-grafted stent and the bare stainless steel stent, while the iron content remained low. This is due to the increase in thickness of the carbon-based layer derived by conjugating the antibody on the polymer.

Table 7. Atomic Composition of Surface-modified Stents (at. %)

Sample	C	O	Cr	Fe
Bare stent	13.8	3.3	18.9	50.6
PEG-grafted stent	31.4	14.9	1.8	30.7
Antibody-conjugated stent	35.5	15.4	2.2	24.6

Secondary Antibody Immnoassay

We performed the immunofluorescent staining of anti-VE-cadherin antibodies with anti-rabbit IgG antibodies on our EPC-capturing stent to clearly demonstrate whether anti-VE-cadherin antibody was immobilized on the stent after surface activation or not. **Figure 35** showed that homogenous fluorescence was detected from the EPC-capturing stent, which proved to even distribution of the antibody, but only partial fluorescence was observed from the bare stainless steel stent, which was expected due to the non-specific binding of Alexa Fluor-conjugated secondary antibody.

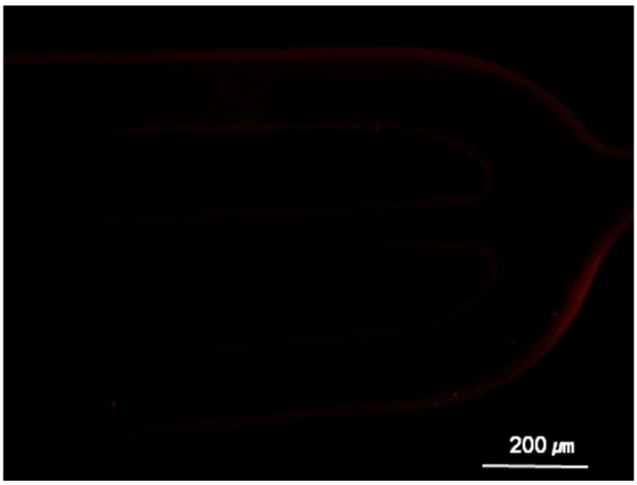

(a)

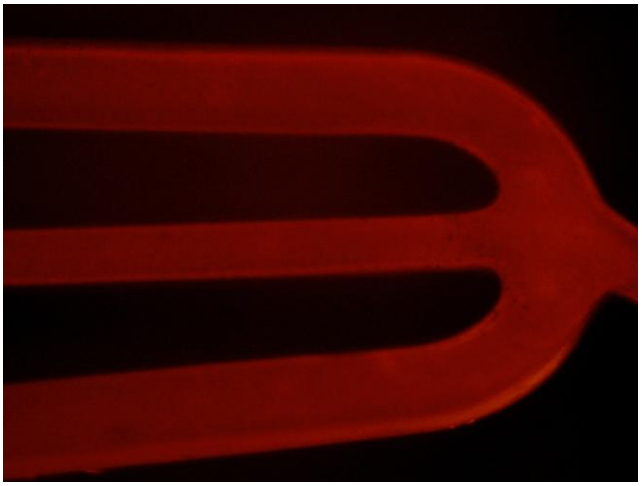

(b)

Figure 35. Confocal laser scanning microscopy (CLSM) images of (a) Alexa Fluor-conjugated secondary antibody-treated bare stent and (b) Alexa Fluor-conjugated secondary antibody-treated EPC-capturing stent.

Macro Level Surface Coating Integrity

Even though all surface modification steps of stent were performed in collapsed state, the surface modification should not be changed after stent expansion. Therefore, we checked the overall quality of the surface-modified stent at the expanded state. FE-SEM image of our EPC-capturing stents demonstrated fully smooth and complete surface integrity. Also, we could not observe any tear and delamination of surface coating which is composed of polymers and antibody (**Figure 36**). Thus, the surface of our EPC-capturing stent was proved to be homogeneous and robust.

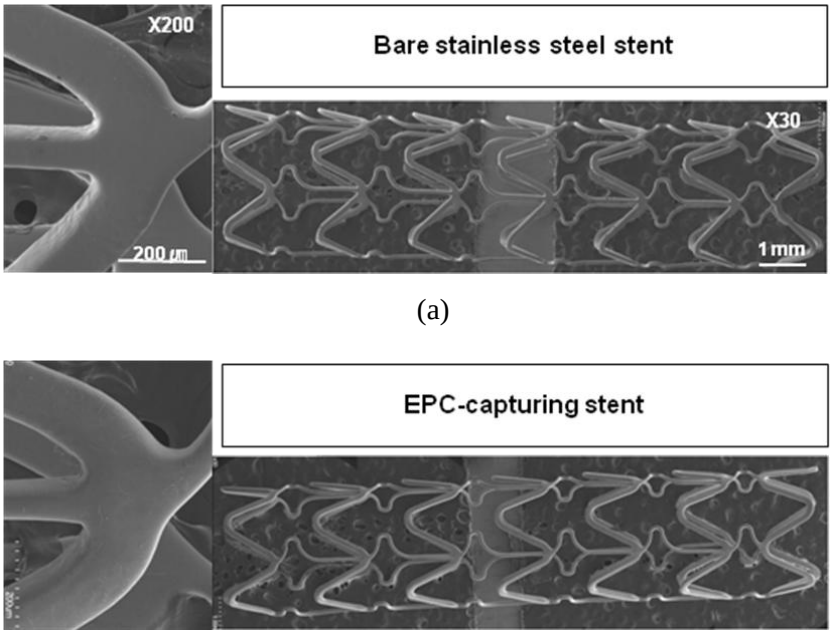

Figure 36. Field-emission scanning electron microscopy (FE-SEM) images of (a) bare stainless steel stent and (b) EPC-capturing stent after stent expansion.

III.3. Capability of EPC-capture and Endothelialization

EPC and Vascular Injury

Endothelial denudation is a primary event after balloon angioplasty and stent deployment[110]. The lack of functional endothelium and subsequent inflammatory cell infiltration into the injured site cause the failure of stenting surgery. Herein, EPCs can play a key role in repairing the vascular injury.

EPCs are heterogeneous cell populations and can be largely divided into 2 different types; early myeloid EPC vs. late EPC. They have quite different characteristics in their morphology, proliferation rate, and survival ability. Early EPCs are spindle-shaped, have a short lifespan, and enhance neovasculogenesis by secreting angiogenic cytokines. On the other hand, late EPCs have cobblestone appearance, show a long lifespan, and contribute to neovasculogenesis by providing endothelial cells based on their high proliferation and differentiation potency[111].

VE-cadherin as an EPC-capturing Target

As we have previously mentioned, the choice of EPC-capturing molecule is crucially important. Although CD34 is one of the representative markers of EPC, it is not enough to capture only EPC.

We suggested that late EPCs are more desirable target for our surface-modified stent because late EPCs are actual building blocks for re-endothelialization. Previous study reported that late EPC expressed VE-cadherin abundantly on their surfaces while early EPC and other leukocytes did not express it. Therefore, VE-cadherin is considered as an ideal surface

marker to recruit circulating EPCs, exclusively late EPCs. VE-cadherin is expressed in adherent junctions of endothelial cells and exerts important functions such as intracellular signaling as well as cell-cell adhesion[112]. Additionally, it is known to regulate diverse cellular processes such as cell proliferation and apoptosis, and modulates the functions of VEGF receptor[113].

III.3.1. Cell Specificity of Surface-modified Stents

We performed head-to-head comparison of EPC specificity between the surface-modified stent and the unmodified one to confirm whether our approach is effective at the cellular level. Suspended late EPCs were perfused from side to side in a cell-stock tube to confirm the effect of our surface-modified stent on EPC capture. After 30 min, the surface-modified stents captured 93 ± 5 EPC per strut, whereas the bare stainless steel stent captured 16 ± 2 EPCs per strut on their surface as shown in **Figure 37** and **Figure 38a, b**. In conclusion, our EPC-capturing stents captured significantly more late EPCs than the bare stainless steel stents ($p=0.015$).

In contrast, when incubating the stents with THP-1, THP-1 was adsorbed on the bare stainless steel at similar level as EPCs, whereas less THP-1 was adsorbed on our EPC-capturing stent (**Figure 38c, d**). This result indicates that the BMS has no cell specificity, whereas the EPC-capturing stent selectively recruited EPCs. This high specificity is totally due to our surface modification. We could say that the hydrophilic polymer grafting played a significant role to repel unwanted proteins and cells. Furthermore, we could determine that the anti-VE-cadherin antibody did not capture other cells such

as monocytes and that the THP-1 did not bind to the F_c portion of the anti-VE-cadherin antibody. Therefore, we suggest that our strategy of combining hydrophilic polymer grafting and antibody coupling effectively provide stents with cell specificity, and thus our EPC-capturing stent worked successfully.

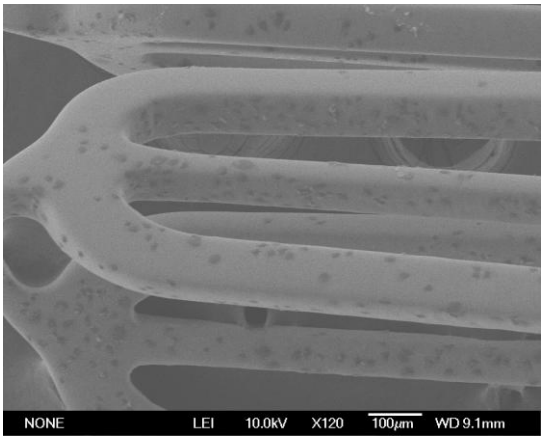

(a)

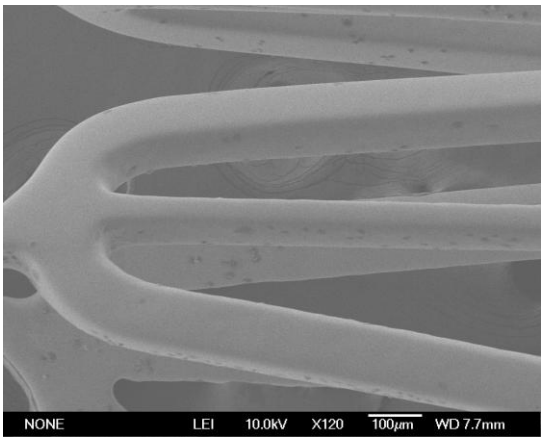

(b)

Figure 37. Field-emission scanning electron microscopy (FE-SEM) images for EPC capture on (a) surface-modified stent and (b) unmodified stent.

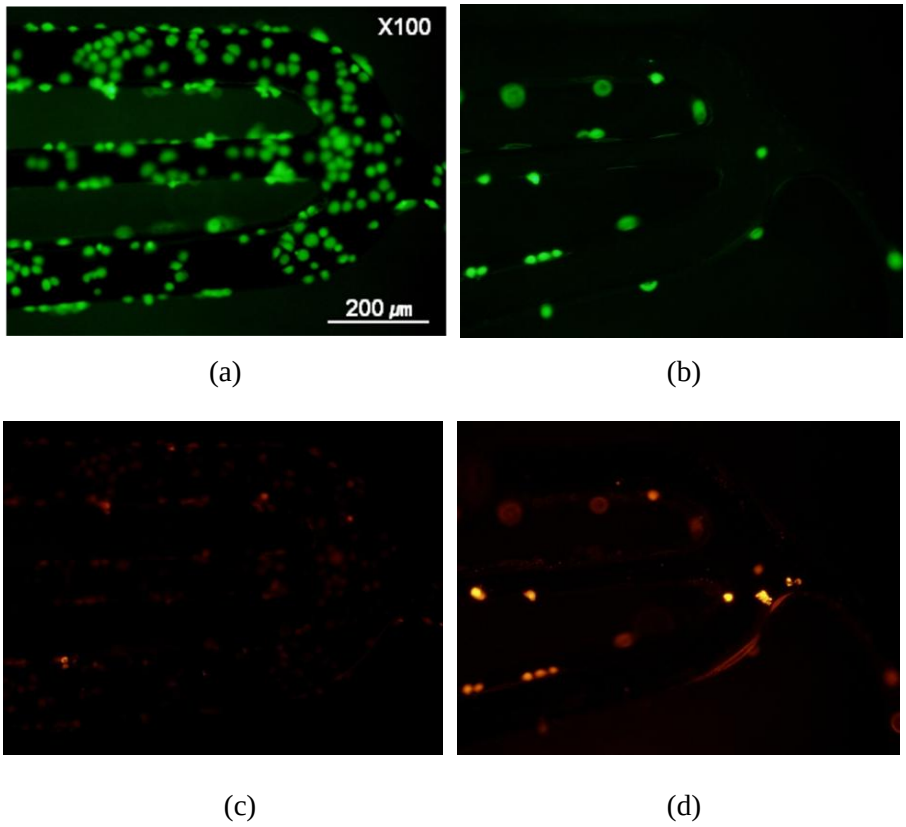

Figure 38. Fluorescence images of (a) surface-modified stent capturing endothelial progenitor cells (EPCs) labeled with CFSE (green), (b) unmodified stent adsorbing a small number of EPCs, (c) surface-modified stent minimally adsorbing THP-1 cells tagged with cell stalker (red), and (d) unmodified stent adsorbing a small number of THP-1 cells.

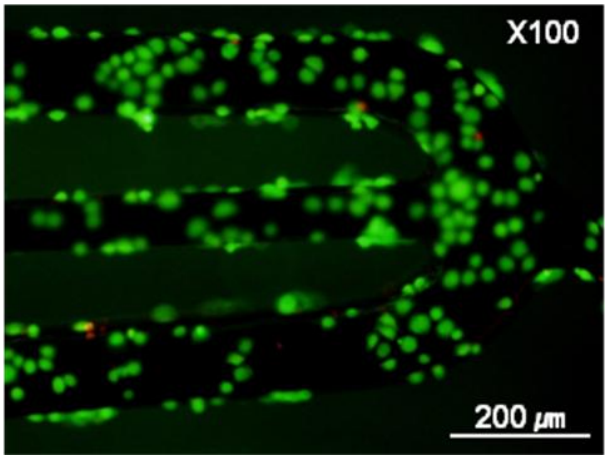

(a)

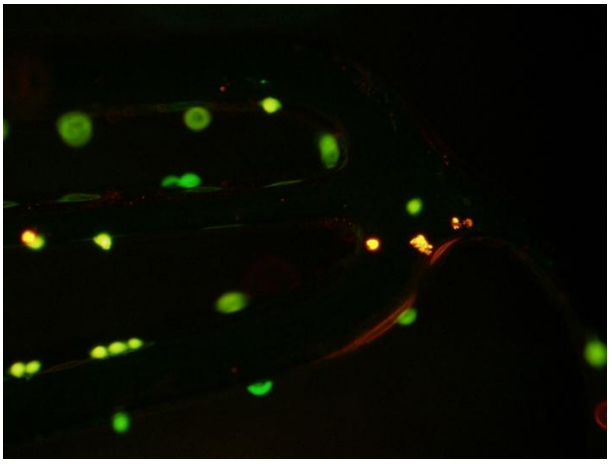

(b)

Figure 39. Comparison of cellular specificity between our EPC- capturing stent and bare stainless steel stent. Merged images of
(a) surface-modified stent of EPC and THP-1 and
(b) unmodified stent of EPC and THP-1.

III.3.2. Endothelialization on the EPC-capturing Stent

Immediately after attachment of suspended late EPCs onto the surface of EPC-capturing stents, spherical-shaped EPCs spread out laterally, became flat and smooth, and finally started to endothelialize the stent surface. The image in **Figure 40** is obvious evidence to represent the cell proliferation on a stent surface.

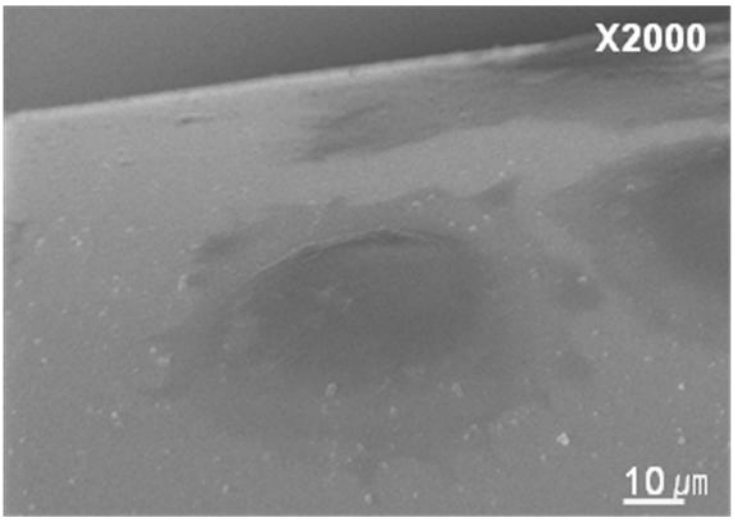

Figure 40. Field-emission scanning electron microscopy (FE-SEM) image of endothelial progenitor cells (EPCs) spread on stent surface.

Additionally, EPC-capturing stents were treated with late EPC suspensions and then captured EPCs were incubated for 48 hr to observe the growth and endothelialization of late EPCs on the stent surface. At 1 hr, a number of cells were observed on the stent surface, but it was only partly endothelialized (**Figure 41a**). However, after 48 hr incubation, EPCs had

largely proliferated and grown to near-confluence level; thus, the stent surface was mostly endothelialized (**Figure 41b**). This endothelialization is attributed to the exclusive expression of VE-cadherin on late EPC, contributing to endothelialization based on its high proliferation ability.

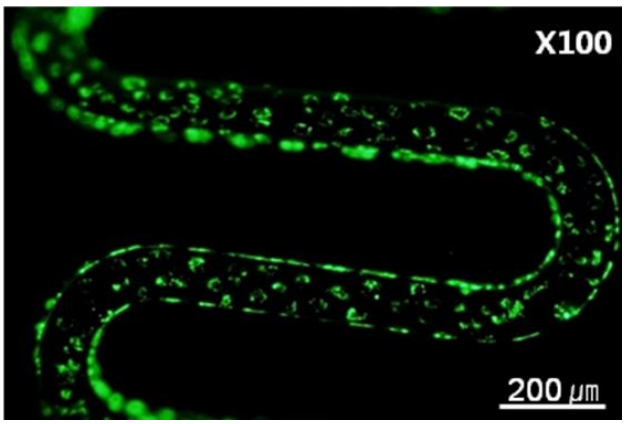

(a)

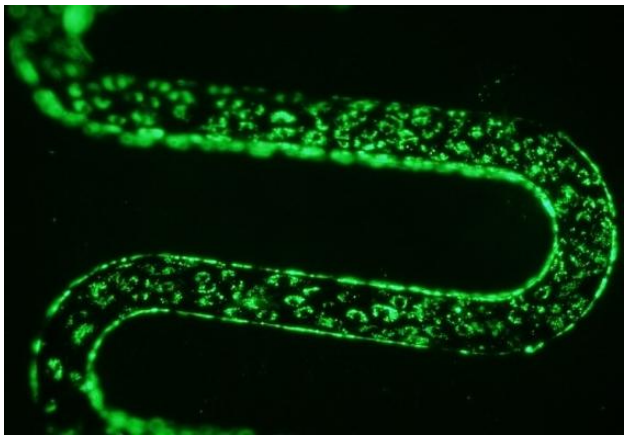

(b)

Figure 41. Endothelialization on the antibody-conjugated stent after endothelial progenitor cells (EPCs) capture. Confocal laser scanning microscopy (CLSM) images of EPC-incubated stent after (a) 1 hr and (b) 48 hr.

III.4. Vascular Re-endothelialization and Neointimal Hyperplasia after Stenting

Comparative Paired Rabbit Iliac Artery Model

Many animal models have been used for clinical study of stent. Common animal models include rodents (rats, mice, rabbits), pigs, dogs, or primates[114].

In this study, we chose a comparative paired rabbit iliac artery model to perform head-to-head clinical comparison of bare stainless steel stent and EPC-capturing stent, because rabbit iliac arteries are paired[115]. Moreover, their dimensions (~3 mm) and blood flow rates (~17 cm/sec) are similar with those of the human coronary artery[116]. Two stents, identical in material, size and design but different in surface properties, were simultaneously implanted under identical conditions in left and right iliac arteries of each rabbit (**Figure 42**). Therefore, we could identify the effect specific to the surface coating, based on its own control concept. The cholesterol diet was fed to the rabbit to reproduce conditions that predispose to the need for human arterial angioplasty such as atherosclerosis.

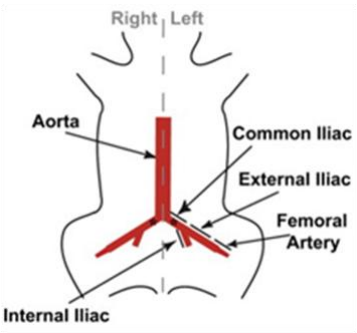

Figure 42. Schematic illustration of stenting in two rabbit iliac arteries[117].

III.4.1. Endothelialization in the Vessel

We investigated *in vivo* efficacy and relevance of our EPC-capturing stents. Schematic diagram of study design and end points are previously illustrated in section II.4.3. At 3 days after stenting of EPC-capturing stents or bare stainless steel on the right and left iliac arteries in the same animal, we directly evaluated the vascular re-endothelialization by FE-SEM. We could identify not only definite difference between them but also rapidness of endothelialization of our EPC-capturing stent. Detailed morphology showed that over 90% of the surface of the EPC-capturing stent was covered with endothelium, while bare stainless steel stent was covered less than 10% of the surface (**Figure 43**).

As demonstrated above, the surfaces of the EPC-capturing stent were almost completely re-endothelialized on the third day of stent implantation. To further analyze status of the initial cells attaching on the EPC-capturing stent, we harvested the stented rabbit iliac arteries and explanted vessels were stained with CD31/PECAM-1 at 48 hr after stent deployment. At this time, the stent surface was not yet fully re-endothelialized. Confocal microscopic examination showed that many cells were attached on the EPC-capturing stent and most of them were stained with antibody against CD31/PECAM-1 (**Figure 44a**). As CD31/PECAM-1 molecules are expressed at high levels specifically localized to endothelial cell junctions, their antibodies have been frequently used as endothelial marker. Based on a large number of cells positive for CD31/PECAM-1 expression (red), we can clearly confirm that the initial captured cells are in endothelial lineage. In contrast, a few cells were found on the bare stainless steel stent and there was no CD31/PECAM-1 expression (**Figure 44b**).

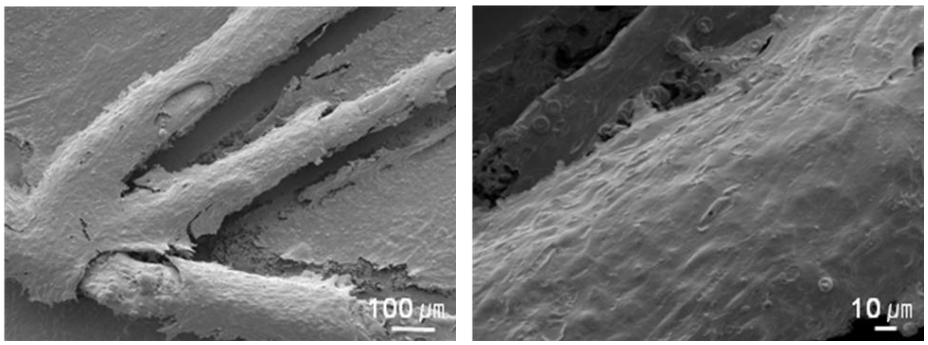

(a)

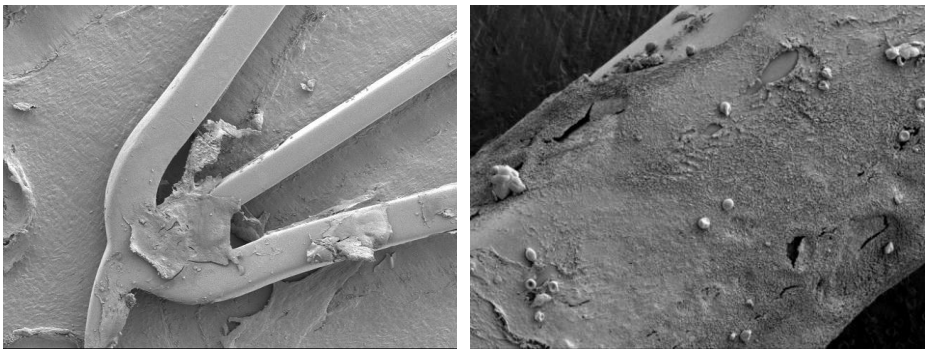

(b)

Figure 43. *In vivo* confirmation of vascular re-endothelialization after implantation to rabbit iliac artery; (a) EPC-capturing stent, (b) bare stainless steel stent.

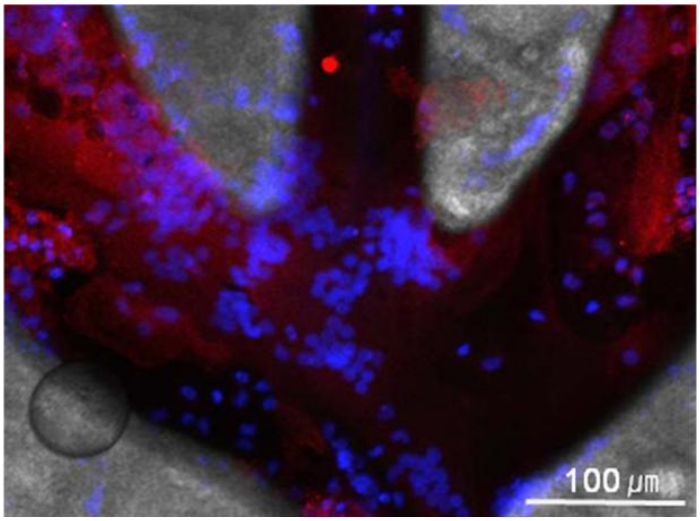

(a)

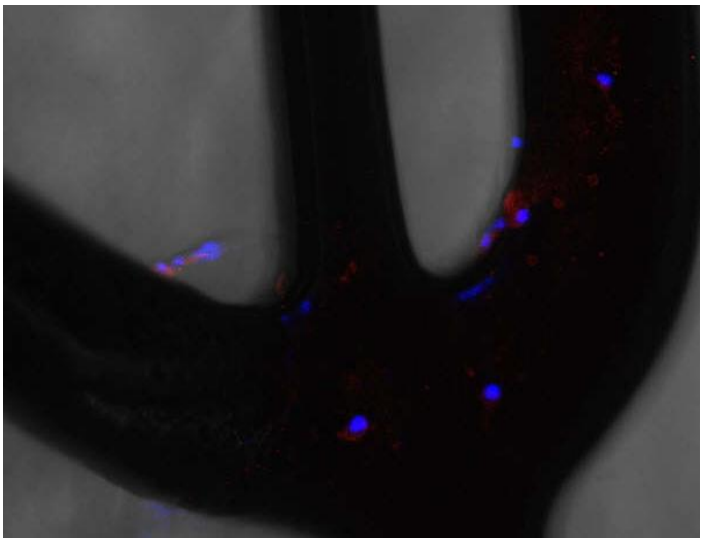

(b)

Figure 44. Confocal microscopic images of luminal surface stained with CD31/PECAM-1 antibody at 48 hr after stent deployment; (a) EPC-capturing stent, (b) bare stainless steel stent. Red color means CE31/PECAM-1 expression and blue color is DAPI's nuclear counterstain.

III.4.2. Neointimal Hyperplasia Measurement

As described in section I.4.1, in-stent-restenosis is closely related to neointimal hyperplasia. Neointimal hyperplasia is influenced by re-endotheliazation, because vascular SMC migration and mobilization of smooth muscle progenitor cells to vascular injury site arises within 24 hr after the endothelial denudation[118]. In this regard, we would investigate the long-term neointimal hyperplasia derived from the difference of re-endothlialization rate in short period.

At 6 weeks after stenting, we harvested iliac arteries to evaluate the degree of neointimal hyperplasia. In morphometric view, our EPC-capturing stents showed a significantly smaller neointimal area than bare stainless steel stent (**Figure 45**). This histology demonstrated that our surface modification can effectively reduce neointimal hyperplasia. It is due to the capability of specific capturing EPCs and facilitating re-endothelialization within 3 days. The measured neointimal areas are 0.95 ± 0.22 mm^2 in EPC-capturing stent and 1.34 ± 0.43 mm^2 in bare stainless steel stent, respectively ($p=0.02$, $n=10$). Converting into a rate roughly, EPC-capturing stent can inhibit neointimal hyperplasia, about 29.1% at 6 weeks. Given that the experimental rabbits were very young and healthy, this rate is excellent. Taken these *in vivo* data together, we can conclude that our EPC-capturing stents capture endothelial lineage cells, accelerate re-endothelialization and reduce neointimal formation.

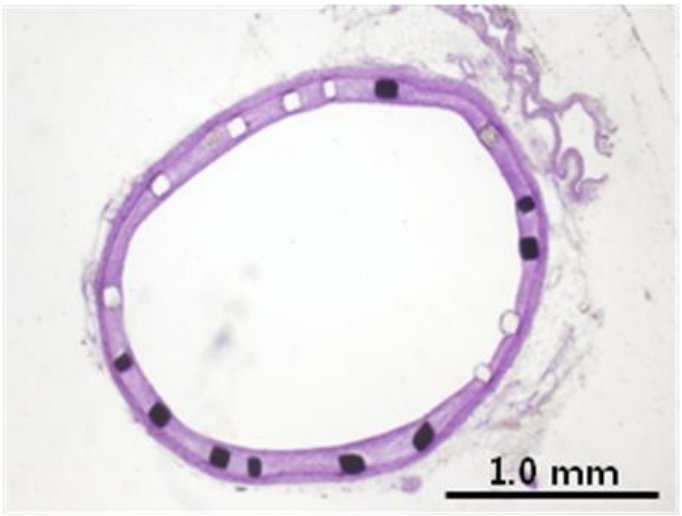

(a)

(b)

Figure 45. Dissected histologic images of the iliac arteries at 42 days after stent deployment; (a) EPC-capturing stent, (b) bare stainless steel stent.

III.4.3. Immunohistochemical Analysis of the Neointima

To address the potential concerns about non-specific inflammation due to surface coating, we performed immunohistochemical staining on neointimal area of the iliac arteries obtained at 6 weeks after stent implantation. Macrophage infiltration into the stented arteries was assessed by staining with RAM11. RAM11 has been commonly used for immunohistochemical analysis of rabbit macrophages, especially in the cellular analysis of the atherosclerotic lesions[119]. The degree of RAM11 staining can be translated to inflammatory activity, because the inflammation cascade is initiated by mainly resident macrophages. Although there is the additional coating composed of silane, polymer, and antibody in our EPC-capturing stent, the detected difference between EPC-capturing stent and bare stainless steel stent was limited and two staining images were similar as shown in **Figure 46**.

These data indicate that anti-VE-cadherin antibodies as well as polymers coated on the stent struts do not cause any non-specific inflammation at least at the time of 6 weeks after stent deployment. Through this result, we suggest that the rapid re-endothelialization fundamentally blocks innate inflammation for foreign stent and our coating itself causes any special non-specific inflammation.

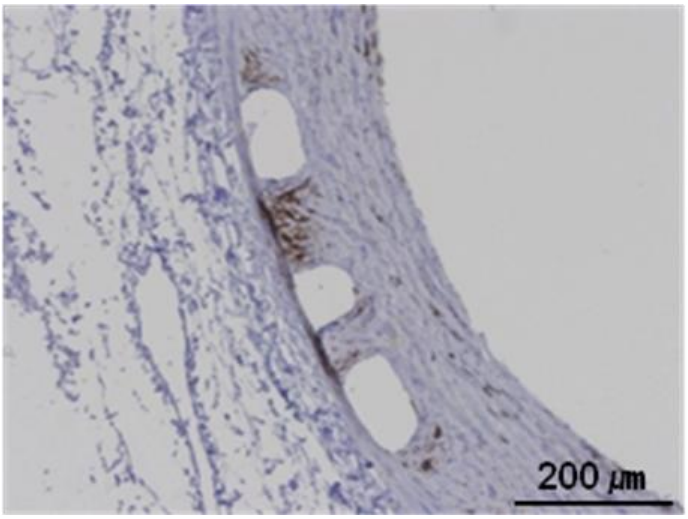

(a)

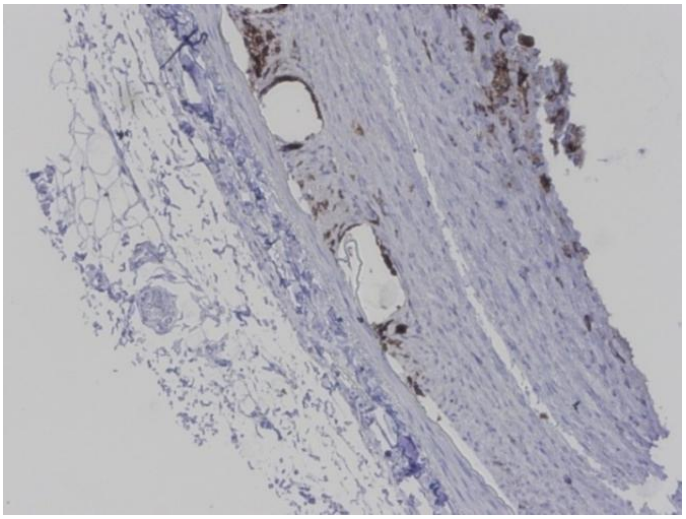

(b)

Figure 46. Immunohistochemical images stained with RAM11 antibody at 6 weeks after stent deployment; (a) EPC-capturing stent, (b) bare stainless steel stent.

In addition to macrophage infiltration, we assayed the PCNA expression to check the possibility of further neointimal hyperplasia in the stented vessel. PCNA is originally identified as a protein that is expressed in the nuclei of cells during the DNA synthesis phase of the cell cycle and thus its immunocytochemistry can represent the present activity of neointima.

Immunohistologic staining with PCNA demonstrated that a considerable number of proliferating cells were found in the neointimal area of the both stent groups, EPC-capturing stent and bare stainless steel stent. However, the proportion of proliferating cells was much higher in the bare stainless steel group, compared with the EPC-capturing stent group (**Figure 47**). Calculating the proliferating cell count in 1 mm^2 area, the number in EPC-capturing stent was 1650 ± 578 and it is less than half of the number in bare stainless steel stent, 3921 ± 101. This result suggested that the proliferative activity of the neointimal area at 6 weeks after stent deployment is still higher in bare stainless steel stented segment than EPC-capturing stented one. Therefore, we can deduce that the vessel stented by bare stainless steel will proceed with the neointimal hyperplasia. On the other hand, as EPC-capturing stent showed the lower proliferative activity, it is expected to result in smaller neointima, which is due to rapid re-endothelialization.

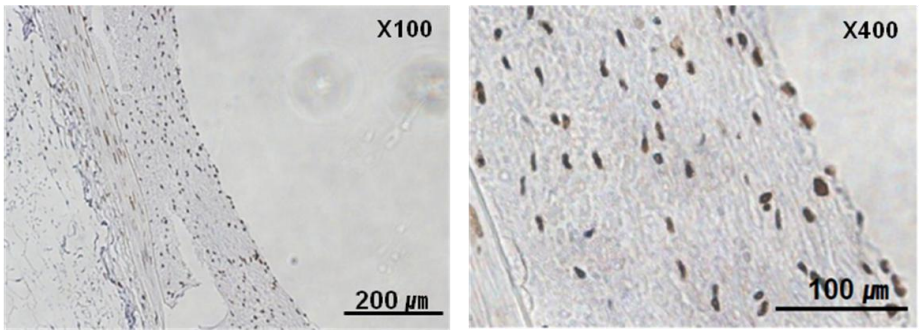

(a)

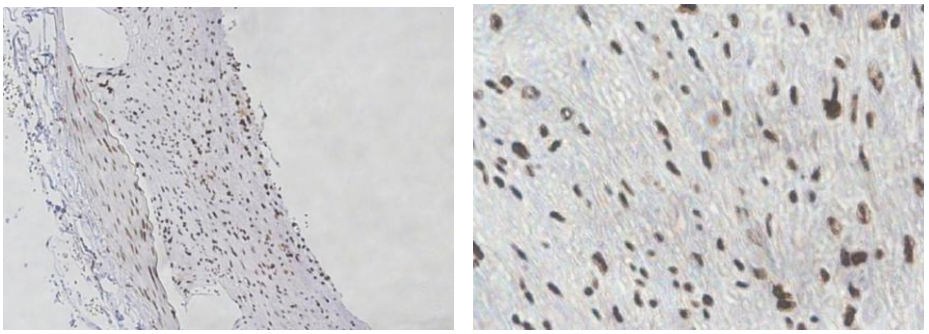

(b)

Figure 47. Immunohistochemical images stained with PCNA antibody at 6 weeks after stent deployment; (a) EPC-capturing stent, (b) bare stainless steel stent.

IV. Conclusion

Our study demonstrates a facile method to fabricate biofunctional stents with EPC specificity by combining acid-treatment, silanization, polymer grafting and antibody immobilization. It is a simple dip-coating process that can be widely applied to various devices of any geometry in addition to stents. A variety of analyses including AFM, AES, FE-SEM, and CLSM showed that our strategy resulted in successful covalent immobilization of antibody on the biocompatible surface. Here, the hydrophilic polymer layer served to create a non-biofouling interface and the immobilized antibody provided specific biological functionality.

As a basic study, we presented a correlation between the surface properties and the protein adsorption in terms of the roughness and hydrophilicity. For this correlation study, various surfaces (smooth vs. rough, hydrophilic vs. hydrophobic) were prepared by elecropolishing and polymer grafting. The fibrinogen adsorption assay on bare and the surface-modified stainless steel plates revealed that we could reduce non-specific protein adsorption as much as ~80%, comparing to bare stainless steel plate. Thus, smoothened and hydrophilic polymer-grafted surface was the best of choice for fabricating biofunctional EPC-capturing stent as it can effectively decrease bio-fouling such as protein adsorption and thrombogenesis.

As a result of this study, the surface modification procedures for EPC-capturing were established. Each of experimental steps and analysis results were as follows.

Firstly, we generated biocompatible stent through electropolishing and hydrophilic polymer grafting as we expected. This surface-modified stent dramatically reduced the non-specific adsorption and uniformly introduced functional groups. Using these functional groups, we could immobilize anti-VE-cadherin antibody which is the powerful ligand to capture late EPCs from bloodstream.

Secondly, it is confirmed that our EPC-capturing stent selectively recruited EPCs and promoted endothelialization on the interface, indicating that it can induce re-endothelialization on the stent surface as soon as stenting. *In vitro* cell adsorption test showed that the surface-modified stent could interact with EPCs, but not with THP-1, another blood cell. On the other hand, bare metal stent adsorbed both EPC and THP-1 without any preference. Through this head-to-head comparison between the EPC-capturing stent and the bare metal stent, we proved the EPC specificity of our approach.

Finally, through *in vivo* animal experiment, we demonstrated that our EPC-capturing stent rapidly completed re-endothelialization within 3 days and prevented re-narrowing of vessels at 42 days. Being different from commercial stents, the stented vessel was fully re-endothelialized in a few days and thus the risk of in-stent thrombosis is expected to decrease significantly. On the contrary, in the case of bare metal stent, the only partial surface of stent was covered with cells at 3 days and its restenosis area was bigger. Additionally, the surface coating with silane, polymer and antibody did not induce any further inflammation in terms of macrophage infiltration. Our surface modification technology to selectively capture circulating late EPCs can actually induce not only the prevention of stent thrombosis but also the inhibition of neointimal growth, thereby unraveling major problems after stenting.

This opens a new prospect to develop high-performance EPC-capturing stents that can effectively prevent stent thrombosis and restenosis as well. It will also give significant impacts on blood-contacting devices such as artificial vessels, if provided with specific cells or molecules which exist in the biological system. Far beyond this, our bioconjugation chemistry can be widely applied to other biomaterial functionalization, biosensor development, and therapeutic design as well as next-generation stent fabrication.

V. Future Work

Recently, we comparatively evaluated whether anti-VE-cadherin antibody-coated stents might accelerate vascular re-endothelialization and reduce neointimal formation more than anti-CD34 antibody-coated stents[120]. Herein, the stainless steel stents were immobilized with anti-VE-cadherin antibodies or anti-CD34-antibodies under the same condition such as PEG grafting. The anti-VE-cadherin antibody-coated stents showed higher number of captured EPC (823.6±182.2 vs. 379.2±137.2) and smaller neointima (0.92±0.38 vs. 1.24±0.41 mm^2) at 42 days in the rabbit iliac artery study. However, this study only focused on the efficacy of two antibodies and we have not compared our EPC-capturing stents to commercial OrbusNeich's Genous R™ stents. Hereafter, the direct comparison with Genous R™ stents is necessary to show superiority of our EPC-capturing stent.

In immobilizing anti-VE-cadherin antibodies on the PEG-grafted stent, the orientation was not controlled. Partly, Fab portions of the antibody might be coupled with the polymer surface and thus the EPC-capturing ability was not maximized. To improve the efficacy of capturing EPCs, the controlled antibody orientation on stent should be investigated.

For closer investigation, more information of anti-VE-cadherin antibody and EPC are required. However, the biology of EPC such as surface antigens is not fully understood. If we know the dimension of antibody and the VE-cadherin expression level on EPC membrane, the EPC-capturing ability per stent strut could be estimated. The biology of EPC should be regularly tracked and updated in the future.

VI. Reference

1. Colombo, A., Stankovic, G., and Moses, J.W. Selection of coronary stents. *J. Am. Coll. Cardiol.* **40**, 1021-1033. (2002)

2. Gruntzig, A. R., Senning, A., and Siegenthaler, W. E. Nonoperative dilatation of coronary artery stenosis percutaneous transluminal coronary angioplasty. *N. Engl. J. Med.* **301**, 61-68. (1979)

3. Sigwart, U., Puel, J., Mirkovitch, V., Joffre, F., and Kappenberger, L. Intravascular stents to prevent occlusion and re-stenosis after transluminal angioplasty. *N. Engl. J. Med.* **316**, 701-706. (1987)

4. Grines, C. L., Cox, D. A., Stone, G. W., Garcia, E., Mattos, L. A., Giambartolomei, A., Brodie, B.R., Madonna, O., Eijgelshoven, M., Lansky, A. J., O'neill, W. W., and Morice, M. C. Coronary angioplasty with or without stent implantation for acute myocardial infaction. *N. Engl. J. Med.* **341**, 1949-1956. (1999)

5. Williams, D. O., Holubkov, R., Yeh, W., Bourassa, M. G., Al-Bassam, M., Block, P. C., Coady, P., Cohen, H., Cowley, M., Dorros, G., Faxon, D., Holmes, D. R., Jacobs, A., Kelsey, S. F., King III, S. B., Myler, R., Slater, J., Stanek, V., Vlachos, H. A., and Detre, K. M. Percutaneous coronary intervention in the current era compared with 1985-1986: The national heart, lung, and blood institute registries. *Circulation* **102**, 2945-2951. (2000)

6. Stables, R. H. and Sigwart, U. Advances in coronary stenting. *Acc Curr. J.*

Rev. **7**, 27-30. (1998)

7. Jain, S. P., Ramee, S. R., White, C. J., Mehra, M. R., Ventura, H. O., Zhang, S., Jenkins, J. S., and Collins, T. J. Coronary stenting in cardiac allograft vasculopathy. *J. Am. Coll. Cardiol.* **32**, 1636-1640. (1998)

8. Palmaz, J. C., Bailey, S., Marton, D., and Sprague, E. Influence of stent design and material composition on procedure outcome. *J. Vasc. Surg.* **36**, 1031-1039. (2002)

9. Elezi, S., Kastrati, A., Hadamitzky, M., Dirschinger, J., Nuemann, F. J., and Schomig, A. Clinical and angiographic follow-up after ballon angioplasty with provisional stenting for coronary in-stent restenosis. *Cathet. Cardiovasc. Intervent.* **48**, 151-156. (1999)

10. Lowe, H. C., Oesterle, S. N., and Khachigian, L. M. Coronary in-stent restenosis; Current status and future strategies FREE. *J. Am. Coll. Cardiol.* **39**, 183-193. (2002)

11. Hoffmann, R., Mintz, G. S., Dussaillant, G. R., Popma, J. J., Pichard, A. D., Satler, L. F., Kent, K. M., Griffin, J., and Leon, M. B. Patterns and mechanisms of in-stent restenosis. *Circulation* **94**, 1247-1254. (1996)

12. Scheerder, I. D., Verbeken, E., and Humbeeck, J. V. Metallic surface modification. *Semin. Intervent. Cardiol*. **3**, 139-144. (1998)

13. Takagi, T., Akasaka, T., Yamamuro, A., Honda, Y., Hozumi, T., Morioka, S., and Yoshida, K. Impact of insulin resistance on neointimal tissue

proliferation after coronary stent implantation: Intravascular ultrasound studies. *Journal of Diabetes and its Complications* **16**, 50-55. (2002)

14. Kraitzer, A., Kloog, Y., and Zilberman, M. Approaches for prevention of restenosis. *J. Biomed. Mater. Res.* **85**, 583-603. (2008)

15. Garza, L., Aude, Y. W., and Saucedo, J. F. Can we prevent in-stent restenosis? *Curr. Opin. Cardiol*. **17**, 518-525. (2002)

16. Freed, M., Safian, R. D., and Grines, C. Manual of interventional cardiology. Birmingham, *MI; Physicians' Press*, 818. (1996)

17. Kimura, T., Yokoi, H., Nakagawa, Y., Tamura, T., Kaburagi, S., Sawada, Y., Sato, Y., Yokoi, H., Hamasaki, N., Nosaka, H., and Nobuyoshi, M. Three-year follow-up after implantation of metallic coronary artery stents. *N. Engl. J. Med.* **334**, 561-566. (1996)

18. Duda, S. H., Poerner, T. C., Wiesinger, B., Rundback, J. H., Tepe, G., Wiskirchen, J., and Haase, K. K. Drug-eluting stents: Potential applications for peripheral arterial occlusive disease. *J. Vasc. Interv. Radiol*. **14**, 291-301. (2003)

19. Wimmer, N. J., and Yeh, R. W. Another view of personalized medicine: Optimizing stent selection on the basis of predicted benefit in percutaneous coronary intervention. *Trend Cardiovasc. Med.* **22**, 23-28. (2012)

20. Blindt, R., Vogt, F., Astafieva, I., Fach, C., Hristov, M., Krott, N., Seitz, B., Kapurniotu, A., Kwok, C., Dewor, M., Bosserhoff, A.-K., Bernhagen, J.,

Hanrath, P., Hoffmann, R., and Weber, C. A novel drug-eluting stent coated with an integrin-binding cyclic Arg-Gly-Asp peptide inhibits neointimal hyperplasia by recruiting endothelial progenitor cells. *J. Am. Coll. Cardiol.* **47**, 1786-1795. (2006)

21. Fattori, R. and Piva, T. Drug-eluting stents in vascular intervention. *Lancet* **361**, 247-249. (2003)

22. Hara, H., Nakamura, M., Palmaz, J. C., and Schwartz, R. S. Role of stent design and coatings on restenosis and thrombosis. *Adv. Drug Delivery Rev.* **58**, 377-386. (2006)

23. Kim, T.G., Lee, H., Jang, Y., and Park, T. G. Controlled release of paclitaxel from heparinized metal stent fabricated by layer-by-layer assembly of polylysine and hyaluronic acid-g-poly(lactic-co-glycolic acid) micelles encapsulating paclitaxel. *Biomacromolecules* **10**, 1532-1539. (2009)

24. Takahashi, H., Letourneur, D., and Grainger, D. W. Delivery of large biopharmaceuticals from cardiovascular stents: A review. *Biomacromolecules* **8**, 3281-3293. (2007)

25. Garg, S. and Serruys, P. W. Coronary stents: Looking forward. *J. Am. Coll. Cardiol.* **56**, S43-S78. (2010)

26. Carter, A. J., Aggarwal, M., Kopia, G. A., Tio, F., Tsao, P. S., Kolata, R., Yeung, A. C., Llanos, G., Dooley, J., and Falotico, R. Long-term effects of polymer-based, slow-release, sirolimus-eluting stents in a porcine coronary model. *Cardiovasc. Res.* **63**, 617-624. (2004)

27. Luscher, T. F., Steffel, J., Eberli, F. R., Joner, M., Nakazawa, G., Tanner, F. C., and Virmani, R. Drug-eluting stent and coronary thrombosis: Biological mechanisms and clinical implications. *Circulation* **115**, 1051-1058. (2007)

28. Schomig, A., Neumann, F-J., Kastrati, A., Schuhlen, H., Blasini, R., Hadamitzky, M., Walter, H., Zitzmann-Roth, E-M., Richardt, G., Alt, E., Schmitt, C., and Ulm, K. A randomized comparison of antiplatelet and anticoagulant therapy after the placement of coronary-artery stents. *N. Engl. J. Med.* **334**, 1084-1089. (1996)

29. Bertrand, M. E., Rupprecht, H-J., Urban, P., and Gershlick, A. H. Double-blind study of the safety of clopidogrel with and without a loading dose in combination with aspirin compared with ticlopidine in combination with aspirin after coronary stenting: the clopidogrel aspirin stent international cooperative study (CLASSICS). *Circulation* **102**, 624-629. (2000)

30. McFadden, E. P., Stabile, E., Regar, E., Cheneau, E., Ong, A. T., Kinnaird, T., suddath, W. O., Weissman, N. J., Torguson, R., kent, K. M., Pichard, A. D., Satler, L. F., Waksman, R., and Serruys, P. W. Late thrombosis in drug-eluting coronary stents after discontinuation of antiplatelet therapy. *Lancet* **364**, 1519-1521. (2004)

31. Daemen, J., Wenaweser, P., Tsuchida, K., Vaina, S., Abrecht, L., Morger, C., Kukreja, N., Juni, P., Sianos, G., Hellige, G., van Domburg, R., Hess, O. M., Boersma, E., Meier, B., Windecker, S., and Serruys, P. W. Early and late coronary stent thrombosis of sirolimus-eluting and paclitaxel-eluting stents in routine clinical practice: Data from a large two-institutional cohort study.

Lancet **369**, 667-678. (2007)

32. Kereiakes, D. J., Cox, D. A., Hermiller, J. B., Midei, M. G., Bachinsky, W. B., Nukta, E. D., Leon, M. B., Fink, S., Marin, L., and Lansky, A. J. Usefulness of cobalt chromium coronary stent alloy. *Am. J. Cardiol.* **92**, 463-466. (2003)

33. Krucoff, M. W., Kereiakes, D. J., Petersen, J. L., mehran, R., Hasselblad, V., Lansky, A. J., Fitzgerald, P. J., Garg, J., Turco, M. A., Simonton, C. A., Verheye, S., Dubois, C. L., Gammon, R., Batchelor, W. B., O'shaughnessy, C. D., Hermiller, J. B., Schofer, J., Buchbinder, M., and Wijns, W. A novel bioresorbable polymer paclitaxel-eluting stent for the treatment of single and multivessel coronary disease: Primary results of the COSTAR II Study. *J. Am. Coll. Cardiol*. **51**, 1543-1552. (2008)

34. Ormiston, J. A., Serruys, P. W., Regar, E., Dudek, D., Thuesen, L., Webster, M. W. Onuma, Y., Garcia-Garcia, H. M., McGreevy, R., and Veldhof, S. A bioabsorbable everolimus-eluting coronary stent system for patients with single de-novo coronary artery lesions (ABSORB): A prospective open-label trial. *Lancet* **371**, 899-907. (2008)

35. Griffiths, H., Peeters, P., Verbist, J., Bosiers, M., Deloose, K., Heublein, B., Rohde, R., Kasese, V., Ilsley, C., and Di Mario, C. Future devices: Bioabsorbable stents. *Br. J. Cardiol. (Acute. Interv. Cardiol.)* **11**, AIC 80 – AIC 84. (2004)

36. Heublein, B., Rohde, R., Kaese, V., Niemeyer, M., Hartung, W., and Haverich, A. Biocorrosion of magnesium alloys: A new principle in

cardiovascular implant technology? *Heart* **89**, 651-656. (2003)

37. Barlis, P., Tanigawa, J., and Di Mario, C. Coronary bioabsorbable magnesium stent: 15-month intravascular ultrasound and optical coherency findings. *Eur. Heart. J.* **28**, 2319. (2007)

38. Caster, D.G. and Ratner, B. D. Biomedical surface science: Foundations to frontiers. *Surf. Sci.* **500**, 28-60. (2002)

39. O'Brien, B. and Carroll, W. The evolution of cardiovascular stent materials and surfaces in response to clinical drivers: A review. *Acta Biomater.* **5**, 945-958. (2009)

40. Tirrell, M., Kokkoli, E., and Biesalski, M. The role of surface science in bioengineered materials. *Surf. Sci.* **500**, 61-83. (2002)

41. Abrahams, J. M., Diamond, S. L., Hurst, R. W., Zager, E. L., and Grady, M. S. Topic review: Surface modifications enhancing biological activity of Guglielmi detachable coils in treating intracranial aneurysms. *Surg. Neurol.* **54**, 34-40. (2000)

42. Kukreja, N., Onuma, Y., Daemen, J., and Serruys, P. W. The future of drug-eluting stents. *Pharmacol. Res.* **57**, 171-180. (2008)

43. Seeger, J. M., Ingegno, M. D., Bigatan, E., Klingman, N., Amery, D., Widenhouse, C., and Goldberg, E. P. Hydrophilic surface modification of metallic endoluminal stents. *J. Vasc. Surg.* **22**, 327-336. (1995)

44. Lahann, J., Klee, D., Thelen, H., Bienert, H., Vorwerk, D., and Hocker, H. Improvement of haemocompatibility of metallic stents by polymer coating. *J. Mater. Sci.: Mater. Med.* **10**, 443-448. (1999)

45. Lewis, A. L., Cumming, Z. L., Goreish, H. H., Kirkwood, L. C., Tolhurst, L. A., and Stratford, P. W. Crosslinkable coatings from phosphorylcholine-based polymers. *Biomaterials* **22**, 99-111. (2001)

46. Bertrand, O. F., Sipehia, R., Mongrain, R., Rodes, J. R., Tardif, J. C., Bilodeau, L., Cote, G., and Bourassa, M. G. Biocompatibility aspects of new stent technology. *J. Am. Coll. Cardiol.* **32**, 562-571. (1998)

47. Palmaz, J. C., Bailey, S., Marton, D., and Sprague, E. Influence of stent design and material composition on procedure outcome. *J. Vasc. Surg.* **36**, 1031-1039. (2002)

48. Kastrati, A., Schomig, A., Dirschinger, J., Mehilli, J., von Welser, N., Pache, J., Schuhlen, H., Schilling, T., Schmitt, C., and Neumann, F-J. Increased risk of restenosis after placement of gold-coated stents: Results of arandomized trial comparing gold-coated with uncoated steel stents in patients with coronary artery disease. *Circulation* **101**, 2478-2483. (2000)

49. Unverdorben, M., Sippel, B., Degenhardt, R., Sattler, K., Fries, R., Abt, B., Wagner, E., Koehler, H., Daemgen, G., Scholz, M., Ibrahim, H., Tews, K-H., Hennen, B., Berthold, H. K., and Vallbracht, C. Comparison of a silicon carbide-coated stent versus a noncoated stent in human beings: the Tenax versus Nir Stent Study's long-term outcome. *Am. Heart. J.* **145**, e17. (2003)

50. Tanajura, L. F., Abizaid, A. A., Feres, F., Pinto, I., Mattos, L., Staico, R., de Paula, J., Abizaid, A. S., Centemero, M., Chaves, A., J., Paes, A., Seixas, A., Sousa, A., and Sousa, J. E. M. Randomized intravascular ultrasound comparison between patients that underwent amorphous hydrogenated silicon-carbide coated stent deployment versus uncoated stents FREE. *J. Am. Coll. Cardiol.* **41**, 58A. (2003)

51. Wohrle, J., Al-Khayer, E., Grotzinger, U., Schindler, C., Kochs, M., Hombach, V., and Hoher, M. Comparison of the heparin coated vs the uncoated Jostent – no influence on restenosis or clinical outcome. *Eur. Heart. J*. **22**, 1808-1816. (2001)

52. Lewis, A.L., Cumming, Z.L., Goreish, H.H., Kirkwood, L.C., Tolhurst, L.A., Stratford, P.W. Crosslinkable coatings from phosphorylcholine-based polymers. *Biomaterials* **22**, 99-111. (2001)

53. Babapulle, M., N. and Eisenberg, M. J. Coated stents for the prevention of restenosis: Part II. *Circulation* **106**, 2859-2866. (2002)

54. Lewis, A.L., Vick, T.A., Collias, A.C.M., Hughes, L.G., Palmer, R.R., Leppard, S.W., Furze, J.D., Taylor, A.S., Stratford, P.W. Phosphorylcholine-based polymer coatings for stent drug delivery. *J. Mater. Sci.: Mater. Med.* **12**, 1389-1398. (2007)

55. Yang, Z. L., Tu, Q. F., Zhu, Y., Luo, R. F., Li, X., Xie, Y. C., Maitz, M. F., Wang, J., and Huang, N. Mussel-inspired coating of polydopamine directs endothelial and smooth muscle cell fate for re-endothelialization of vascular devices. *Adv. Healthcare Mater.* **1**, 548-559. (2012)

56. Morice, M-C. Serruys, P. W., Sousa, F. E., Fajadet, J., Ban Hayashi, E., Perin, M., Colombo, A., Schuler, G., Barragan, P., Guagliumi, G., Molnar, F., and Falotico, R. A randomized comparison of a sirolimus-eluting stent with a standard stent for coronary reascularization. *N. Engl. J. Med.* **346**, 1773-1780. (2002)

57. Marxand, S. O. and Marks, A. R. Bench to bedside: The development of rapamycin and its application to stent restenosis. *Circulation* **104**, 852-855. (2001)

58. Finn, A. V., Nakazawa, G., Joner, M., Kolodgie, F. D., Mont, E. K., Gold, H. K., and Virmani, R. Vascular responses to drug-eluting stents: Importance of delayed healing. *Arterioscler. Thromb. Vasc. Biol*. **27**, 1500-1510. (2007)

59. Colombo, A., Drzewiecki, J., Banning, A., Grube, E., Hauptmann, K., Silber, S., Dudek, D., Fort, S., Schiele, F., Zmudka, K., Guagliumi, G., and Russell, M. E. Rondomized study to assess the effectiveness of slow- and moderate-release polymer-based paclitaxel-eluting stents for coronary artery lesions. *Circulation* **108**, 788-794. (2003)

60. Schuler, W., Sedrani, R., Cottens, S., Haberlin, B., Schulz, M., Schuurman, H. J., Zenke, G., Zerwes, H-G., and Schreier, M. H. SDZ RAD, a new rapamycin derivative: Pharmacological properties in vitro and in vivo. *Transplantation* **64**, 36-42. (1997)

61. Meredith, I. T., Ormiston, J., Whitbourn, R., Kay I. P., Muller, D., Bonan,R., Popma, J. J., Cutlip, D. E., Fitzgerald, P., Prpic, R., and Kuntz, R. E.

First-in-human study of the Endeavor ABT-578-eluting phosphorylcholine-encapsulated stent system in de novo native coronary artery lesions: Endeavor I trial. *Eurointervention* **48**, 2440-2447. (2006)

62. Kandzari, D. E., Leon, M. B., Popma, J. J., Fitzgerald, P. J. O'Shaughnessy, C., Ball, M. W., Turco, M., Applegate, R. J., Gurbel, P. A., Midei, M. G., Badre, S. S., Mauri, L., Thompson, K. P., LeNarz, L. A., and Kuntz, R. E. Comparison of zotarolimus-eluting and sirolimus-eluting stents in patients with native coronary artery disease: A randomized controlled trial. *J. Am. Coll. Cardiol.* **48**, 2440-2447. (2006)

63. Miyazawa, A., Ako, J., Hongo, Y., Hur, S. H., Tsujino, I., Courtney, B. K., Hassan, A. H., Kanazari, D. E., Honda, Y., and Fitzgerald, P. J. Comparions of vascular response to zotarolimus-eluting stent vs. sirolimus-eluting stent: intravascular ultrasound results from ENDEAVOR III. *Am. Heart. J.* **155**, 108-113. (2008)

64. Kukreja, N., Onuma, Y., Daemen, J., and Serruys, P. W. The future of drug-eluting stents. *Pharmaco. Res.* **57**, 171-180. (2008)

65. Iakovou, I., Schmidt, T., Bonizzoni, E., Ge, L., Sangiorgi, G. M., Stankovic, G., Airoldi, F., Chieffo, A., Montorfano, M., Carlino, M., Michev, I., Corvaja, N., Briguori, C., Gerckens, U., Grub, E., and Colombo, A. Incidence, predictors, and outcome of thrombosis after successful implantation of drug-eluting stent. *JAMA* **293**, 2126-2130. (2005)

66. Daemen J., Wenaweser, P., Tsuchida, K., Abrecht, L., Vaina, S., Morger, C., Kukreja, N., Juni, P., Sianos, G., Hellige, G., van Domburg, R. T. Hess, O. M.,

Boersma, E., Meier, B., Windecker, S., and Serruys, P. W. Early and late coronary stent thrombosis of sirolimus-eluting and paclitaxel-eluting stents in routine clinical practice: data from a large two-institutional cohort study. *Lancet* **369**, 667-678. (2007)

67. Kawamoto, A. and Asahara, T. Role of progenitor endothelial cells in cardiovascular disease and upcoming therapies. *Cathete. Cardio. Inte.* **70**, 477-484. (2007)

68. de Mel, A., Jell, G., Stevens, M. M., and Seifalian, A. M. Biofunctionalization of biomaterials for accelerated in situ endothelialization: A review. *Biomacromolecules* **9**, 2969-2979. (2008)

69. Meyers, S. R., Kenan, D. J., Khoo, X. J., and Grinstaff, M. W. Bioactive stent surface coating that promotes endothelialization while preventing platelet adhesion. *Biomacromolecules* **12**, 533-539. (2011)

70. Asahara, T., Murohara, T., Sullivan, A., van der Zee, R., Li, T., Witzenbichler, B., Schatteman, G., and Isner, J. M. Isolation of putative progenitor endothelial cells for angiogenesis. *Science*. **275**, 964-966. (1997)

71. Aoki, J., Serruys, P. W., van Beusekom, H., Ong, A. T. L., McFadden, E. P., Sianos, G., van der Giessen, W. J., Regar, E., de Feyter, P. J., Davis, H. R., Rowland, S., and Kutryk, M. J. B. Endothelial progenitor cell capture by stents coated with antibody against CD34. *J. Am. Coll. Cardiol*. **45**, 1574-1579. (2005)

72. Yin, M., Yuan, Y., Liu, C., and Wang, J. Combinatorial coating of adhesive polypeptide and anti-CD34 antibody for improved endothelial cell adhesion and proliferation. *J. Mater. Sci.: Mater. Med.* **20**, 1513-1523. (2009)

73. Szmitko, P. E., Kutryk, M. J. B., Stewart, D. J., Strauss, M. H., and Verma, S. Endothelial progenitor cell-coated stents under scrutiny. *Can. J. Cardiol.* **22**, 1117-1119. (2006)

74. Chong, E., Poh, K. K., Liang, S., Lee, R. C.-H., Low, A., Teo, S.-G., and Tan, H. C. Two-year clinical registry follow-up of endothelial progenitor cell capture stent versus sirolimus-eluting bioabsorbable polymer-coated stent versus bare metal stents in patients undergoing primary percutaneous coronary intervention for ST elevation myocardial infarction. *J. Intervent. Cardiol.* **23**, 101-108. (2010)

75. Wendel, H. P., Avci-Adali, M., and Ziemer, G. Endothelial progenitor cell capture stents — hype or hope? *Int. J. Cardiol.* **145**, 115-117. (2010)

76. OrbusNeich Medical Incoporate. Coating which promotes endothelial cell adherence. *International Patent*, PCT/US2001/008244. (2001)

77. Aoki, J., Serruys, P. W., Beusekom, H., Ong, A. T., Mcfadden, E. P., Sianos, G., van der Giessen, W. J., Regar, E. de Feyter, P. J., Davis, R., Rowland, S., and Kutryk. M. J. Endothelial progenitor cell capture by stents coated with antibody against CD34: The HEALING-FIM registry. *J. Am. Coll. Cardiol.* **45**, 1574-1579. (2005)

78. Bejik, M. A. M., Klomp, M., Verouden, N. K. W., van Geloven, N., Koch,

K. T., Henriques, J. P. S., Baan, J., Vis, M. M., Scheunhage, E., Piek, J. J., Tijssen, J. G. P., and de Winter, R. J. Genous endothelial progenitor cell capturing stent vs. the Taxus Liberte stent in patients with de novo coronary lesions with a high-risk of coronary restenosis: A randomized, single-centre, pilot study. *Eur. Heart. J.* **31**, 1055-1064. (2010)

79. Beijk, M. A., Klomp, M., van Geloven, N., Koch, K. T., Henriques, J. P., Baan, J. Marije, M., Vis, M. M., Tijssen, J. G. P., Piek, J. J., and de Winter, R. J. Two-year follow-up of the Genous endothelial progenitor cell capturing stent vs. the Taxus Liberte stent in patients with de novo coronary artery lesions with a high-risk of restenosis: A randomized, single-centre, pilot study. *Catheter. Cardiovasc. Interv.* **78**, 189-195. (2011)

80. Bystron, M., Cervinka, P., Spacek, R., Kvasnak, M., Jakabcin, J., Cervinkova, M., Kala, P., and Widimsky, P. Randomized comparison of endothelial progenitor cells capture stent vs. cobalt-chromium stent for treatment of ST-elevation myocardial infarction: Six-month clinical, angiographic, and IVUS follow-up. *Catheter. Cardiovasc. Interv.* **76**, 627-631. (2010)

81. Garg, S., Duckers, H. J., and Serruys, P. W. Endothelial progenitor cell capture stents: Will this technology find its niche in contemporary practice? *Eur. Heart. J.* **31**, 1032-1035. (2010)

82. Falsey, J. R., Renil M., Park S., Li S., and Lam K. S. Peptide and small molecule microarray for high throuput cell adhesion and functional assays. *Bioconjugate Chem.* **12**, 346-353. (2001)

83 . Cheng, F., Shang, J., and Ratner, D.M. A versatile method for functionalizing surfaces with bioactive glycans. *Bioconjugate Chem.* **22**, 50-57. (2011)

84. Nanci, A., Wuest, J. D., Peru, L., Brunet, P., Sharma, V., Zalzal, S., and Mckee, M. D. Chemical modification of titanium surfaces for covalent attachment of biological molecules. *J. Biomed. Mater. Res*. **40**, 324-335. (1998)

85. Huang, N. P., Michel, R., Voros, J., Textor, M., Hofer, R., Rossi, A., Elbert, D. L., Hubbell, J. A., and Spencer, N. D. Poly(L-lysine)-g-poly(ethylene glycol) layers on metal oxide surfaces: Surface-analytical characterization and resistance to serum and fibrinogen adsorption. *Langmuir* **17**, 489-498. (2001)

86. Prime, K. L. and Whitesides, G. M. Self-assembled organic monolayers: Model systems for studying adsorption of proteins at surfaces. *Science* **252**, 1164-1167. (1991)

87. Tegoulia V. A., Rao, W., Kalambur, A. T., Rabolt, J. F., and Cooper, S. L. Surface properties, fibrinogen adsorption, and cellular interactions of a novel phosphorylcholine-containing self-assembled monolayer on gold. *Langmuir* **17**, 4396-4404. (2001)

88. Piehler, J., Brecht, A., Geckeler, K. E., and Gauglitz, G. A high-density poly(ethylene glycol) polymer brush for immobilization on glass-type surfaces. *Biosens. Bioelectron*. **11**, 579-590. (1996)

89. Shin, D.-S., Lee, K.-N., Jang, K.-H., Kim, J.-K., Chung, W.-J., Kim, Y.-K., and Lee, Y.-S. Protein patterning by maskless photolithography on hydrophilic polymer-grafted surface. *Biosens. Bioelectron.* **19**, 485-494. (2003)

90. Sharma, S., Popat, K. C., and Desai, T. A. Controlling nonspecific protein interactions in silicon biomicrosystems with nanostructured poly(ethylene glycol) films. *Langmuir* **18**, 8728-8731. (2002)

91. Ulman, A. Formation and structure of self-assembled monolayers. *Chem. Rev.* **96**, 1533-1554. (1996)

92. Carmeliet, P., Lampugnani, M. G., Moons, L., Breviario, F., Compernolle, V., Bono, F., Balconi, G., Spagnuolo, R., Oosthuyse, B., Dewerchin, M., Zanetti, A., Angellilo, A., Mattot, V., Nuyens, D., Lutgens, E., Clotman, F., de Ruiter, M. C., Gittenberger-de Groot, A., Poelmann, R., Lupu, F., Herbert, J. M., Collen, D., and Dejana, E. Targeted deficiency or cytosolic truncation of the VE-cadherin gene in mice impairs VEGF-mediated endothelial survival and angiogenesis. *Cell* **98**, 147-157. (1999)

93. Yoon, C. H., Hur, J., Park, K. W., Kim, J. H., Lee, C. S., Oh, I. Y., Kim, T. Y., Cho, H. J., Kang, H. J., Chae, I. H., Yang, H. K., Oh, B. H., Park, Y. B., and Kim, H. S. Synergistic Neovascularization by mixed transplantation of early endothelial progenitor cells and late outgrowth endothelial cells - The role of angiogenic cytokines and matrix metalloproteinases. *Circulation* **112**, 1618-1627. (2005)

94. Cho, H. J., Kim, H. S., Lee, M. M., Kim, D. H., Yang, H. J., Hur, J.,

Hwang, K. K., Oh, S., Choi, Y. J., Chae, I. H., Oh, B. h., Choi, Y. S., Walsh, K., and Park, Y. B. Mobilized endothelial progenitor cells by granulocyte-macrophage colony-stimulating factor accelerate reendothelialization and reduce vascular inflammation after intravascular radiation. *Circulation* **108**, 2918-2925. (2003)

95. Kang, C. K. and Lee, Y. S. Carbohydrate polymer grafting on stainless steel surface and its biocompatibility study. *J. Ind. Eng. Chem.* **18**, 1670-1675. (2012)

96. Horbett, T. A. The role of adsorbed proteins in animal cell adhesion. *Coll. and Surf. B.* **2**, 225-240. (1994)

97. Zhang, M., Desai, T., and Ferrari, M. Proteins and cells on PEG immobilized silicone surfaces. *Biomaterials* **19**, 953-960. (1998)

98. Yang, Z., Galloway, J.A., and Yu, H. Protein interactions with poly(ethylene glycol) self-assembled monolayers on glass substrates: Diffusion and adsorption. *Langmuir* **15**, 8405-8411. (1999)

99. Eidelmann, R.S. and Hennekens, C.H. Fibrinogen: A predictor of stroke and marker of atherosclerosis. *Eur. Heart. J.* **24**, 499-500. (2003)

100. Thierry, B., Merhi, Y., Bilodeau, L., Trepanier, C., and Tabrizian, M. Nitinol versus stainless steel stents: Acute thrombogenicity study in an ex vivo porcine model. *Biomaterials* **23**, 2997-3005. (2002)

101. Herrwerth, S., Eck, W., Reinhardt, S., and Grunze, M. Factors that

determine the protein resistance of oligoether self-assembled monolayers – internal hydrophilicity, terminal hydrophilicity, and lateral packing density. *J. Am. Chem. Soc.* **125**, 9359-9366. (2003)

102. Zhdanov, V. P. and Kasemo, B. Van der waals interaction during protein adsorption on a solid covered by a thin film. *Langmuir* **17**, 5407-5409. (2001)

103. Palmaz, J. C., Benson, A., and Sprague, E. A. Influence of surface topography on endothelialization of intravascular metallic material. *JVIR* **10**, 439-444. (1999)

104. Otsuka, H., Nagasaki, Y., and Kataoka, K. PEGylated nanoparticles for biological and pharmaceutical applications. *Adv. Drug Delivery Rev.* **55**, 403-419. (2003)

105. Tomizaki K-Y., Usui K., and Mihara H. Protein-detecting microarrays: Current accomplishments and requirements. *Chembiochem* **6**, 782-799. (2005)

106. Kang, C. K. and Lee, Y. S. The surface modification of stainless steel and the correlation between the surface properties and protein adsorption. *J. Mater. Sci.: Mater. Med.* **18**, 1389-1398. (2007)

107 . Zhao, H., Van Humbeeck, J., Sohier, J., and De Scheerder, I. Electrochemical polishing of 316L stainless steel slotted tube coronary stents. *J. Mater. Sci.: Mater. Med.* **13**, 911-916. (2002)

108. Mansfeld, F., Breslin, C. B., Pardo, A., and Perez, F. J. Surface modification of stainless steels: Green technology for corrosion protection. *Surf. Coat. Technol.* **90**, 224-228. (1997)

109. Hermanson, G. T. Bioconjugate Techniques. *Academic Press: New York*. 137-226. (1996)

110. Komatsu, R., Ueda, M., Naruko, T., Kojima, A., and Becker, A. E. Neointimal tissue response at sites of coronary stenting in humans: Macroscopic, histological, and immunohistochemical analyses. *Circulation* **98**, 224-233. (1998)

111. Hur, J., Yoon, C. H., Kim, H. S., Choi, J. H., Kang, H. J., Hwang, K. K., Oh, B. H., Lee, M. M., and Park. Y. B. Characterization of two types of endothelial progenitor cells and their different contributions to neovasculogenesis. *Arterioscler. Thromb. Vasc. Biol.* **24**, 288-293. (2004)

112. Lampugnani, M. G., Resnati, M., Raiteri, M., Pigott, R., Pisacane, A., Houen, G., Ruco, L. P., and Dejana, E. A novel endothelial-specific membrane protein is a marker of cell-cell contact. *J. Cell. Biol*. **118**, 1511-1522. (1992)

113. Vestweber, D. VE-cadherin: The major endothelial adhesion molecule controlling cellular junctions and blood vessel formation. *Arterioscler. Thromb. Vasc. Biol.* **28**, 223-232. (2008)

114. Touchard, A. G., and Schwartz, R. S. Preclinical restenosis models: Challenges and successes. *Toxicol. Pathol*. **34**, 11-18. (2006)

115. Robert, R., Rioufol, G., Finet, G., Cottin, Y., Tabib, A., Zeller, M., Wolf, J. E., Lievre, M., and Bricca, G. Experimental assessment of new stent technologies: Validation of a comparative paired rabbit iliac artery study model. *J. Biomed. Mater. Res.* **70**, 303-310. (2004)

116. Yamashita, A., Asada, Y., Sugimura, H., Yamamoto, H., Marutsuka, K., Hatakeyama, K., Tamura, S., Ikeda, Y., and Sumiyoshi, A. Contribution of von willebrand factor to thrombus formation on neointima of rabbit stenotic iliac artery under high blood-flow velocity. *Arterioscler. Thromb. Vasc. Biol.* **23**, 1105-1110. (2003)

117. Waterhouse, A., Wise, S. G., Yin, Y., Wu, B., James, B., Zreiqat, H., McKenzie, D. R., Bao, S., Weiss, A. S., Ng, M. K. C., and Bilek, M. M. M. In vivo biocompatibility of a plasma-activated, coronary stent coating. *Biomaterials* **33**, 7984-7992. (2012)

118. Reidy, M. A., Clowes, A. W., and Schwartz, S. M. Endothelial regeneration. V. Inhibition of endothelial regrowth in arteries of rat and rabbit. *Lab. Invest*. **49**, 569-575. (1983)

119. Lis, G. J., Litwin, J. A., Furgal-Borzych, A., Zarzecka, J., and Cichocki, T. Macrophage-specific RAM11 monoclonal antibody cross-reacts with basal cells of stratified squamous epithelia. *Folia Histochemica et Cytobiologica* **45**, 229-232. (2007)

120. Lee, J. M., Choe, W., Kim, B. K., Seo, W. W., Lim, W.H., Kang, C. K., Kyeong, S., Eom, K. D., Cho, H. J., Kim, Y. C., Hur, J., Yang, H. M., Cho, H. J., Lee, Y. S., and Kim, H. S. Comparison of endothelialization and neointimal

formation with stents coated with antibodies against CD34 and vascular endothelial-cadherin. *Biomaterials* **33**, 8917-8927. (2012)

Appendix

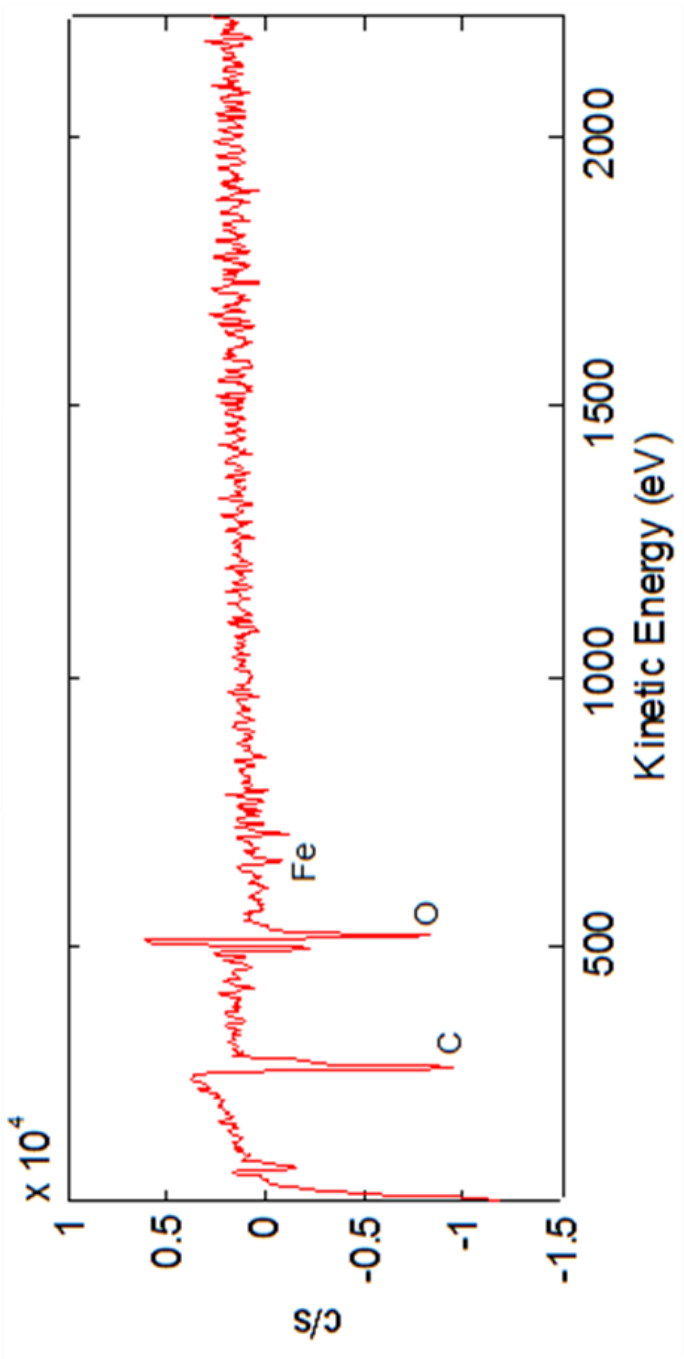

Figure A.1. AES spectra of bare stainless steel stent.

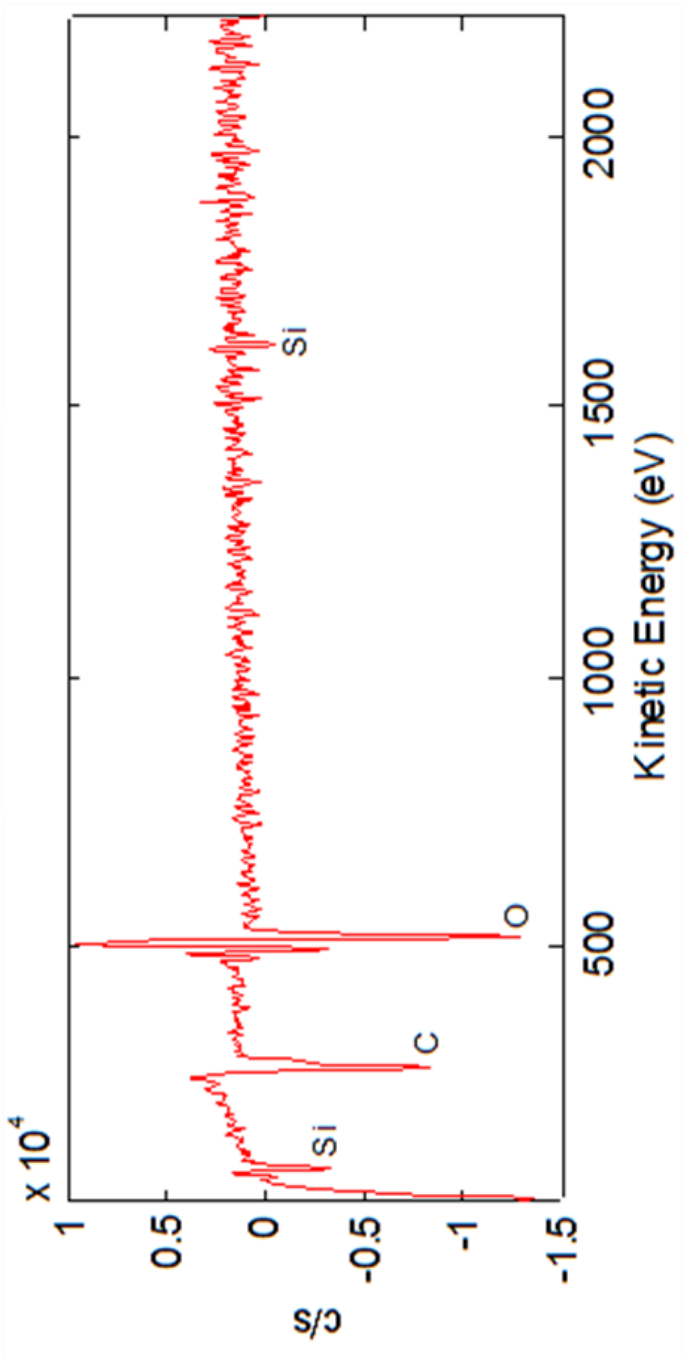

Figure A.2. AES spectra of silanized stainless steel stent.

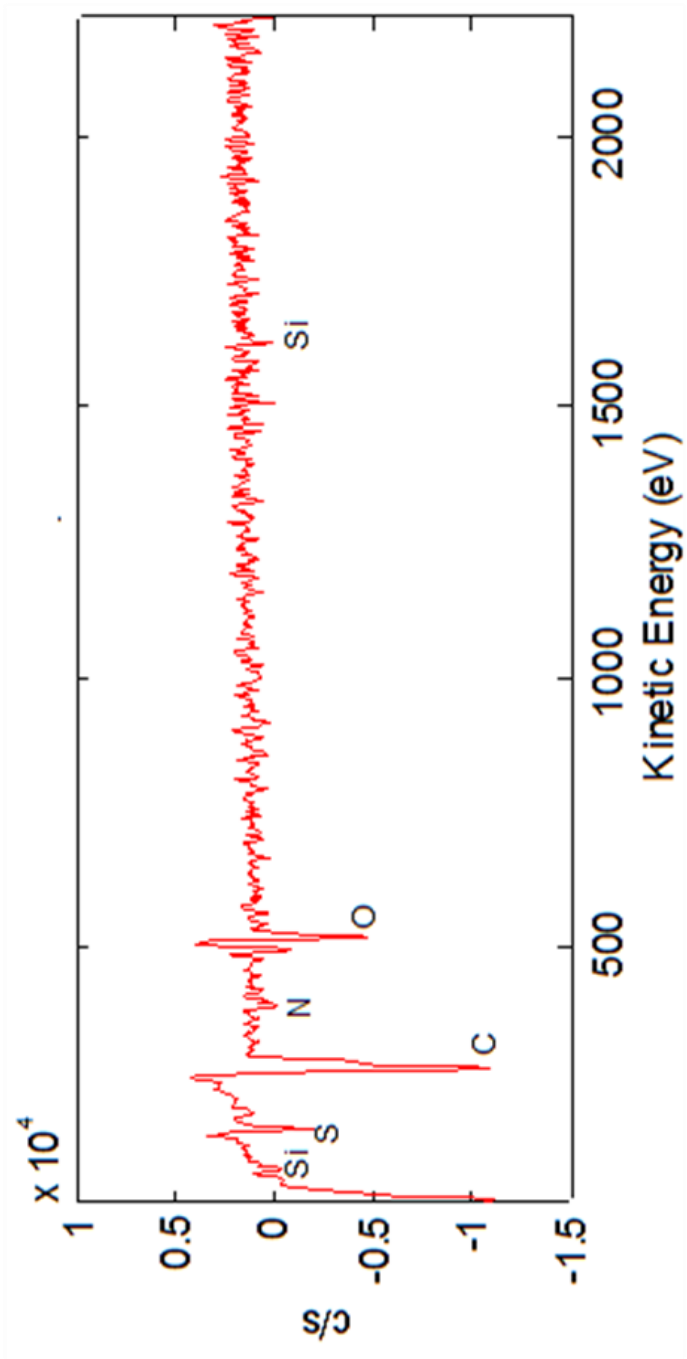

Figure A.3. AES spectra of PEG-grafted stainless steel stent.

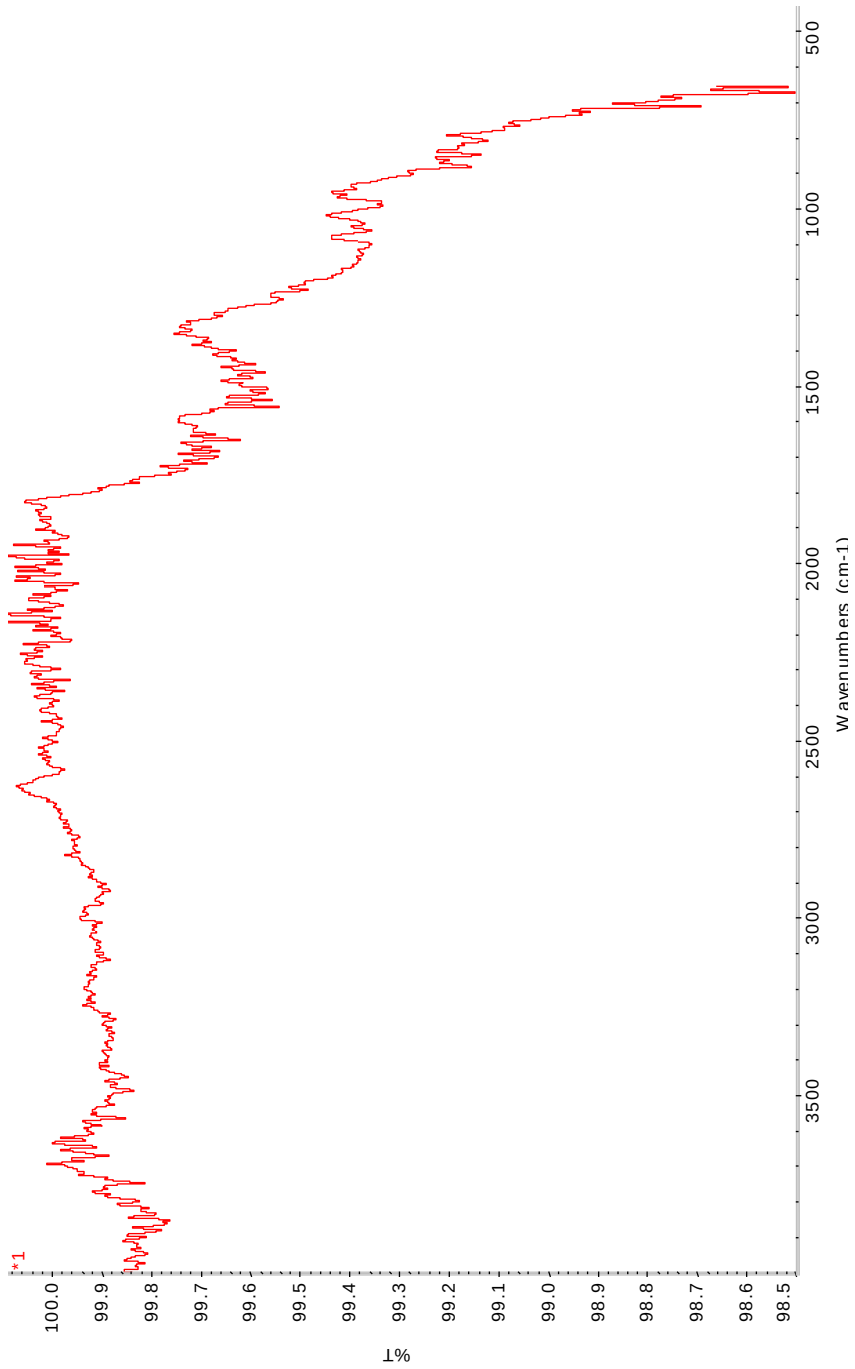

Figure A.4. ATR-FTIR spectra of bare stainless steel stent.

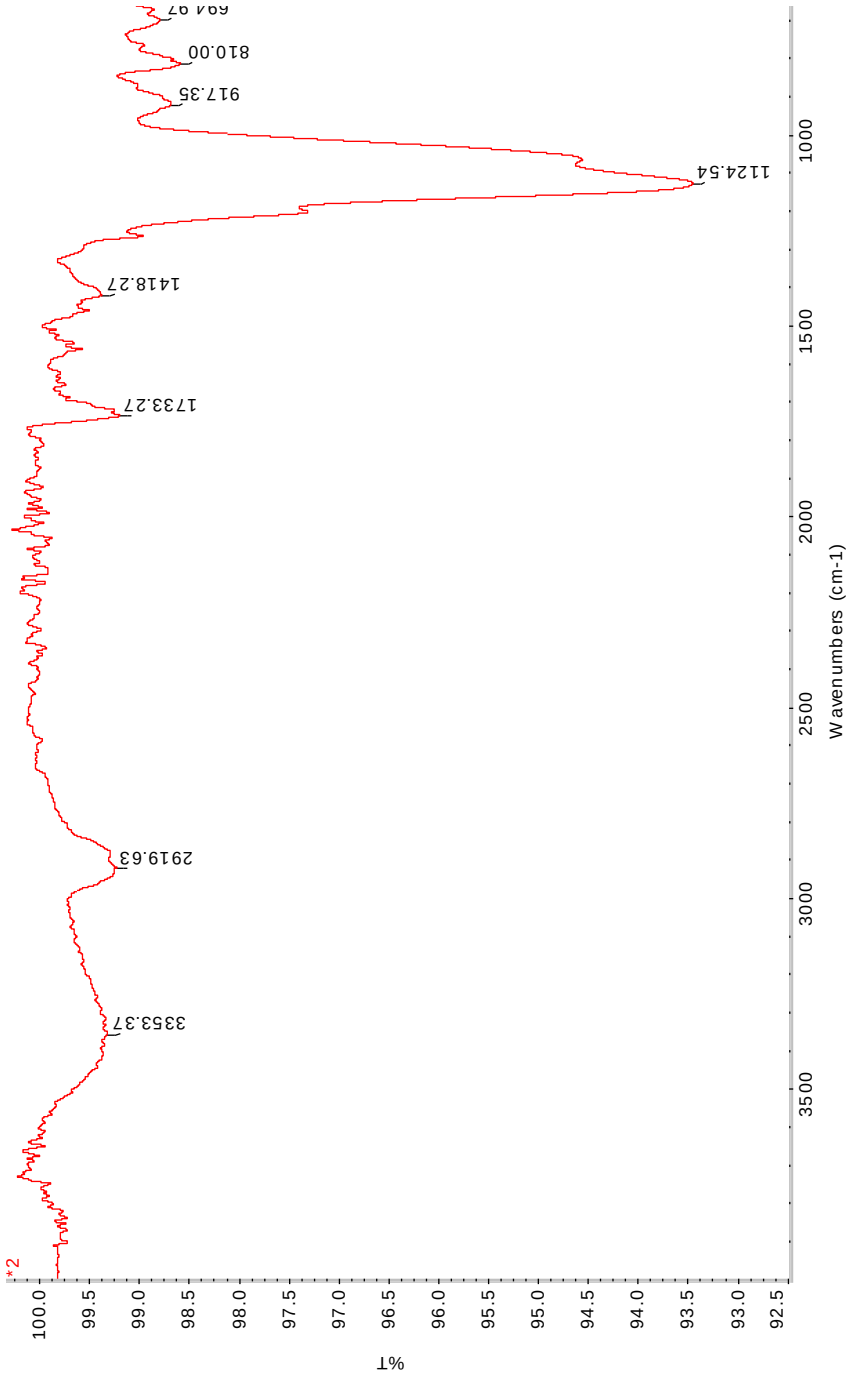

Figure A.5. ATR-FTIR spectra of silanized stainless steel stent.

Abstract in Korean

심혈관질환 치료에 널리 사용되는 스텐트는 최근 기술적 진보를 거듭하며 성능이 개선되고 있지만, 재협착 및 혈전증 문제가 여전히 발생하고 있다. 이에, 혈관내피 줄기세포(EPC)를 선택적으로 포획함으로써 기존 문제를 한번에 해결하는 EPC 포획 스텐트에 대한 개발이 활발히 진행되고 있다.

본 연구에서는 친수성 고분자를 그래프팅하고 VE-cadherin 항체를 고정화하여 혈관내피 줄기세포만 선택적으로 포획하는 스텐트를 개발하고자 하였다. 먼저 스텐트의 재료인 스테인리스 스틸의 표면성질과 단백질 흡착간의 상관관계를 정량 분석했다. 스텐트 표면에 단백질 등의 생체분자가 비특이적으로 흡착하면 부작용이 발생할 뿐만 아니라, 혈관내피 줄기세포의 포획효율도 떨어지기 때문에 단백질 흡착을 억제하는 표면개질 연구는 매우 중요하다. 실험 결과, 표면이 매끄럽고 친수성을 보일수록 단백질의 흡착을 효과적으로 억제하는 것으로 나타났다. 따라서 이 표면성질을 스텐트 개발에 가장 적합한 것으로 판단하였다.

이를 바탕으로, 스텐트 표면을 산처리, 실란화 반응, 고분자 그래프팅, 항체 고정화의 순으로 개질하였다. 표면개질의 방법은 혈관내부의 가혹한 물리화학적 환경을 감안하여 안정성이 떨어지는 물리적 흡착이 아닌, 공유결합 기반의 화학적 합성법을 채택하였다. 그리고 각각의 단계는 AFM, AES, FE-SEM, CLSM 등 다양한 표면분석기기를 통해 그 진행여부를 확인하였다.

EPC 및 THP-1 세포와 반응을 시켜본 결과, VE-cadherin

항체가 고정화된 스텐트는 일반 금속 스텐트에 비해 EPC는 더 많이 포획하는 반면, THP-1의 흡착은 효과적으로 억제하는 모습을 보였다. 또한 포획된 EPC는 스텐트에 흡착되자마자 바로 증식을 시작하면서 빠르게 내피화를 진행하였다.

더 나아가 이렇게 표면개질된 스텐트가 일반 금속 스텐트에 비해 실제 임상적 효능이 우수한지를 토끼 장골혈관내에 스텐트를 삽입하는 비교실험을 통해 확인하였다. 스텐트 시술 3일후 일반 금속 스텐트의 내피화 수준은 10% 미만에 불과했으나, 표면개질된 스텐트는 90% 넘게 내피화가 진행되었다. 또한 42일 후 측정한 신생내막 분석에서도 표면개질된 스텐트가 일반 금속 스텐트 대비 30% 가량 과증식이 억제되었음을 관찰할 수 있었다. 또한 본 연구의 표면 코팅기술은 면역조직검사에서 특별한 염증반응을 유발하지 않은 것으로 확인되어 체내안전성도 우수한 것으로 판명되었다.

본 연구를 통해 새롭게 개발된 스텐트는 세포 및 동물실험 모두에서 일반 금속 스텐트 대비 월등히 우수한 결과를 보여주었다. 이 표면처리기술은 생체물질에 대한 높은 특이성을 가지기 때문에 향후 차세대 스텐트 개발은 물론 바이오센서, 바이오칩, 생체재료 등 다양한 연구분야에서 활발히 적용될 수 있을 것으로 기대된다.

주요어: 스텐트, 표면개질, 단백질 흡착, 혈관내피 줄기세포, 혈관내피화, 재협착

학 번: 2009-30265